MECHANICAL AND MICROSTRUCTURAL PROPERTIES OF STEEL FIBRE REINFORCED CEMENT - BASED MATERIALS

by

Alan David Morris

A dissertation submitted to the University of Cape Town in partial fulfilment of the requirements for the degree of Master of Science.

Dept. of Metallurgy and
Materials Science

June, 1978.

CONTENTS

GRAPHICAL NOTATION

The following symbols were used for graphical representation in Chapters 4 and 5:

(a) ● unreinforced matrix ○ reinforced matrix

(b) Figs: 4.5 - 6; 11 - 12; 14 - 15; Figs. 5.6 - 8

test sample 1 : ●
" " 2 : ■
" " 3 : ◆
" " 4 : ▲
" " 5 : ▼
" " 6 : ▶
" " 7 " ◀

(c) Figs: 4.8, 10, 13, 19, 20, 21, 23

80% stress level : ■
75% " " : ●
70% " " : ▲
65% " " : ▼
60% " " : ◆
55% " " : ▶

CHAPTER 1

1. GENERAL INTRODUCTION

"Concrete is a simple material. It consists of a heterogeneous system of solid, discrete, gradiently-sized inorganic mineral aggregates, usually plutonic (feldspatho-siliceous or ferro-magnesian) or sedimentary-calcareous in origin, embedded in a matrix compounded of synthesized poly-basic alkaline and alkaloidal silicates held in an aqueous solution and co-precipitate dispersion with other amphoteric oxides; this matrix being originally capable of progressive dissolution, hydration, reprecipitation, gel-atinization and solidification through a con-tinuous and co-existent series of crystalline, amorphous, colloidal and crypto-crystalline states, and ultimately subject to thermo-allotriomorphic alteration. The system when first conjoined is transiently plastic during which stage it is impressed to a predetermined form into which it finally consolidates, thus providing a simple man-made constructional material relatively impermeable and with useful capacity to transmit compressive, tensile, shear and bond stresses"

_____ Dr. R.N. Swamy[+]

[+] Concrete, Editor's Comment, August 1973, p. 15.

Concrete?

Portland cement is one of the most common construction materials today, yet it is relatively under-researched compared to metals and plastics which have produced highly sophisticated industries. With the present-day economic climate and rising costs of fuel it becomes increasingly important to conserve energy. Current annual consumption of energy in the United Kingdom has been quoted at 340×10^6 tonnes of coal equivalent (or $9{,}6 \times 10^{18}$J) by Kelly (1), with the estimated energy production in the 1990s some 500×10^6 tonnes of coal equivalent (14×10^{18}J). Kelly notes that were the difference in these two figures available for export at current world prices, it would pay for the U.K.'s total net food and materials imports. Therefore, energy conservation in industrial processes, and in the commercial and domestic sectors, would be economically very worthwhile.

Is this quite true? I am not sure!

consumption?

One strategy suggested for a more efficient usage of available energy is the possibility of making better use of, and extending the use of, materials of construction which require rather little energy to produce and to fabricate (1). These materials are the simple inorganics such as glasses and Portland cement. In terms of cost of energy per cubic metre of material produced, the United Kingdom Cement Industry consumes approximately 5% of that of the steel industry. (Glass manufacture consumes approximately 6% relative to steel.) Cost of energy in fabricating materials after their production must also be considered. These remain very high for metals (forging, rolling, welding and machining, etc.) whereas with regard to the cheap inorganics fabrication does not require large forces or even high temperatures.

It is perhaps important, therefore, in the national interest, that engineers should look even more seriously towards materials like cement for man's building requirements currently reserved explicitly for metals and alloys. However, cement-based materials, as with most ostensibly brittle materials, are severely limited in many applications by their relatively low tensile strength (~3 MPa). This compares very poorly against materials like steel (~1000 MPa) and even timber (~100 MPa). In order to understand the factors that

Contradiction to the way first sentence!

may contribute to this deficiency it is necessary to have an appreciation of the structure of cement products.

The two main cementitious compounds in cement are the two calcium silicates (tricalcium silicate, C_3S; dicalcium silicate, C_2S); the mechanical behaviour of the cement hydrate is very similar to that of these two compounds alone. The hydration products consist essentially of the cement gel (hydrates of the various compounds), calcium hydroxide (CH) crystals (produced as a by-product of the hydration reaction), unhydrated cement, free water in the capillary pores (this is unreacted water as opposed to chemically combined adsorbed water) and some other minor components. In addition to these hydration products there are many voids and inherent flaws (or discontinuities) resulting from aggregate interfacial bond cracks or shrinkage cracks. It is well established that the low tensile strength of concrete is caused by the propagation of cracks which originate from these voids and flaws. It becomes evident, therefore, that inhibiting the growth of these internal flaws will prevent, or at least retard, crack propagation and may well afford the opportunity to improve the tensile strength and ductility of the material.

1.1. PROJECT MOTIVATION

The concept of a concrete which is strengthened by the addition of a random, uniform distribution of short, discontinuous pieces of steel is not new and an early mention of both experimental work and the underlying philosophy of crack growth resistance was made as far back as 1910 by Porter (2). Nevertheless, it was not until the early 1960s that interest was regenerated when Romualdi and Batson (3) published work claiming significant improvements on the mechanical properties of plain concrete and mortar by including short, randomly-distributed steel fibres in the mix. However, more recently other works have disagreed substantially with these claims, and the state-of-the-art is

still at a stage where the mechanisms contributing to crack-growth resistance still appear to be unclear; certainly, a reliable method of proportioning ingredients to achieve a matrix of high bond characteristics is still in the development stage. Subject to the hitherto-established properties of fibre concrete, applications of steel-fibre reinforced concrete have been in the areas of refractories, pavements (including jet aircraft runways), overlays, patching, concrete armour for jetties and mine tunnel lining.

Relative to work carried out in plain cement systems, steel fibre reinforced cement composites have received little attention. It is usual practice to design concrete members for purely compressive or flexural stresses and it is under these loading conditions that previous investigations have been mainly involved.

It is surprising, also, that only a relatively limited number of investigations have been carried out with a view to determining the uniaxial tensile properties of fibre-reinforced cement products since this is where the direct consequences of fibre addition are going to be realised. Moreover, reports of steel-fibre reinforced cement-based materials have almost entirely been devoted to static loading. Thus, virtually no information is available describing the behaviour of the composite under dynamic loading, or fatigue conditions.

Fatigue, which has been defined as the weakening and subsequent failure of a material resulting from a cyclically-varying applied stress which is less than the ultimate static failure stress, has been extensively investigated in compression of plain cements. Van Orrum (4) in 1903 first investigated the compressive fatigue characteristics of concrete, introducing the S - N curve for concrete as used conventionally with metals.

It would be hoped that a better understanding of the properties and microstructure of the cement hydrate and its interaction with steel fibres would contribute to the more efficient use of the cement and fibre-reinforced composite, as well as a more reliable assessment of its potential as a

construction material.

1.2. PROJECT OBJECTIVE

The prime aim of this thesis was to examine the comparative mechanical properties of plain and steel-fibre reinforced cement-based materials, and attempt to interpret the behaviour through microstructural considerations.

Based on previous studies of steel fibre reinforced cements, an examination of the uniaxial, static compressive properties was initially undertaken. These investigations were then extended to the fatigue situation. A knowledge of the properties in compression can be justified in view of the fact that concrete is extensively designed based on its compressive properties.

However, in order to attempt to understand more fully the various factors contributing to steel-fibre reinforcement in cement-based materials, it is considered necessary to carry out tests in direct tension. Another aim was therefore to develop and utilise such a suitable method for comparative purposes under both static and fatigue conditions.

CHAPTER 2

2. FUNDAMENTALS OF FIBRE-REINFORCEMENT OF CEMENT-BASED MATERIALS

2.1. INTRODUCTION

The concept of ductile-fibre reinforcement is to utilise the deformation of a brittle matrix under stress to transfer load to the fibre thereby inhibiting crack propagation within the matrix. When the composite is stressed the axial elastic displacements in the fibre and the matrix will be different because of the difference in the elastic moduli of the two components. This means that shear strains are produced on all planes parallel to the axis of the fibres in the direction of this axis. These strains and the resulting shear stresses are the means whereby the loads supported by the fibre and matrix are distributed between the two components. The continuity of elastic displacement at the interface will, therefore, control the efficiency of load transfer; if large stresses are built up in the fibres the accompanying large shear stresses at the interface will lead to failure at the interface or in the matrix, elastic continuity being destroyed, resulting in the fibres becoming debonded. Once debonding has occurred the transfer of shear stress at the interface is no longer possible so that the load-bearing capacity of the fibres is not utilised resulting in failure of the matrix and the ultimate failure of the composite.

One of the objects of fibre-composite theory is to attempt to interpret, and thereby to be able to predict, the mechanical properties of a composite (in terms of the established behaviour of its two components); often this will require an understanding of the interaction between the two components in the region of the interface. Engineering design, on the other hand, is typically concerned only with the 'effective' properties of the composite.

This chapter deals with several theoretical approaches that have been proposed to predict the influence of uniformly-distributed, but randomly-oriented, steel fibres within a cement matrix. It also provides a background to

the fundamental concepts and parameters associated with the mechanical properties discussed in chapters to follow. Further details concerned with fibre reinforcement can be found elsewhere (5, 6, 7).

2.2. THEORETICAL CONSIDERATIONS

Romualdi and Batson (3, 8) have claimed that the tensile strength of concrete could be increased to 1000 lbs/in^2 (6,9N/mm^2) with the random addition of steel fibres. (A value of approximately 3N/mm^2 is typically quoted for tensile strength under ordinary circumstances.) The theoretical analysis upon which these claims were made was based on linear elastic fracture mechanics (LEFM). These authors predicted the first crack tensile strength to be inversely proportional to the geometrical spacing of the fibres (fig. 2.1.) for a given volume of fibres, i.e. Griffith's formula (9) could be rewritten in the form:

$$\sigma^2 = G_c.E./(1-\mu^2).\pi.a \qquad \text{2.1}$$

where, σ = average tensile failure stress,
G_c = critical elastic energy release rate,
E = Young's modulus,
μ = Poisson's ratio,
a = half the length of the critical flaw.

The theory (3, 8) was based on the assumptions that:

(i) cement-based materials are notch-sensitive, i.e. a fracture mechanics approach is applicable; and

(ii) reducing the fibre spacing, given by:

$$s = 13,8.d.\sqrt{\frac{1}{V_f}} \qquad \text{2.2}$$

where, s = average fibre spacing (inches)
V_f = percentage fibre volume content
d = fibre diameter (inches)

results in a reduction of the length of the

critical flaw giving rise to an increased cracking stress.

The analysis was reportedly verified by Romualdi and Mandel (10). It is important to note that this proposed analysis (3, 8) is based entirely on energy considerations and that, although the LEFM concepts used are based on direct tensile stresses, experimental verification was carried out in flexure (10).

Linear elastic fracture mechanics has been applied to cement-based materials with varying degrees of success (11-17), based on the assumption that these materials are notch-sensitive. Kesler et al. (18) report that the concepts of LEFM are not directly applicable to cement-based materials since they found the critical stress intensity factor to vary with varying specimen geometry. (LEFM implies that the mechanism by which a crack propagates is independent of specimen geometry.) Similarly, Higgins and Bailey (17) found that the zone of stress disturbance due to the inhomogeneity of the material or non-linear elastic behaviour was large compared with their specimen dimensions, concluding that the size of specimen convenient for laboratory use was too small for LEFM to apply. A similar observation is made by Gjorv et al. (19). Kanninen and co-workers (20) observe that fracture mechanics applications to fibre-reinforced composites have so far not been as effective as has the analysis of many other commonly-used structural materials and that LEFM is " ... not capable of coping with the complexity of the crack extension process as seen from the micromechanical point of view".

It is hardly surprising, therefore, that direct tensile experimental results were found to be inconsistent with Romualdi's theory, as shown in fig. 2.2. (21, 22, 23).

Shah and Rangan (21), for example, suggested that the reinforcing action of the fibres was in fact similar to that of conventional reinforcement and could be predicted by the properties of the individual components. Although no such analysis was carried out they used a two-phase composite materials approach to predict the <u>compressive</u> stress-strain

behaviour which they found to be consistent with experimental results. The stress for the fibre reinforced composite for a strain of ε_c was calculated to be:

$$\sigma_{RC} = E_{RC}.\varepsilon_c \qquad \text{2.3}$$

where, σ_{RC} = composite stress,
E_{RC} = elastic modulus of fibre composite ( ),
ε_c = strain in the unreinforced material (equal to strain in the reinforced composite) at reinforced composite stress, σ_{RC} (i.e. $\varepsilon_c = \varepsilon_{RC}$). Although this alternative composite materials approach, based on the law of mixtures, may be applied to predict the compressive stress-strain behaviour of the composite, the theory has not yet been satisfactorily correlated with experimental data (24). Furthermore, the law of mixtures approach is only strictly applicable to direct tensile stresses.

It is of interest to note that nearly a decade after Romualdi and Batson proposed their spacing theory Aveston and co-workers (6, 25) proposed a similar theory based on force and energy balance criteria, i.e. utilising fracture mechanics concepts again, from which they were able to predict the tensile stress-strain behaviour of the composite. They proposed that under stress the composite initially deforms in a linear elastic manner until reaching the limit of proportionality (assumed to be the failure strain of the matrix, ε_{mu}) at which point the fibres will support the entire load provided the breaking stress of the fibres, σ_{fu}, satisfies the inequality:

$$\sigma_{fu}.V_f \geq \sigma_{mu}.V_m + \sigma'.V_f \qquad \text{2.4}$$

where, σ_{mu} = breaking stress of matrix,
σ' = load transfer from matrix to fibre (equal to $E_f.\varepsilon_{mu}$ for the elastic region),
V_m, V_f = volume fraction of matrix and fibre, respectively.

Progressive multiple cracking of the matrix will then occur (fig. 2.3.(a)). V_f in the equation above is defined as the critical fibre volume (for $V_f < V_{crit.}$ the composite will

fail by so-called 'single' fracture, i.e. when one component fails the other cannot sustain the load). The initial slope of Aveston et al.'s predicted curve (fig. 2.3.(b) - region 1) is similar to that predicted by the simple law of mixtures (5) which is strictly valid for continuous fibres and assumes no slippage between fibres and matrix, i.e.

$$E_c = E_m.V_m + E_f.V_f \qquad \text{2.5}$$

where E_c, E_m and E_f are the respective elastic moduli of the composite, matrix and fibres. According to Aveston and his co-workers, during multiple cracking (fig. 2.3.(b) - region 2) the cement matrix is broken into a series of blocks of dimensions between x' and $2x'$, i.e. there is a limiting crack separation. By a simple force balance they derived x' as follows:

$$2.N.\pi.r.\tau.x' = \sigma_{mu}.V_m \qquad \text{2.6.a}$$

where N is the number of fibres per unit area and equal to $V_f/\pi r^2$; x' is determined by the rate of stress transfer between fibre and matrix which in turn is determined by the maximum stress τ which the interface (or the matrix) can sustain; r is the fibre radius; and, τ is the interfacial shear stress. Further, therefore:

$$x' = (V_m / V_f).(\sigma_{mu} r / 2.\tau) \qquad \text{2.6.b}$$

Once multiple cracking is complete it is assumed that load is supported by the fibres which stretch and slide until the composite fails (slope of the curve now given by $E_f.V_f$ with failure stress of $\sigma_{fu}.V_f$ - region 3 shown in fig. 2.3.(b)).

The theory proposed by Aveston et al. (6, 25) predicts the cracking stress of fibre cement to be inversely proportional to the square root of the fibre spacing; also, the predicted increases in cracking strain of the composite compared to the unreinforced cement are rather larger than those achieved in practice (26). However, the concept of multiple fracture is of great significance in fibre cement composites as it enables the material to behave in a "pseudo-ductile" manner.

In view of the apparently strong dependence of crack growth on fibre spacing and the practical difficulties

involved in casting, it has been suggested that theoretical considerations thus far discussed have only limited scope for large-scale application; they fail to take into account bond deficiency of discontinuous fibres and their orientation within the cement matrix (27, 28). Kar and Pal (27) have formulated an effective wire spacing equation taking into consideration these two factors. They assume that: (1) all wires are straight; (2) geometric centres of the fibres are uniformly distributed in space; and (3) a fibre has an equal probability of being oriented at any angle with the direction of stress. The theoretical distribution of bond stress along a continuous length of fibre due to the presence of a crack and its idealised situation is shown in figs. 2.4. (a,b). Kar and Pal calculated the bond efficiency as:

$$\frac{\int_0^l \frac{2y}{kd}\left(1 - \frac{y}{2kd}\right)dy}{\int_0^l dy} = \frac{l}{kd}\left(1 - \frac{l}{3kd}\right) \qquad \text{2.7}$$

where, l = half fibre length,
d = fibre diameter, and
k = bond length coefficient (fig. 2.4.),
given that there is an equal probability of the crack being formed anywhere within the length of the wire.

Their effective spacing equation they presented as:

$$s_e = 8.85\, d \sqrt{\frac{1}{p\eta l.(1 - l/3kd)/.kd}} \qquad \text{2.8}$$

where, s_e = effective spacing,
η = orientation factor (27),
p = volume fraction of fibres.

Kar and Pal find a good correlation between the fibre spacing equation above and the tensile strength ratio (expressed with respect to the tensile strength of plain concrete at the same w/c ratio) of concrete. However, their shear-stress distribution at the fibre-matrix interface is only due to the presence of a crack in the immediate vicinity

of the fibre with no consideration given to fibres that are not affected by the crack. Thus they assume that before a fibre contributes to the composite properties it must be subjected to matrix cracking. Previous theories have also assumed zero interfacial shear stresses until the initiation of a crack at the fibre interface (3, 6, 8).

Based on a combined crack-control/composite mechanics approach, Swamy et al. (28, 29) have, with reasonable success (30 - 33), predicted the first crack and ultimate flexural strength of randomly oriented steel fibrous concrete beams. They suggested that three basic considerations must be taken into account in deriving an effective spacing equation: (1) the critical fibre length; (2) the interfacial bond; and (3) fibre orientation.

The critical fibre length (i.e. length at which the fibre should theoretically yield at the point of composite failure) they obtained by considering a fibre of length l and diameter d embedded in the cement matrix, with load transferred by an average interfacial shear stress, τ ; the longitudinal tensile stress in the fibre σ_f , they assumed varies from zero at the ends of the fibre to the fracture stress σ_{fu} , if the fibre is long enough (fig. 2.5.) - $l_c/2$ is defined as the transfer length where l_c is the critical fibre length. From equilibrium considerations:

$$\frac{\pi d^2}{4} \cdot \frac{d\sigma}{dl} = \pi d.\tau$$

or

$$\frac{dl}{d\sigma} = \frac{d}{4\tau}$$

The fracture stress can be reached only when:

$$\frac{l_c}{2} = \sigma_{fu} \frac{d}{4\tau}$$

or

$$l_c = \sigma_{fu} \frac{d}{2\tau}, \qquad \text{2.9}$$

The aspect ratio of the fibre must then be: $\frac{l_c}{d} \geq \frac{\sigma_{fu}}{2\tau}$ 2.10

Swamy and his co-workers assumed the fibre tensile stress to have linear distribution (fig. 2.5.) - fibre tensile stress is also not constant along the fibre length (fig. 2.6.) - and used an average stress of σ_{fu}. These authors, therefore, show that the interfacial bond stress and the fibre tensile stress are closely related to the fibre aspect ratio. They also considered the interfacial bond stress to be of two parts: firstly, the stress due to load transfer from matrix to fibre, fig. 2.6.(other spacing equations (3, 6, 27) have overlooked the shear stress distribution at the fibre-matrix interface in the absence of a crack); and secondly, stress due to the presence of a crack (fig. 2.7.).

Although various orientation factors have been derived based upon various assumptions (see reference 34), Swamy et al. (29) considered the orientation factor obtained by Romualdi and Mandel (10) to be exact, such a factor being necessary since some fibres are less effectively oriented than others and contribute to a lesser degree to the crack arrest mechanism (Romualdi's earlier geometrical fibre spacing concept (3, 8) did not fully recognise the influence of the geometry of the fibre). The orientation factor was given as (10):

$$V_{fc} = 0{,}41.V_f \qquad \text{2.11.a.}$$

or

$$l_{fc} = 0{,}41.l_f \qquad \text{2.11.b.}$$

where V_{fc} is the effective volume for a nominal fibre volume V_f and l_{fc} the effective fibre length from a nominal fibre length l_f.

From the factors discussed above, a more general spacing equation, taking into account fibre aspect ratio, was obtained (28,29):

$$s_e = 15{,}287 . \sqrt{\frac{\sigma_{fu}.\bar{d}^2}{\tau} . \frac{d}{V_f.l}} \qquad \text{2.12}$$

By evaluating σ_{fu} and $\bar{d}$, Swamy, Mangat and Rao (28) were able to obtain the effective spacing for the first crack stress and ultimate modulus of rupture. The predicted

flexural strength of steel-fibre reinforced concrete beams was:

$$\sigma_c = \sigma_{mu} V_m + 0.82 \tau (l/d) V_f \qquad 2.13$$

which they derived from the law of mixtures (5):

$$\sigma_c = \sigma_{mu} . V_m + \sigma_{fu} . V_f \qquad 2.14$$

Although verified experimentally (31, 32) a number of objections have been raised (35). For example, it has been questioned whether the assumption of a linear stress bond is strictly valid since it has been reported that the stress distribution can be shown to be non-linear (35). Also the derivation of the critical length parameter, based on equilibrium considerations and the orientation factor are only strictly applicable to direct tensile stresses, as is the simple law of mixtures approach. The analysis discussed above, however, has been used for flexural stress prediction.

2.3. SUMMARY

Two basic approaches have been utilised to predict the 'first crack strength' or the proportional limit of fibre-reinforced cement-based materials.

One mechanism is based on the crack arrest action by the fibres and energy considerations, i.e. utilising linear elastic fracture mechanics concepts, and relates the cracking stress to the spacing, s_e, of the fibre reinforcement.

The other mechanism is based on the laws of mixtures of composite materials which relates the proportional limit to the volume, V_f , orientation, η , and aspect ratio, l/d , of the fibres.

The composite materials approach would appear to be the more satisfactory of the two approaches since the former approach does not apply beyond the proportional limit and does not fully explain the mechanism of fibre reinforcement. Although yet to be satisfactorily correlated with experimental data, it is generally agreed that the ultimate strength of the fibre composite is relatively insensitive to fibre spacing

and depends primarily on volume, aspect ratio and the bond characteristics of the fibres (24, 34).

These theoretical approaches have been used to ascertain how well they predict the properties of the fibre reinforced composite studied in this investigation by comparing with the experimental data obtained in Chapters 4 and 5 - see table 2.1.

cryptic

EQUATION	PREDICTED	EXPERIMENTAL
(2.2): $S = 13.8d \frac{1}{V_f}$	S = 4,9mm	
(2.1): $\sigma_c^2 = G_c E \vert (1-\mu^2)\pi a$	σ_c = 18,9 MPa	5,64 MPa
(2.4): $\sigma_{fu} V_f > \sigma_{mu} V_m + \sigma' V_f$ for fibre load-bearing	21 MPa > 3,82	confirmed
(2.5): $E_c = E_m V_m + E_f V_f$	$E_{Rc} = 30,95.10^3$ MPa	29,7 MPa
(2.3): $\sigma_c = E_{Rc} \varepsilon_c$	σ_c = 3,40 MPa (tension) σ_c = 69,9 MPa (compression)	5,64 MPa 32,24 MPa
(2.9): $l_c = \frac{\sigma_{fu} d}{2\tau}$ $l > l_c$ for fibre fracture	l_c = 157mm	l = 38mm ie. fibre pull-out
(2.13): $\sigma_c = \sigma_{mu} V_m + 0,82\tau \frac{l}{d} V_f$	σ_c = 5,46 MPa	5,64 MPa
(2.14): $\sigma_c = \sigma_{mu} V_m + \sigma_{fu} V_f$	σ_c = 24,38 MPa	5,64 MPa

values assumed:

G_c = 0,01 MPa	ε_{mu} = 110με
μ = 0,13	τ = 1,67 MPa
$E_m = 27,5.10^3$ MPa	σ_{mu} = 3,45 MPa
$E_f = 200.10^3$ MPa	σ_{fu} = 1050 MPa

TABLE 2.1

Comparison Between Theoretical Predicted Values and Experimental Data.

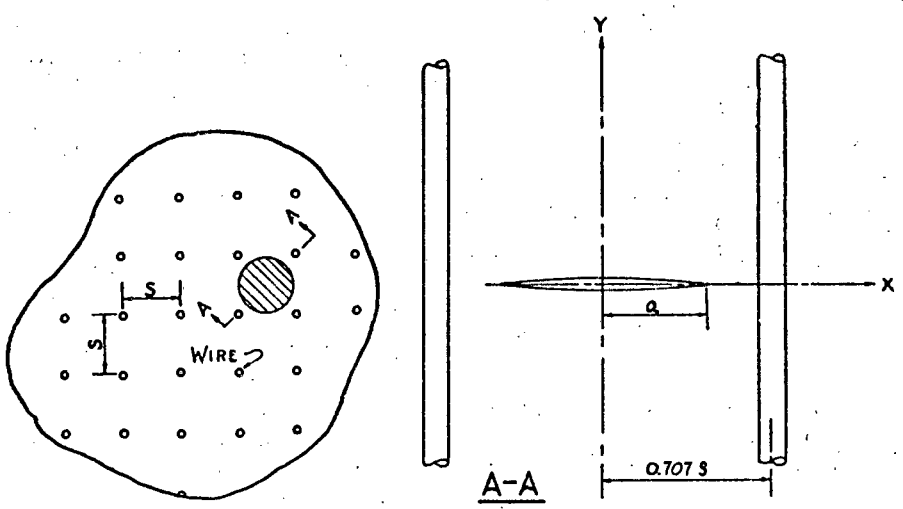

Fig. 2.1: Geometrical Spacing concept proposed by Romualdi and Batson (3).

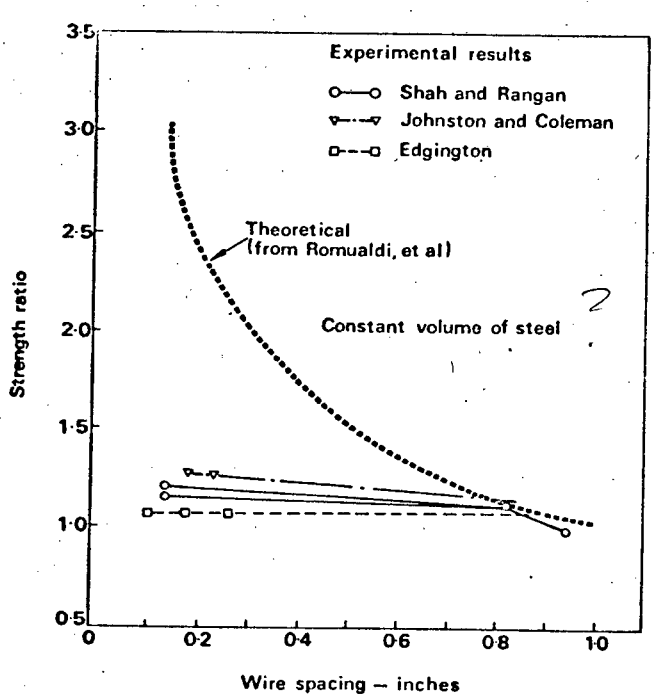

surely not if spacing changing

Fig. 2.2: Effect of Fibre Spacing on first tensile cracking strength of concrete (43).

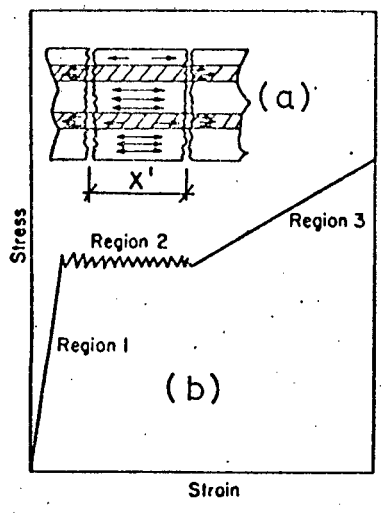

Fig. 2.3: Idealised tensile stress-strain curve (6).

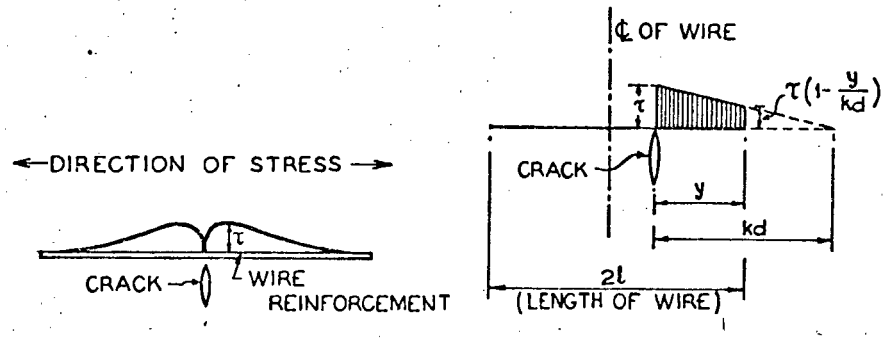

Fig. 2.4: Bond Stress Distribution, (a) Theoretical versus distance from crack, (b) Idealised along length of fibre (27).

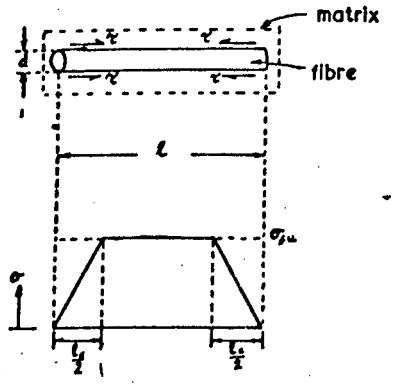

l_c - critical fibre length

$\frac{l_t}{2}$ - transfer length

Fig. 2.5: Fibre Stress Distribution (28).

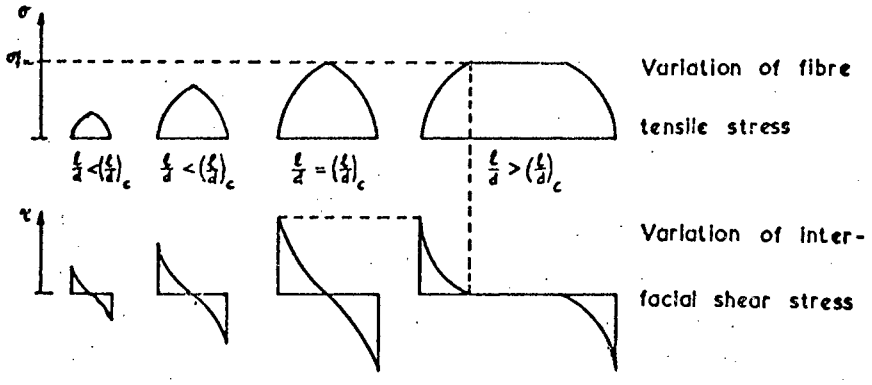

Fig. 2.6: Variation of Interfacial shear stress and fibre tensile stress (28).

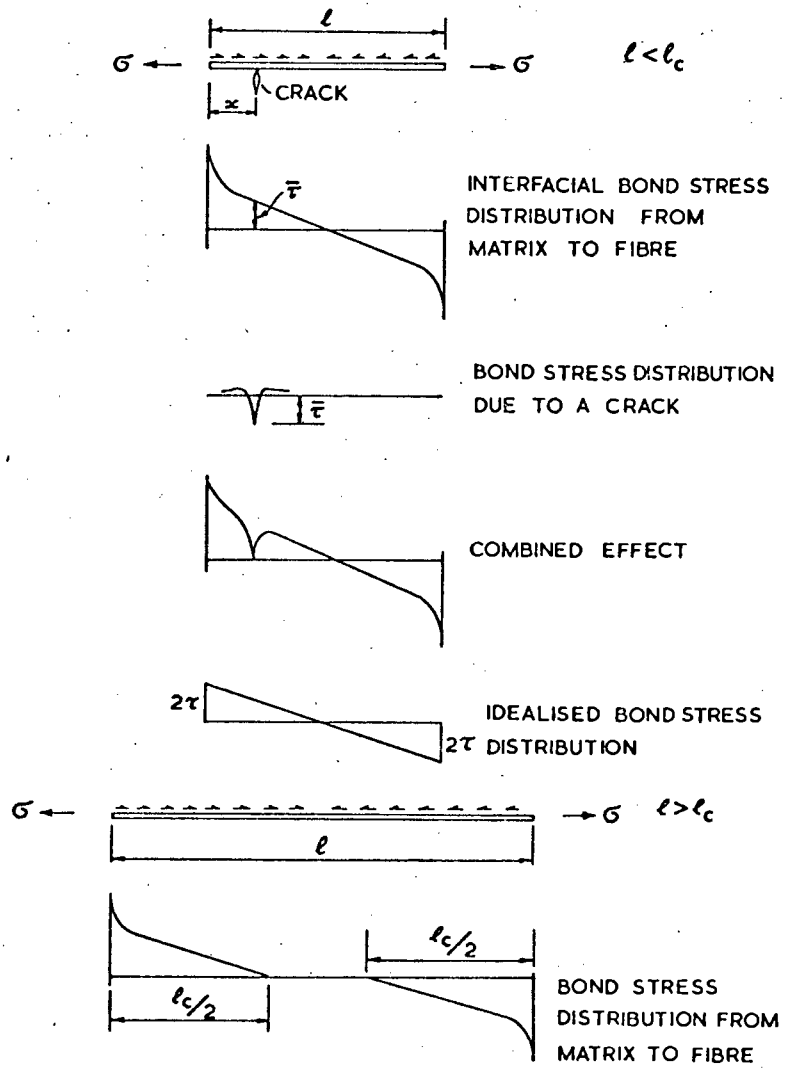

Fig. 2.7: Bond Stress Distribution at Fibre Matrix interface (28).

CHAPTER 3

3. GENERAL EXPERIMENTAL DETAILS

3.1. MATERIALS

3.1.1. Cement

Rapid Hardening Portland Cement (RHPC) supplied by the National Portland Cement Company Limited, Philippi, Cape, was used throughout in this thesis.

In order to minimise experimental scatter due to variations in cement composition, 60 bags of cement were purchased directly from the cement factory as a single batch obtained consecutively from the same production run and numbered 1 to 60. In the laboratory the bags were divided into 15 sets of 4, e.g. the first set consisted of bags numbered 1, 16, 31 and 46; the last consisted of bags numbered 15, 30, 45 and 60. The cement bags were sealed in polythene bags until such time they were required for mixing; four bags from a set were at that time thoroughly blended and stored in an airtight steel container for use. When this cement had been completely used the next set of cement bags were removed from their polythene bags and blended and stored prior to use.

The chemical analysis and physical properties of the cement are given in tables 3.1 and 3.2, respectively.

3.1.2. Aggregate

The aggregate used was a fine, natural siliceous sand (Cape Flats sand). The sand was first thoroughly dried in the laboratory over a period of several days and then stored in airtight containers in order to maintain a negligibly-small moisture content prior to mixing.

Results of the grading analysis of the sand are given in fig. 3.1.

Not good enough! What was the moisture content?

3.1.3. Steel Fibres

From previous investigations (36 - 38) it has been reported that Duoform fibres have shown superior mechanical properties compared to plain round fibres as a reinforcing medium for cement-based materials. Fig. 3.2 shows the physical difference between these two types of fibre.

In order to limit the variables under study it was decided to confine the experimental investigation to one fibre type, of fixed dimensions. (Duoform, 0,5 mm diameter, 38 mm long, having an aspect ratio of 76.) The mechanical properties of these fibres in comparison to a number of others used in cement matrices are given in table 3.3; for comparison, also given are the corresponding cement matrix properties.

3.2. SPECIMEN FABRICATION

3.2.1. Specimen Geometry

(i) In order to reduce end restraints, due to the relative difference in Poisson's ratio between the compression test platens and compression test specimens (39-41), compression specimens were cast vertically as 60x60x180 mm prisms in accurately machined steel moulds (fig. 3.3(a)). Each cast consisted of at least 6 prisms - as work progressed a further 2 moulds were made enabling 8 prisms to be cast in one batch.

(ii) Tensile specimens were horizontally cast 76x76x325 mm prisms with a 'waisted' mid-section reduced to 38 mm; steel moulds were also accurately machined (fig. 3.3(b)).

3.2.2. Specimen Manufacture

3.2.2.(a) Mix Proportions:

In order to examine in detail the influence of steel fibres on the tensile and compressive, static and fatigue behaviour, a single mix design was chosen for investigation.

The mix proportions used and their derivation are given in table 3.4 (by weight to an accuracy of ± 0,1 kg). The particular mix composition was chosen on the basis of previous similar studies (21, 23, 24, 34, 42).

It has been noted elsewhere (34) that steel fibre contents in excess of 2% by volume are generally difficult to incorporate into a cement mix (depending on mix design and aspect ratio of the fibre). Problems can arise due to non-uniform segregation and balling of the fibres during mixing (24, 43). Therefore, in selecting a single volume fraction for study (again limiting the number of variables for examination), 2% was chosen. In mixing, this was proportioned to an equivalent weight (table 3.4) to an accuracy of ± 0,001 kg. The fibres were added in the 'as-received' condition ('degreasing' the fibres has been found to have only marginal effects on the mechanical properties of the fibrous composite - see Chapter 6).

3.2.2.(b) Mixing Method

Experience gained from previous work reported in the literature (44) has shown that different mixing procedures may induce significant changes to the mechanical properties of the cement mix. Mixing methods, therefore, were standardised throughout. All mixing was done in a 0,06 m^3 rotating pan-and-paddle type mixer.

The mixing procedure adopted for plain samples was as follows:

(i) The aggregate and cement, in proportioned quantities, were dry mixed for 60 secs.

(ii) All the water to be mixed was added; the cement slurry was then mixed for a further 240 secs.

(iii) The mortar mix was then ready for casting.

Problems experienced during mixing steel fibre in cement/mortar, as mentioned previously, were overcome to a satisfactory degree by adopting the following mixing procedure:

(i) The sand aggregate and cement, in proportioned

quantities, were dry mixed for 60 secs.

(ii) All the water to be mixed was then added and mixed for a further 60 secs.

(iii) While the mixing drum was still rotating, the steel fibres were added. At this point it was most important to eliminate any tangled lumps of fibres before adding the fibres to avoid mixing conditions that would promote the formation of fibre agglomerates. Various mechanical methods have been suggested for adding fibres during this stage (23, 30, 34); in this investigation the fibres were added by hand.

(iv) After the last fibre had been added the composite was mixed for a further 120 secs.

3.2.2.(c) Casting Technique

Methods of casting and compaction can also strongly influence mechanical properties (24). Since this thesis was basically of a comparative nature, a standardised technique was adopted, as follows:

(i) Both plain and fibrous compression samples were cast in three approximately equal lifts (layers), each layer compacted into the mould with a compacting rod. After the last layer had been placed, the moulds were externally vibrated for 20 secs., after which the free surface was trowelled smooth. X-ray radiography confirmed that this procedure resulted in a uniform random distribution of steel fibres (fig. 3.4(a)). It should be noted that vibration times longer than 20 secs., in order to achieve greater compaction, tended to result in fibre segregation (fig. 3.4(b)).

(ii) Tension samples were also placed in three approximately equal lifts. However, after each lift the mould was externally vibrated for 5 secs. After the last layer had been vibrated, the specimen surface was trowelled smooth and the specimen vibrated for a further 10 secs. Resulting failure surfaces of test specimens confirmed that this procedure resulted in a uniform fibre distribution (fig. 3.4(c)).

3.2.3. Curing Conditions

Variations in curing methods have been shown to have significant effects upon the strength of concrete (45), necessitating a completely standardised curing procedure.

Approximately 4 hours after casting a damp hessian cloth, covered by a polythene sheet, was placed over the moulds to restrict the evaporation of 'free' water from the specimen surface. Specimens were removed from their moulds 24 hours after casting and submerged in a saturated lime water solution curing bath which was kept at a constant temperature of 20 ± 2°C. The lime solution limited the leaching of calcium hydroxide from the cement hydrate.

Compression test specimens were removed from the curing bath and tested at 7 days age (equivalent to 28 day strength of Ordinary Portland Cement, OPC). Due to the longer preparation time (to be described in the following sections), tensile samples were removed from the curing bath at 9 days age and tested at 10 days age because of the small associated strength variations in comparison to 7 day OPC (44).

3.2.4. Preparation for Testing

(i) At 6 days age compression samples were capped using a quick-set putty (Pratley Quick-set Epoxy) to ensure that the compressive load transmitted to the test specimen was purely uniaxial and evenly distributed (B.S. 1881: 1970 (46) recommends plane-end surfaces to within 0,05 mm). Indeed, Gonnerman (47), for example, has reported 30% strength losses for 0,25 mm difference in 'planeness' between ends. Capping was done between the test platens, the orientation of the specimen in the machine being noted at the time of capping so that the specimen could be replaced between the platens in precisely the same orientation when tested; any stress distribution variations due to the platens being slightly out of parallel was thus entirely avoided. After capping, the specimens were replaced in the curing bath until tested.

(ii) Tensile test specimens, as mentioned previously, required a somewhat longer preparation time.

The pronounced effect of casting direction upon the direct tensile strength due to 'bleeding' has been noted by Hannant (48). This is the migration of water to the surface of freshly-placed cement resulting in a porous, and therefore, weaker upper layer in each specimen. Since tensile specimens were all cast horizontally in this investigation, the surface layer is considerably weaker than the bottom layers, resulting in differential deformation under load which is applied parallel to the planes of variation. (In compression this effect is not so apparent because the applied load is normal to the planes of variation.) To minimise this effect, ~ 15 mm was cut off the top of all tension specimens at 7 days age. All cutting was carried out under water using a silicon carbide cutting disc at 2890 r.p.m., after which the specimens were then replaced in the curing bath.

At 9 days age, tension specimens were removed from the curing bath. After 30 mins., when the specimens were relatively free of excess surface water, side plates were glued onto the specimens to be tested in fatigue with an epoxy resin (discussed in more detail in section 3.3.1). This process took approximately 60 mins. A number of studies (45, 49 - 51) have shown that the moisture content of the test specimen can affect the static and fatigue properties. However, Neville (44) states that if the drying period, in air, is less than 6 hours, variation in specimen properties is generally less than 5%. Therefore, to avoid any excess moisture loss whilst the epoxy resin set (~12 hours) the 6 specimens were sealed separately in plastic bags. At 10 days age the tension samples were removed from the plastic bags and prepared for testing.

All test specimens (compression and tension) were tested at 1 hour, and not later than 3 hours, after removing from the water bath (compression) or sealed bags (tension). Specimens, therefore, may be regarded as having approximately 100% moisture contents at the time of testing.

Prior to testing, strain transducer blocks were glued onto the specimens using a Pratley Quick-set epoxy glue. Ultrasonic transducers (see section 3.3.2) were also attached to the specimens. Figs. 3.5(a-c) show both compression and tension samples ready for testing.

3.3 EXPERIMENTAL PROCEDURE

3.3.1. Testing Mode and Grip Design

The method of testing in compression is relatively straightforward. The problems of testing cement-based materials in tension, however, are considerably more involved. Certainly from the literature available it would appear that there is no direct tensile fatigue testing method for cement-based materials, although various methods have been suggested for static tests. These are summarised by a RILEM enquiry (52).

One of the requirements of this thesis work, therefore, was to develop a dual purpose system suited for both fatigue and static loading. The method finally chosen, after considerable experimentation, involved the transfer of the static or cyclic tensile load by shear to the test piece through side plates glued onto the sides of the tension test specimen. The side plates were manufactured from mild-steel angle section (75x75x8 mm) with the internal surfaces being accurately machined to right-angles between one another. An Epophen Epoxide resin (Genkem - RSA - Pack 'D') was used for attaching the side plates. Hose clips kept the plates in position while the epoxy set ($\sim$12 hours) - see fig. 3.5(b). The side plates were re-usable after removing from the tested specimen and cleaning.

This method was restricted to fatigue tests; for static testing a more convenient method based on transferring load by friction (c.f. references 23, 53) was used. The frictional force was applied by a further two plates (fig. 3.5(a)), each bolt having a torque moment of 20 N.M (this corresponds to a negligible stress of $\sim$ 5% of the maximum compressive stress upon the specimen).

The tensile, pulley-housing grip attachments required for loading the specimen in the machine are shown in fig. 3.6. The high tensile chains (2000 kg breaking force) are able to rotate around the freely revolving pulley which is centrally fitted within the pulley-housing, thus ensuring no eccentric loading of the test piece. The load transmitted to the side plates, therefore, was equal on each side of the test specimen, so avoiding induced bending stresses. The 'D-shape' shackles are made from stainless steel (2000 kg maximum bending load) with a 8 mm diameter pin.

To ensure no torsional stresses were exerted upon the tensile test specimen, the crosshead was lowered until the two grip attachments were a few millimetres apart. Using a straight edge they were aligned and locked into position (with the spiral wedges). The crosshead was then raised to working height and tightened ready for testing.

3.3.2 Mechanical Testing

All tests were performed using an E.S.H. 'Universal' Testing machine with a maximum load capacity of 250kN. This is a servo-controlled, electro-hydraulic, closed-loop testing machine being able to apply a controlled stroke (deflection), strain or load to the test piece.

Static, uniaxial loads may be applied at varying ramp rates in either of the above three control modes, as may fluctuating loads with varying waveforms; a built-in cycle counter monitors the number of cycles during a fatigue test. Fig. 3.7 shows the machine and associated instrumentation operating in compression.

LVDT = Linear variable differential transformer.

Strains on each specimen were measured using linear voltage displacement transducers (LVDT) attached by holder blocks glued on to the specimen. During fatigue tests (10Hz) these were monitored using a SE Labs. model 3006 ultraviolet recorder, with a B420 galvanometer (response 420Hz). In compression, both longitudinal and lateral strains were measured (gauge length 98 mm and 49 mm respectively); in tension only longitudinal strains were

measured, over a fixed gauge length of 115 mm.

The accumulation of damage was also monitored using the ultrasonic pulse transit time (UPTT) method (54 - 57), i.e. by measuring the time taken for a 50 kH sound pulse to travel through the specimen under test. A Harwell system 3127-1, the operating principle of which is schematically illustrated in fig. 3.8, was used with 50 kHz piezo - electric crystal transducers, the transmitting transducer being excited at a pulse rate of 10 Hz. The output signal, as a signal acquired by an integrating capacitor, was calibrated against time and recorded on a Bryans X-Y-Y-T 26000 A3 chart recorder.

The ultrasonic transducers were attached to the specimens (laterally in compression; longitudinally in tension, as suggested by Jones (57)), with a thin film of high viscosity grease (Shell Barbatia) between transducer and specimen to ensure minimum loss of energy at the interface and a steady pulse during the tests. In attaching the transducers, as shown in figs. 3.5(a-c), it was found that the most efficient coupling was obtained if no pressure was applied prior to securing the rubber bands, i.e. purely the pressure of the rubber bands was able to maintain the transducers in position with an efficient coupling between transducer and specimen. Attempting to secure the transducers too tightly resulted in an inadequate coupling system.

3.3.3. Static Tests

The maximum failure stress in compression is dependent upon the rate of application of static load (44,58,59)and, therefore, in order for test results to be comparable, the rate of application of load has been standardised (46).

On the other hand, due to relatively limited work in direct tension, no standardised test (and therefore loading rate) has yet been proposed for uniaxial tensile strength determination. A similar rate of load application to that of the compression static tests was therefore used.

Consequently, all static tests were carried out in

the stroke control mode at a ramp rate of 0,02 mm/sec (stroke range : ± 10 mm) which is in accordance with BS 1881 : 1970(46). The maximum load at failure was recorded directly from the E.S.H. testing machine (load range - compression : ± 250 kN; tension : ± 50 kN) as were strain values from the LVDTs (strain range - compression, longitudinal : ± 2 mm; lateral : ± 0,5; and tension, longitudinal : ± 1 mm).

Three specimens were tested statically to determine the mean strength of the particular batch, the remaining samples tested in fatigue.

3.3.4. Fatigue Tests

There are a number of factors, which are independent of static strength, that can significantly affect the fatigue behaviour of mortar or concrete when subjected to repeated loading. Before embarking upon such an investigation an appreciation of these factors was necessary in order to decide upon the test procedure. Briefly, these are listed as follows:

(i) Range of loading, i.e. difference between minimum stress level and maximum stress level, when altered can affect fatigue life (60 - 62).

(ii) Rest periods during the application of the cyclic stress can increase the fatigue resistance of concrete (62).

(iii) Rate of loading, i.e. test frequency, may have significant effects upon fatigue strength (63, 64).

(iv) Specimens with varying moisture contents at the beginning of a test may have varying fatigue lives (50, 51).

In order to be able to neglect the influence of any of these factors specimens were continuously, sinusoidally cycled until failure, or 1 million cycles, whichever occurred first, at a constant frequency of 10 Hz between some predetermined maximum stress level (some percentage of the ultimate mean strength) and a fixed minimum stress level (~5% of the ultimate mean strength). It has already been mentioned that specimens could reliably be considered as 100% saturated at the time of testing.

Ignition loss	1,7%
Ca O	64,1%
$Si\ O_2$	21,7%
Al_2O_3	6,1%
Fe_2O_3	2,4%
SO_3	2,3%
Mg O	1,3%
Others	0,4%
Total	100,0%

Free CaO	2,2%
Insoluble Residue	1,8%

Cement Consistency Compound Composition (Bare Composition)?	
C_3S	49,7%
C_2S	19,6%
C_3A	12,1%
C_4AF	7,3%
Total	88,7%

TABLE 3.1.

Chemical Analysis of RHPC

Specific surface?

Surface Fineness:

Blaine	5018 cm^2/gr

Soundness:

Le Chatelier Expansion,	
unboiled	2 mm
boiled	1 mm

Setting Time:

Initial	100 min
Final (28% water used)	2 hrs. 45 min

Compressive Strength: (SABS 743)

3 days cured	41,5 MPa
7 days cured	52,0 MPa

TABLE 3.2.

Physical Properties of RHPC

FIBRE	Young's Modulus MPa x 10^4	Tensile Strength MPa	Density x10^3 kg/m	Elongation at fracture (%)
Chrysotile Asbestos	8 - 16	550-4500	2,55-3,12	0,6 - 3
Glass	6,9-7,2	1000-4000	2,6	1,5 - 3.5
Polypropylene	0,35-0,5	500-750	0,9	20 - 25
Duoform (low carbon steel)	20	1000-3000	7,8	0,5 - 4
Stainless Steel	15 - 21	2048-2552	7,7-8,0	35 - 55
Cement paste Mortar Concrete	1,5 - 4,5	2,8-7,0	2-2,3	,04 - 0,06

TABLE 3.3.

Properties of Fibres and Cement Matrix (24, 26, 34)

Components	Ratio	Mix Proportions by Weight (kg)+	
		Compression	Tension
Cement	1.0	5,00	8,00
Sand	2.0	10,00	16,00
Water	0.5	2,50	4,00
Fibres	2% (by vol)	1,229	1,966

TABLE 3.4(a)

Mix Proportions

+ See table 3.4(b).

This is for 8 moulds

COMPRESSION

Volume of Moulds		=	$5{,}184.\ 10^{-3}\ m^3$
cement : 5,0 kg	: 3120 kg/m^3	=	$1{,}603.\ 10^{-3}\ m^3$
sand : 10,0 kg	: 2650 "	=	$3{,}774.\ 10^{-3}\ m^3$
water : 2,5 kg	: 1000 "	=	$2{,}500.\ 10^{-3}\ m^3$
			$7{,}88.\ 10^{-3}\ m^3$
2% (by vol). $7{,}88.\ 10^{-3}\ m^3$		=	$1{,}575.\ 10^{-4}\ m^3$
fibres (by weight)		=	1,229 kg

For 6 moulds - waist ?

TENSION

Volume of Moulds		=	$11{,}09.\ 10^{-3}\ m^3$
cement : 8,0 kg	: 3120 kg/m^3	=	$2{,}56.\ 10^{-3}\ m^3$
sand : 16,0 kg	: 2650 "	=	$6{,}04.\ 10^{-3}\ m^3$
water : 4,0 kg	: 1000 "	=	$4{,}00.\ 10^{-3}\ m^3$
			$12{,}60.\ 10^{-3}\ m^3$
2% (by vol). $12{,}60.\ 10^{-3}$		=	$2{,}520.\ 10^{-4}$
fibre (by weight)		=	1,966 kg

TABLE 3.4(b)

Derivation of Mix Proportions

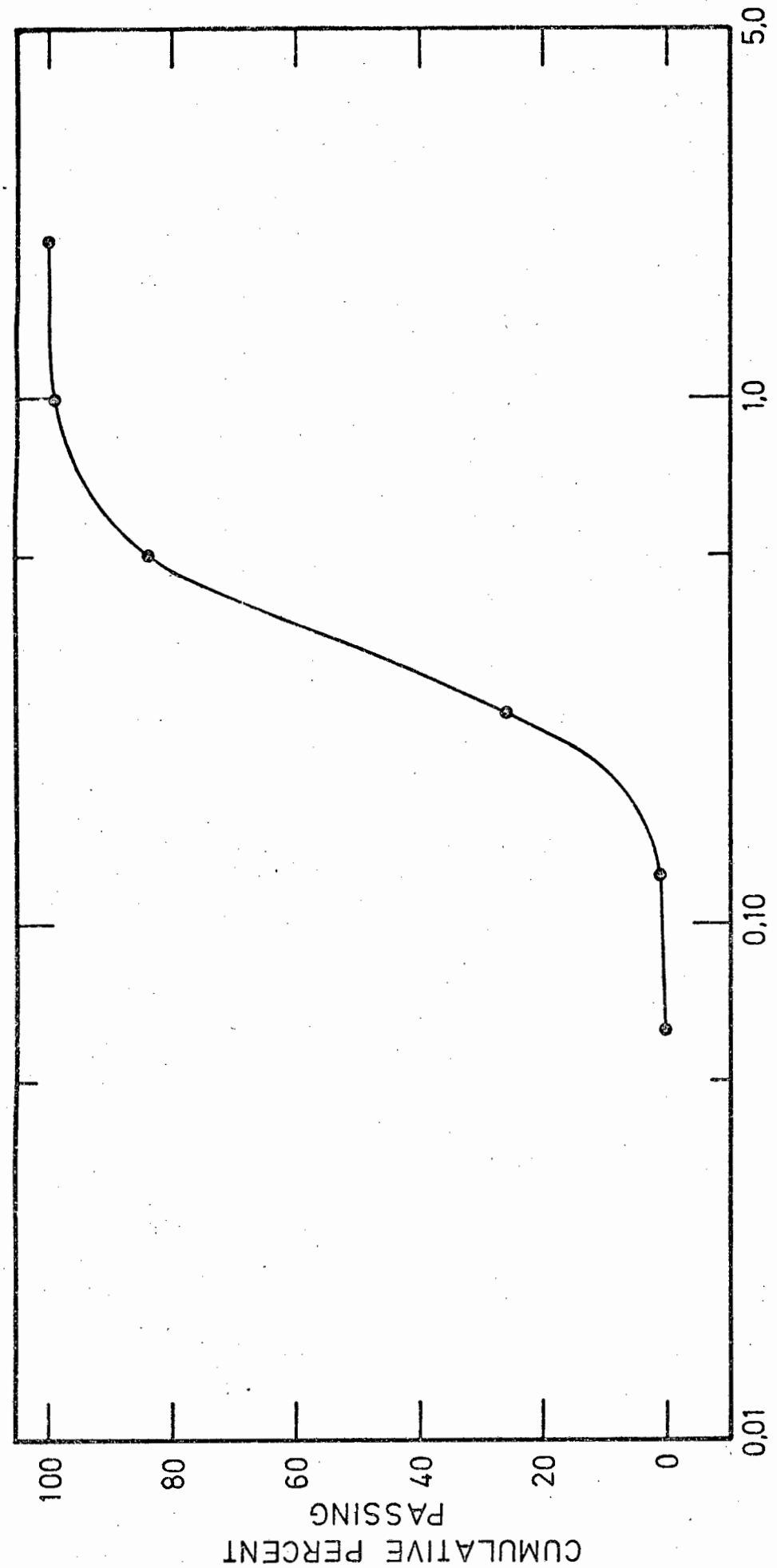

Fig. 3.1: Sand aggregate - Sieve Analysis

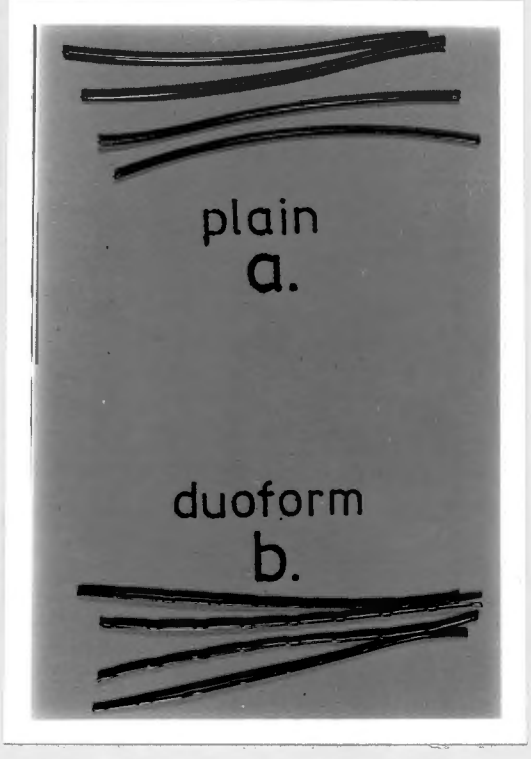

Fig. 3.2: Comparison between (a) plain fibres and (b) Duoform fibres (both are 0,5 dia. x 38 mm long).

Why not a Cube mould?

(a): Compression mould and specimen.

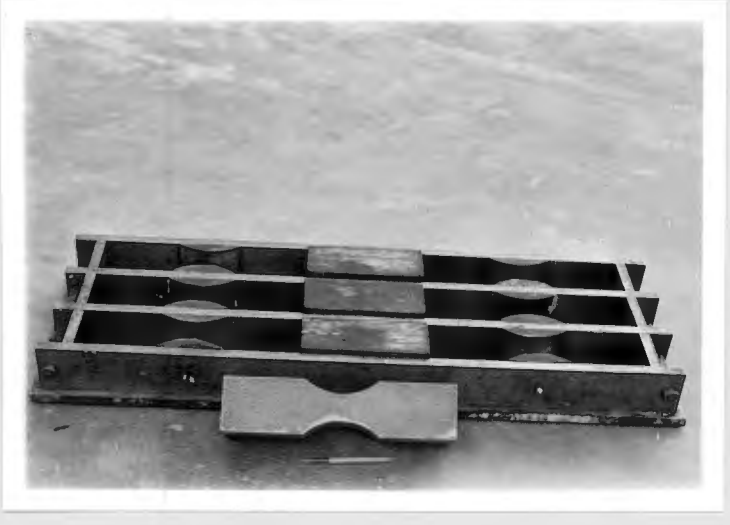

(b): Tension mould and specimen.

Fig. 3.3: Typical specimen moulds and corresponding specimens.

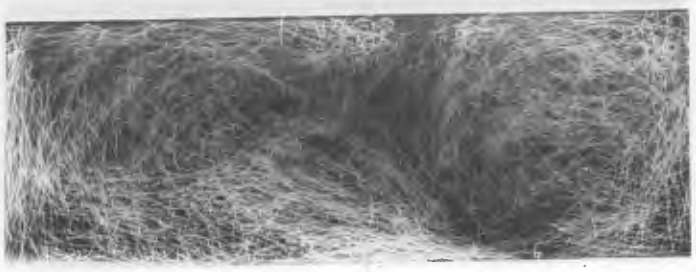

(a): X-ray showing uniform fibre distribution of compression sample (20 secs vibration time).

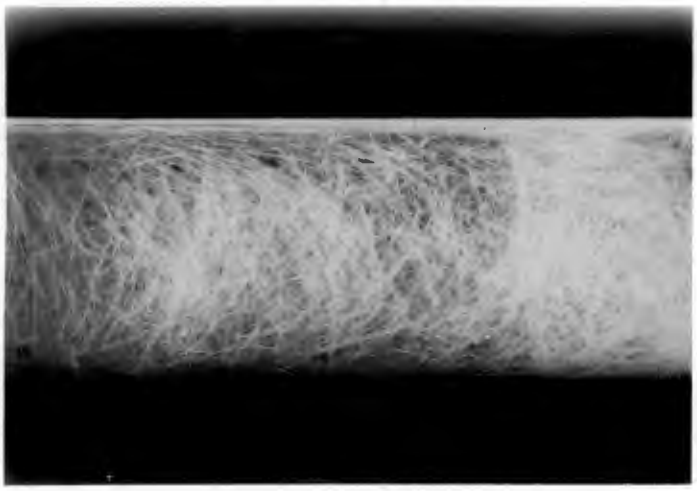

(b): X-ray showing non-uniform fibre distribution of compression sample (20 secs vibration time).

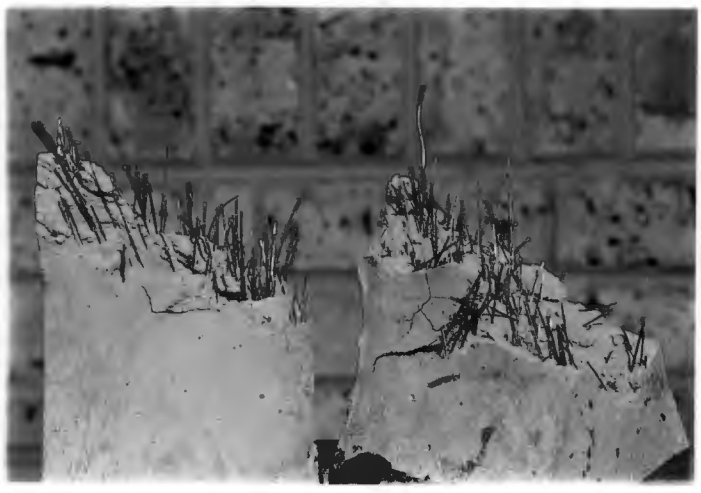

(c): Tensile fracture surface indicates uniform fibre distribution.

Fig. 3.4: Fibre distributions obtained from mixing and casting techniques used.

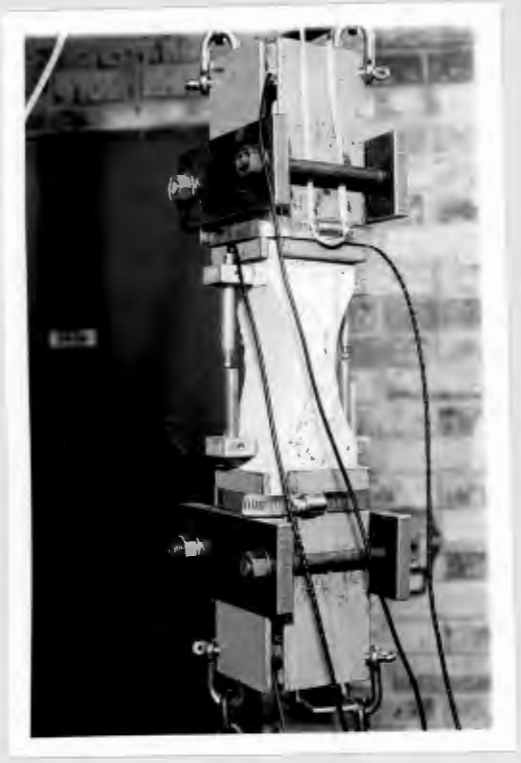

(a) Static tension sample

(b) Fatigue tension sample

(c) Compression sample

Fig. 3.5: Typical specimens ready for testing.

Fig. 3.6: Showing Tensile Testing pulley housing and chains.

Fig. 3.7: ESH Testing Machine in Compression Testing mode with associated instrumentation.

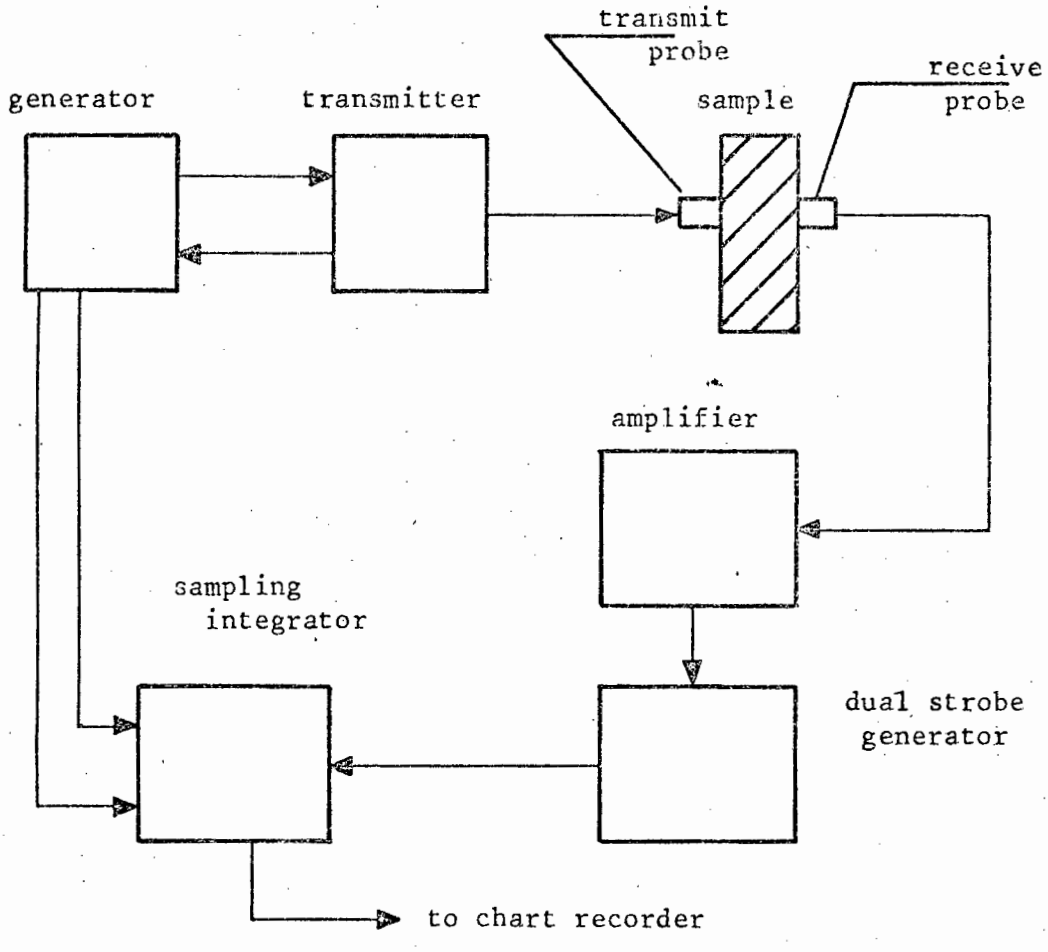

Fig. 3.8: Diagrammatic illustration of operating principle of the Harwell Ultrasonic non-destructive test system 3127-1.

CHAPTER 4

4. COMPRESSIVE BEHAVIOUR OF CEMENT-BASED MATERIALS

4.1. STATIC PROPERTIES

4.1.1. Experimental Results

4.1.1.(a) Mean Strength: A comparison of the static mean strengths of plain mortar and mortar reinforced with a random, uniform distribution of steel fibres (2% by volume) indicates that there is no significant difference between the two (fig. 4.1.). A 't-test' at an α-level of 0.05 confirms this observation statistically (see reference (65)).

4.1.1.(b) Stress-Strain behaviour: With steel-fibres present as reinforcement it is immediately evident that the post-failure characteristics of plain mortar are substantially altered (fig. 4.2.). Toughness of cement materials has conventionally been defined in terms of the amount of energy absorbed by the material during fracture, as measured by the area under the complete stress-strain curve. According to this definition, fig. 4.2. shows steel-fibre reinforcement substantially increases the toughness (or ductility) of the mortar matrix. This more ductile mode of fracture of fibrous mortar is in contrast to the typically brittle, catastrophic mode of failure of plain mortar (fig. 4.3.).

The non-linear characteristics of the stress-strain curve are evident from fig. 4.2. The longitudinal (compressive) failure strains (corresponding to the maximum failure stress) remain essentially unaffected by the presence of steel fibres, for plain mortar. As would be expected from a simple law of mixtures (see Chapter 2) the elastic modulus of plain mortar (defined as the slope of the initial tangent to the stress-strain curve) is unaffected by the addition of steel fibres (2% by volume fibre content).

The steel-fibres, however, significantly affect the

deformation behaviour of mortar in the early stages of loading, illustrated by the respective changes in ultrasonic pulse transit times (ΔUPTT), shown in fig. 4.2. The initiation of 'damage', primarily cracking, occurs at a lower strain in the steel-fibre reinforced mortar.

4.1.2. Discussion

As mentioned previously, a major proportion of previous experimental studies carried out on the effects of fibre reinforcement in plain cement mixes has been almost exclusively restricted to static loading conditions. It would seem reasonable, therefore, to compare such results with those found in the present study before proceeding to discuss fatigue behaviour.

Summarised in table 4.1. are the results of tests measuring relative strengths of steel fibre reinforced cement matrices in both compression and flexure; the wide variability in results is immediately apparent. Similar to results found in this study, Williamson (66), for example, found no significant change in mortar strength with the addition of up to 2,5% steel fibres in compression, although he did find increases varying from 16-23% on concrete with fibre addition, as little as 1% by volume. In direct contradiction, Chen and Carson (67) found no increase in compressive strength for fibrous concrete relative to plain concrete but found a 60% increase in the strength of plain mortar with the addition of only 0,75% volume of steel fibres. Williamson (66) interpreted his observed increase in concrete strength according to the spacing concept formulated by Romualdi (3), by assuming the aggregate, as well as the steel fibres, to inhibit crack growth, i.e. the strength of the fibre-cement composite is inversely proportional to fibre (and aggregate) spacing. However, Williamson can offer no suggestion to explain the corresponding absence of a strength increase in fibre-reinforced mortar, where a similar crack arrest mechanism should be operative. Chen and Carson (67), similarly, do not attempt to explain their observations. Hughes and Fattuhi (68) found a 7% increase in the compressive strength of concrete with the addition of Duoform fibres which they

suggest is caused by the fibres constraining lateral expansion under load thereby reducing the propagation of cracking, offering no mechanism for this process. No appreciable changes in strength were observed from the addition of other types of steel fibres; neither did they investigate effects of varying volume fractions. Shah and Rangan (21) explain their observed absence of a strength increase of concrete reinforced with steel-fibre in terms of a two-phase composite materials approach (see Chapter 2) which predicts the composite failure stress to be proportional to the product of elastic modulus of the composite and the corresponding concrete failure strain, i.e. fibre addition has no influence upon the failure strain. This explanation would appear to be the most reasonable and consistent with results obtained in this thesis since the matrix elastic modulus is found to be unaffected by the presence of steel-fibres.

It is well established that fibre reinforced mixes exhibit a significantly greater post-failure resistance to cracking than plain mixes in both flexure (21, 26, 69, 70) and compression (21, 67, 68, 71). This is clearly illustrated in fig. 4.2. The increase in energy absorption, or toughness, will be a direct result of the ability of fibres to inhibit the propagation of microcracks, i.e. prolong the load-bearing capacity of the material. Large amounts of energy are then consumed arising from fibre pull-out (24, 34). In addition, and resulting from extensive interaction with microcracks, the total fracture surface area of the reinforced composite is significantly increased in comparison to the unreinforced matrix (fig. 4.3.).

Other characteristics of stress-strain behaviour, and the effects of fibre-reinforcement, are shown in table 4.1. Shah and Rangan (21) found the strain corresponding to the maximum load in compression to be unaffected by the presence of steel fibres, which is consistent with the observations made in this study. Shah and Rangan explained this observation in terms of their composite two-phase materials (law of mixtures) approach cited above and in Chapter 2.

However, they found that the strain at which microcracking initiated was unaffected by the addition of steel fibres (measured by the limit of proportionality). Ultrasonic pulse transit time (UPTT) measurements in this thesis have indicated that in the presence of steel fibres cracking initiates at a lower strain than that in plain mortar. (This difference from Shah and Rangan's results may well be a function of the sensitivity of the ultrasonic equipment used.) This would suggest that the fibres themselves play a role in crack initiation. It would seem reasonable, therefore, to suggest that steel fibres can play a dual role, i.e. one promoting crack-initiation and the other crack-arrest (as indicated by the post-maximum stress behaviour); both mechanisms could occur simultaneously, the dominant one being dependent on factors which would include the stress level and the loading conditions.

Under flexural loading, several authors (32, 70) have claimed that steel-fibres can markedly increase the strain at which cracking is initiated (table 4.1.). Swamy and Mangat (32), for example, using both a strain gauge technique and ultrasonic measurements, observed a relative increase in first crack strain of about 70% for a mix containing 2,5% (by volume) of fibres. They found that the first crack strain increases with decreasing effective fibre spacing (increasing fibre volume fraction) which was consistent with their theoretical prediction (Chapter 2 - (28)).

It was mentioned in section 4.1.1.(b) that the elastic modulus in compression is effectively unaltered by the presence of steel fibres (table 4.1.). It is of interest to compare, however, that in flexure, Swamy and co-workers found an increase in modulus in the range 4-30% in comparison with the unreinforced matrix (32, 69). They attribute this to the crack arresting mechanism of the fibre reinforcement which minimises the crack size giving rise to a stiffer material. However, these authors pointed out (69) that such increases are moderate when compared to the reinforced composite's significantly greater ability to resist deformation, i.e. toughness, where a tenfold increase was observed.

4.1.3. Conclusions

From the widely differing results reviewed above and summarised in table 4.1., it becomes obvious that the influence of steel fibres upon both the compressive and flexural behaviour of cement-based materials still remains somewhat in question. It would appear that the inability of researchers to achieve reasonable agreement lies in part with the numerous variables (e.g. types of materials used, specimen configuration, mix design, loading mode) that influence the mechanical behaviour of the composite, coupled with the lack of uniformity and standardisation between experimental procedures.

However, the results of this current investigation are fairly specific:

(1) Fibres have little effect on the static compressive behaviour other than to improve the loading-bearing capacity of the composite following maximum load due to the ability of the fibres to bridge microcracks and thus inhibit their propagation. The large amounts of energy absorption associated with this failure mode is probably due to the fibre pull-out from the cement matrix.

This is not new!

(2) Contrary to previous results reported in the literature, table 4.1., steel-fibres are found to initiate cracking at an earlier strain value compared to the unreinforced matrix. This would suggest that the fibres contribute to two distinct, opposing mechanisms, viz: crack-initiation and crack-arrest.

4.2. FATIGUE PROPERTIES

4.2.1. Experimental Results

4.2.1.(a) S - N Curve: The definition of fatigue and its conventional representation using the S - N curve have been described earlier (see Chapter 1).

Fig. 4.4.(a) presents the results of fatigue tests for both plain mortar and steel fibre reinforced mortar. Fig. 4.4.(b) shows the corresponding S - N curves.

Both systems appear to exhibit linear relationships between the fatigue stress amplitude and the corresponding number of cycles to failure; also the fatigue characteristics of the plain mortar and fibrous mortar are not significantly different, although the fatigue strength at 1 million cycles (run-out) of plain mortar is increased from approximately 55% to about 60-65% of the maximum static stress with the addition of steel fibres. There is no evidence of a fatigue limit as with some metals, in either case.

4.2.1.(b) Strain Results: Figs. 4.5.(a-f) and 4.6.(a-e) show typical strain data at various stress levels for plain and steel fibre reinforced mortar levels respectively. Unfortunately, experimental difficulties have limited the extent to which the lateral strain data could be used, therefore discussion relates entirely to longitudinal strain measurement.

During cyclic stressing the longitudinal (compressive) elastic strain amplitudes, $\Delta\varepsilon$, generally increase linearly to failure. For the run-out tests, however, the compressive elastic strain amplitudes generally remain constant (figs. 4.5.(f), 4.6.(e)) with no evidence of any change prior to run-out.

The initial longitudinal elastic strain amplitudes, $\Delta\varepsilon_o$, which are obviously smaller at smaller applied stress amplitudes, are unaffected by the addition of a random distribution of steel fibres (fig. 4.7.). This observation is consistent with the earlier observations (see section 4.1.1.) that there is no change in elastic modulus with fibre addition to plain mortar. Similarly, the longitudinal elastic strain amplitude

at failure, $\Delta\varepsilon_f$, was found not to be significantly different between plain and fibrous mortar, the ultimate strain amplitude decreasing with increasing fatigue life (fig. 4.8.)/decreasing applied stress level (fig. 4.9.).

The observed change in the residual component of the total longitudinal strain, ε_R , with progressive cycling is found to consist of three distinct regimes (see figs. 4.5. and 4.6.):

I : a primary increase in residual strain

II : a secondary region, showing a constant rate of change in ε_R with increasing number of cycles

III : a final (tertiary) accelerated increase in ε_R just prior to ultimate failure.

The total compressive longitudinal strains at failure (fig. 4.10.) are independent of both fatigue life and stress level and do not appear to approach any definite, critical value. However, the average total strains at fatigue failure for plain and steel-fibre reinforced mortar are ~ 2200 microstrains and ~ 3000 microstrains respectively; the static failure strain corresponding to the maximum static stress (i.e. maximum strain at failure for plain mortar) was ~ 3000 microstrains for both plain and fibrous mortar.

4.2.1.(c) Ultrasonic Pulse Transit Time: Figs. 4.11.(a-f) and 4.12.(a-d) show typical output data for plain and steel-fibre reinforced mortar, respectively.

In the initial stages of this study pulse transit times measured prior to testing were found to be approximately constant with no significant difference between plain and fibrous mortar, consistent with work reported elsewhere (55,56,72).

The increase in ultrasonic pulse transit time (ΔUPTT), similar to changes observed in residual strains during fatigue (for example, fig. 4.6.(b)), also consists of three distinct regimes, the extent of this behaviour being dependent upon stress level. The observed variations in ΔUPTT as a fraction of fatigue life for the stress levels examined is

illustrated in fig. 4.13.(a). (A similar relationship is observed for fibrous mortar, fig. 4.13.(b)). For high stress level tests, for example 80%, only the tertiary regime is evident; for run-out tests, i.e. at low stress levels, only the primary regime is observed after which there is no further increase in UPTT. Intermediate stress level tests exhibited all three regimes.

Replotting figs. 4.11. and 4.12. with a logarithmic abscissa shows ΔUPTT to be within well-defined scatter bands: figs. 4.14.(a-d) are for plain mortar and figs. 4.15.(a-c) are for fibre reinforced mortar. The final, individual data points indicated on the graphs are determined at between 90-100% of fatigue life from the direct output (see section 3.3.2.). Due to this rather subjective analysis there did not appear to be a critical value in UPTT at which failure occurred as has been proposed (54, 73), although imminent failure is certainly readily predicted by the sudden, rapid increase in UPTT which occurs just prior to failure, in agreement with other studies (73, 74), and as shown in figs. 4.13.(a,b).

A comparison of plain and fibrous mortar at corresponding stress levels shows that damage accumulation, primarily due to cracking, initiates at a lower fraction of the fatigue life in reinforced mortar. Although the fatigue lives are not significantly different, the total amount of damage sustained by fibre reinforced mortar is substantially larger than by plain mortar, as indicated by the greater increase in UPTT (figs. 4.16.(a-c)). Both these observations would confirm the suggestion made earlier in section 4.1.2. that the steel fibres have a dual role within the cement matrix in uniaxial compression, i.e. they contribute to the initiation as well as arrest of microcracks.

Finally, although run-out tests have generally shown no increase in $\Delta\varepsilon$ or further increase in UPTT (or ε_R) after region I, when tested statically at run-out they were observed to have an increased maximum static stress compared to similar, non-fatigued control specimens. The results are summarised in fig. 4.17.

4.2.2. Discussion

As mentioned previously, reported work dealing specifically with the behaviour of fibre-reinforced cement-based materials under fatigue loading is very limited: with specific regard to steel fibres only two brief studies, in flexure, have appeared in the literature (75, 76). The fatigue properties of plain cement, mortar and concrete, on the other hand, have received rather more attention. Some of the results obtained are summarised in table 4.2. It is logical, therefore, to attempt to extend the analyses of plain cement materials to that of corresponding fibre reinforced ones, as well as to evaluate the behaviour of the fibre-reinforced materials in a fatigue situation.

Previous studies have shown that the fatigue strength at 1 million cycles (run-out tests) for plain cement-based materials is approximately 55% - 60% of the ultimate static strength of companion specimens tested prior to fatigue loading and there is no evidence for a fatigue limit (60, 61, 73, 75-79, 80, 81). Observations from this thesis are broadly consistent with commonly observed characteristics of fatigue in these materials (table 4.2.).

The increase in compressive fatigue strength at 1 million cycles with the addition of steel fibres observed in this study should be compared with other results obtained in flexure (75, 76). Thus, Batson et al. (76) and Romualdi (75) have respectively reported fatigue strengths of 83% and 95% of the first crack static flexure strength at 2 million cycles for steel fibre reinforced concrete beams, compared with 55% for plain concrete beams. Both Batson et al. (76) and Romualdi (75) correlate these increases in fatigue strength directly to Romualdi's theory on crack-arrest (3).

The fact that there is no significant difference between the S - N curves in compression for plain and fibrous mortar (fig. 4.4.(b)) clearly illustrates the dependence on loading mode, and this aspect will be discussed further in respect of the tensile results reported in Chapter 5.

In passing, it is of interest to note that static tests

carried out at a load rate equivalent to a quarter cycle of the fatigue load rate (see fig. 4.18) exhibited an approximately 35% increase in static strength. Therefore, the stress level of the maximum cyclic stress is only an apparent stress expressed as a percentage of the 100% static strength (determined from the standard load rate), whereas in fact, stress level should be in terms of the 135% equivalent static strength (determined from a load rate equivalent to the fatigue load rate). This observation would have the effect of shifting the S - N curve as shown in fig. 4.18. Neal and Kesler (82) have previously commented on this important consideration, stating that " ... the rate of application of the fatigue load is responsible for an apparent strength greater than the static strength when the curve is extrapolated to one cycle of load ... ".

It may now be argued, having clearly shown that the basic compressive fatigue properties of plain mortar, as with the corresponding static properties, are relatively unaffected by the presence of steel fibres, that further study in compression of this fibre composite may be of little value. Also, Glucklich (13) has suggested that compression testing results in stable crack growth, compared to the predominantly unstable crack growth which occurs in tension. Hopefully, the addition of steel fibres in tension promotes stable crack growth; however the necessity of fibre addition having the desired aim of improving compressive properties must be questioned. On the other hand, it is generally acknowledged that compressive failure arises due to tensile stresses normal to the applied compressive stress. It is these tensile stresses that the fibres would restrain, resulting in changed fatigued characteristics not in evidence from conventional S - N curve representation.

The observed increase in longitudinal elastic strain amplitude with progressive fatigue cycling (figs. 4.5. and 4.6.) indicates a corresponding decrease in modulus of elasticity, E, or stiffness, during a fatigue test. Since stiffness can be considered a measure of the ability to resist crack formation (69), the lower the rate of decrease in stiffness, i.e. the lower the rate of increase in $\Delta\varepsilon$, the

longer should be the fatigue life. This is confirmed experimentally with no significant difference between plain and fibrous mortar (fig. 4.19.). Several authors have reported a reduction in E during fatigue (73, 81, 83) and have found the overall reduction to be independent of stress level (see table 4.2.). Bennett and Raju (73), for example, have observed E, as a ratio of the original modulus E_o, to decrease linearly as a percentage of the fatigue life with an overall reduction in modulus of approximately 30%; other workers (81, 83) report a non-linear decrease in the ratio E/E_o, with an overall reduction in modulus to approximately 55% of the initial value (81). Whaley and Neville (84), on the other hand, observed an increase in the modulus of elasticity as a result of cyclic stressing, although their tests were carried out below a maximum stress level of 50% (with a mean stress of 35%). The results obtained in this work, figs. 4.20.(a,b), show a broad similarity with those obtained by Bennett and Raju (73), the mean reduction in elastic modulus ($\varepsilon_o/\varepsilon = E/E_o$) being approximately 30%. These latter curves are approximately identical in slope, i.e. a 2% volume fibre content is insufficient to contribute to E of the composite as predicted by the law of mixtures (see Chapter 2).

It is of interest to note that Bennett and Raju (73) observed the elastic strain component (longitudinal) to reach a critical value at failure, independent of stress level, and that this critical value was not significantly different to the initial tangent static failure strain. In contrast, Hilsdorf and Kesler (85) found the maximum 'tensile' strain (assumed to be the summation of both the elastic and residual strain components) of concrete beams subjected to repeated flexural loads to be independent of fatigue life, yet all their attempts to establish a limiting maximum strain at failure were unsuccessful (51). However, the maximum tensile strains obtained by Hilsdorf and Kesler (85) were found to be greater than the maximum flexural static failure strain. Award and Hilsdorf (86) observed that repeated compressive loads resulted in the failure strains of concrete to increase with decreasing stress level i.e. increasing fatigue life.

In comparison with all these results, data from the present investigation has shown that the longitudinal elastic strain amplitude at failure, $\Delta\varepsilon_f$, decreases with decreasing stress level and does not attain any critical value at failure independent of applied stress level (fig. 4.9.), i.e. $\Delta\varepsilon_f$ is dependent upon fatigue life, as shown in fig. 4.8.; the addition of steel fibres has essentially no effect on this behaviour.

The non-elastic deformation of concrete, ε_R , during fatigue has been referred to as cyclic creep (77, 74, 84), as distinct from creep occurring under a sustained static load. Indeed, several authors have observed that the residual fatigue strain, ε_R , increases in a characteristic manner (64, 74) similar to sustained-load creep, i.e. it can be divided into three distinct regimes, as observed in fig. 4.13.(a), for example. Whaley and Neville (84), however, explain that the respective mechanisms occurring may, in fact, be different: at high cyclic stress levels microcracking probably occurs during the early stages of fatigue life, while at low ranges of stress strain accumulation is probably similar to that which occurs under a sustained static load - ε_R at failure is not necessarily identical in magnitude in both cases. However, these authors (84) do propose that cyclic stress accelerates the process of accumulation compared to sustained load.

Sparks and Menzies (64) found that the rate of residual strain change, $d\varepsilon_R/dn$, observed during the approximately linearly-increasing section of the curve, was dependent upon fatigue life but independent of the rate of loading (i.e. frequency). Though these authors found the relationship to differ with the type of aggregate used, generally a fivefold order of magnitude change was observed in $d\varepsilon_R/dn$.

The results obtained in this investigation confirm those obtained by Sparks and Menzies (64), (fig. 4.21.(a)), and upon comparison it is seen that the slope of the rate of change in residual strain against fatigue cycles, $d(d\varepsilon_R/dn)/dn$, taken from reference 64 is greater for concrete than for mortar (although a number of factors could account for this

difference). A similar relation is found for fibrous mortar (fig. 4.21.(b)), the slope of the rate of change in ε_R being greater for fibrous mortar than concrete. If the accumulation of residual strain is considered a reliable indication of damage sustained during fatigue, then it can be seen that at corresponding high stress levels/short lifetimes, aggregate and steel fibre addition results in a more rapid increase in damage accumulation; at corresponding low stress levels/ long lifetimes, damage accumulation is much slower compared to plain mortar, (fig. 4.21.(c)); in both instances the fibres exhibit the more extreme behaviour. This would again suggest the possible dual role of the steel fibres as both crack-initiators and crack-arrestors. With reference to the S - N curve in fig. 4.4.(a), this interpretation may explain why at low stress levels the fatigue strength at 1 million cycles of plain mortar is increased by the addition of steel fibres; i.e. the steel fibres predominantly inhibit the formation and development of microcracks leading to eventual fatigue failure; at high stress levels, however, there is no significant difference between the plain and fibrous mortar.

Evidence from UPTT for the steel fibres acting predominantly as crack-arrestors at the lower stress levels can also be found in fig. 4.22. Although damage is initiated at a much earlier stage with fibre addition at high stress levels, the total amount of damage sustained is significantly greater than that of unreinforced mortar, as mentioned earlier (see figs. 4.16.(a-c)).

Raju and co-workers (54, 73) have indicated that the progressive decrease in ultrasonic pulse velocity during fatigue is independent of stress level when related to the percentage of fatigue life. No such trend or critical value in UPTT prior to failure have been found in this study (4.2.1.(c)) although, as noted elsewhere (73, 74), imminent failure is readily predicted by the final rapid increase in UPTT (figs. 4.13.(a,b)).

It was mentioned previously that the increase in UPTT during fatigue characteristically consists of three distinct regimes, as shown in figs. 4.13.(a,b) (cf: residual strain

component, fig. 4.5.(b), for example). Further, in a similar manner to the rate of change in residual strain, $d\varepsilon_R/dn$ (figs. 4.21.(a,b)), the rate of change in pulse transit, $d(u/s)/dn$, as a function of fatigue life is a linear, decreasing function for both plain and fibrous mortar (figs. 4.23.(a,b)). The latter figure shows a more rapid increase in rate at high stress levels and a slower increase rate at low stress levels, relative to plain mortar (fig. 4.23.(c)).

This last observation again ties in with previous comments about the effect of fibres on microcrack development. Thus, although the addition of a random but uniform distribution of steel fibres would appear to have little beneficial effect upon the overall compressive fatigue properties of plain mortar, in terms of extending the fatigue life, the fibres do have a significant influence upon the apparent failure mechanism of plain mortar. It is generally acknowledged (48,87) that microcracks develop in two ways. Interfacial cracks, which may well be present prior to testing, occur between the relatively higher modulus material (aggregate) and the cement matrix. Their occurrence is promoted by the interfacial tensile and shear stresses which result from early volume changes during hydration. Matrix cracks result essentially from the application of an external load. With the addition of the high modulus steel-fibres, numerous sites are made available for crack initiation due to the restraints the fibres have upon hydration volume changes compared to the unreinforced matrix. Scanning electron fractography studies, reported in Chapter 6, have shown that the steel fibres are in fact surrounded by a core of weaker hydrate material relative to the bulk material and this would help to explain, together with the fact that there are physically more sites available for crack initiation, why damage accumulation in the fibre-reinforced mortar occurs earlier than in plain mortar, as illustrated in fig. 4.22.

Although these observations may assist in interpreting the relative fracture modes leading to fatigue failure, it is not possible at this point in time to determine the precise

mechanism of failure due to fatigue loading. Indeed, Glucklich (13), utilising a fracture-mechanics approach, proposed a model of fracture of cement-based materials arising from an increasing compressive static load. The simple Griffith concept of fracture of brittle materials (into which category cement is generally included) states that deformation under a monotonically increasing load should remain elastic until the inherent flaw having the greatest stress distribution at its tip propagates in an unstable manner, resulting in fracture. However, this is not the case in cement and Glucklich (13) recognised that the heterogeneity of the material had a considerable effect upon crack propagation in compression which occurred at stresses much below the ultimate fracture stress. As a result of this heterogeneity, cracks will start growing in the region of highest stress concentration at a given applied load and will cease to propagate if they enter an adjacent region in which the energy demand for crack propagation is increased. This increase in energy demand can be met with an increase in applied stress when such cracks will start to grow again. Therefore, the heterogeneity of the cement provides a crack-arresting mechanism.

Although this argument adequately explains stable microcracking during a static test it is difficult to extrapolate this cracking process to a fatigue situation where the maximum applied stress does not increase. It was mentioned previously that residual strain (ε_R) accumulation has similar characteristics to strain accumulation arising from the application of sustained (or creep) load. It is quite possible, therefore, that the failure mechanisms are similar and that these processes are due to stress-induced migration of water molecules or to gel particle movement which is modified by the presence of varying amounts of water (84), resulting in local stress redistributions. A further contribution to microcracking during dynamic fatigue could arise from the phenomenon of 'static fatigue' (analogous to stress corrosion in metals) similar to that suggested for sustained loading (74); this may also be significantly influenced by the presence of free moisture. (This environmentally-induced slow

crack growth has indeed been observed to occur in cement based materials (88)). It is probable, however, that fatigue failure in compression, at least, develops in three stages:

(i) initiation of flaws and cracks;
(ii) slow stable growth of flaws and cracks to a subcritical size; and
(iii) rapid unstable propagation of the flaws or cracks of a critical size resulting in final fracture.

Such a sequence is clearly suggested by the increase in ε_R (figs. 4.5. and 4.6.) and ΔUPTT (fig. 4.13.(a,b).

Specimens fatigued to 1 million cycles without failing were found to have an average increase in static strength of 20% compared to the pre-fatigued static strength of companion specimens. This phenomenon has been extensively reported elsewhere (34, 62, 73 - 77, 81, 84), probably the first observation being made as far back as 1922 (89).

Various theories have been proposed to explain this phenomenon, generally known as 'fatigue hardening'. Romualdi (75) attributed the increased strength to the apparent relaxation of tensile stresses within the matrix which occur due to curing and shrinkage. Hilsdorf and Kesler (62) also relate the increase in flexural strength to a reduction in residual tensile stresses that are caused by drying shrinkage of the cement paste. Bennett and Raju (73) proposed two possible mechanisms for fatigue hardening, the one due to accelerated curing and loss of capillary moisture caused by a temperature increase during fatigue; the other based upon the effects of a sustained compressive stress in which there is a loss of gel moisture. Shah and Chandra (74) argue that consolidation and the consequent strengthening, cracking and the consequent weakening are two opposing mechanisms during fatigue, their relative magnitudes being dependent upon the level of load. Consolidation, they suggest, results in an increase in secondary bonding forces between the cement paste gel particles causing an increase in strength, which was similar to that proposed by Whaley and Neville (84). It has also been suggested that crack healing takes place due to

continued hydration (62), this hydration only becoming significant for low stress levels where time to run-out is of the order of a few days (86). It is of interest to note that a reduction in static compressive strength after only 30-70% of the total life of the test specimen has been observed whereas slight increases were noted at lower life ratios (86).

From the results shown in fig. 4.17., specimens that were statically tested after removing from the curing bath, i.e. pre-fatigue specimens, have different static strengths to those specimens subjected to the same laboratory environment as the fatigue specimens, i.e. post-fatigue specimens, the latter having the higher strength. This difference could possibly be due to the loss of capillary water in specimens subjected to the laboratory environment since specimens tested immediately on removal from the curing bath after the fatigue period were found to be not significantly different in static strength to similar companion specimens tested prior to fatigue. However, fatigued specimens still exhibited an average 11% increase above specimens subjected to the same environmental conditions but not fatigued. It would be premature, on the basis of these results, to consider an adequate explanation for resolving the obviously complex phenomena of fatigue hardening, since such a process would require an extensive study far beyond the scope of this thesis. Results obtained, however, would certainly emphasise the requirement for such an investigation.

4.2.3. Conclusions

From the preceding discussion it becomes clear that the addition of a random, but uniform, distribution of Duoform steel fibres, 2% by volume, has little beneficial effect upon the fatigue properties of plain mortar in compression. As explained previously, compressive failure is a relatively stable mechanism when compared to tensile failure. Although steel fibre addition may be expected to further stabilise cracking in compression it would appear that fibres also contribute to an opposing mechanism, i.e. one of crack initiation. It was observed, however, that fibre addition significantly affects

tensile failure, as will be shown in the following chapter, thereby suggesting that the complex stress distributions in the compressive mode lead to an unrealistic representation of fibre reinforcement crack stabilisation. Although the observations of this chapter do not form an adequate basis for resolving the question of the mechanism of fatigue failure in either plain or fibre reinforced cement systems, the findings make it possible to consider the fundamental issue; do steel fibres contribute to the fatigue characteristics of cement materials? In this connection a number of conclusions can be drawn from the observations made (see also table 4.2.):

(1) S - N curves are linear with no evidence of a fatigue limit, the addition of steel fibres increasing the fatigue strength of plain mortar at 1 million cycles from 55% to approximately 60-65% of the maximum static stress.

(2) The elastic strains at failure, $\Delta\varepsilon_f$, were found to decrease with increasing fatigue life with no definite critical value being attained, independent of stress level/ fatigue life, (cf: table 4.2.), and further, no significant difference between plain and fibrous mortar. The rate of increase in strain amplitude, $d(\Delta\varepsilon)/dn$, also decreased, for both mixes, with increasing fatigue life. Modulus of Elasticity, E, for both plain and fibre reinforced mortar decreased linearly with an overall reduction of 30% in the initial value, E_o (cf: table 4.2.). The fact that the elastic properties of plain and fibrous mortar are similar would be consistent with the law of mixtures (see Chapter 2) for such a low volume content of fibres (2%).

(3) Both residual strain accumulation and increases in ultrasonic pulse transit time were observed to increase in a characteristic manner; up to 3 distinct regimes may be observed depending on the applied stress level.

(4) From ultrasonic pulse transit time measurements, the failure process of plain mortar is significantly modified in the presence of steel fibres; crack initiation occurs earlier within the fatigue life and the amount of damage (microcracking) which can be sustained is considerably increased. In neither cement mix did there appear to be a

critical increase in transit time although imminent failure was predicted by a sudden increase in UPTT.

(5) A dual role played by the steel fibres in the compressive loading mode is proposed, viz. one of crack-initiation and the other of crack arrest.

(6) Run-out tests to 1 million cycles have shown post-fatigue static strength increases of about 11% when compared to similar unfatigued specimens.

(7) From the results obtained herein (although not discussed as such) a number of possible empirical relationships for failure prediction emerge. These include:

(i) S - N curve (fig. 4.4.(b))

(ii) Ultimate longitudinal elastic strain amplitude against fatigue life (fig. 4.8.)

(iii) Rate of change of elastic strain amplitude as a function of fatigue life (fig. 4.19.)

(iv) Reduction of elastic modulus, E, as a ratio of the initial modulus, E_o, against fatigue life percentage corresponding to that reduction in E (fig. 4.20.)

(v) Rate of increase in residual strain, ε_R, and pulse transit time as a function of fatigue life (figs. 4.21. and 4.23. respectively).

Properties	Decrease	No Significant Change	Increase
Strain at first cracking	AUTHOR	21, 21[1], 43[1]	32, 32[1], 70[1]
Elastic Modulus		21, 26, 43, 66, 117, 118, AUTHOR, 21[1], 26[1], 43[1]	67, 32[1]
Strain at maximum load		21, AUTHOR	67, 119, 32[1], 69[1]
Maximum compressive strength	71, 121[3], 123	21, 43, 66[2], 67[3], 68[3], 120, AUTHOR	66[3], 67[2], 68[3], 121[3], 122
First cracking flexural strength[1]			8, 34, 70, 116, 118
Maximum flexural strength[1]		21, 123	24, 26, 43, 69, 70, 116, 122

1. In flexure
2. Concrete
3. Mortar

} Changes depend on mix design.

TABLE 4.1.

Relative Properties of Steel fibre reinforced cement-based materials compared to the unreinforced matrix.

Properties	Compression	First Crack in Flexure	Flexure
(a) Fatigue Strength at 1.10^6 cycles:			
(i) ~55%;	73, 77, 78, 80, AUTHOR	75, 76	60, 61, 79, 80, 81
(ii) > 55%;	AUTHOR+	75+, 76+,	
(b) Fatigue Limit at 1.10^6 cycles:			
(i) evidence;			
(ii) no evidence;	73, 77, 78, 80, AUTHOR, AUTHOR+	75, 76, 75+, 76+	60, 61, 79, 80, 81
(c) Elastic Modulus:			
(i) Increase;	84		
(ii) Decrease;	73, 81, 83, AUTHOR, AUTHOR+		
(d) Elastic Strain at Failure:			
(i) Limiting value (Indep. of N_f);	54, 73		81, 85
(ii) Dep. of N_f;			
1) Increase	86		
2) Decrease	AUTHOR, AUTHOR+		

+ Steel-fibre reinforced matrix

TABLE 4.2

Summary of Fatigue Properties

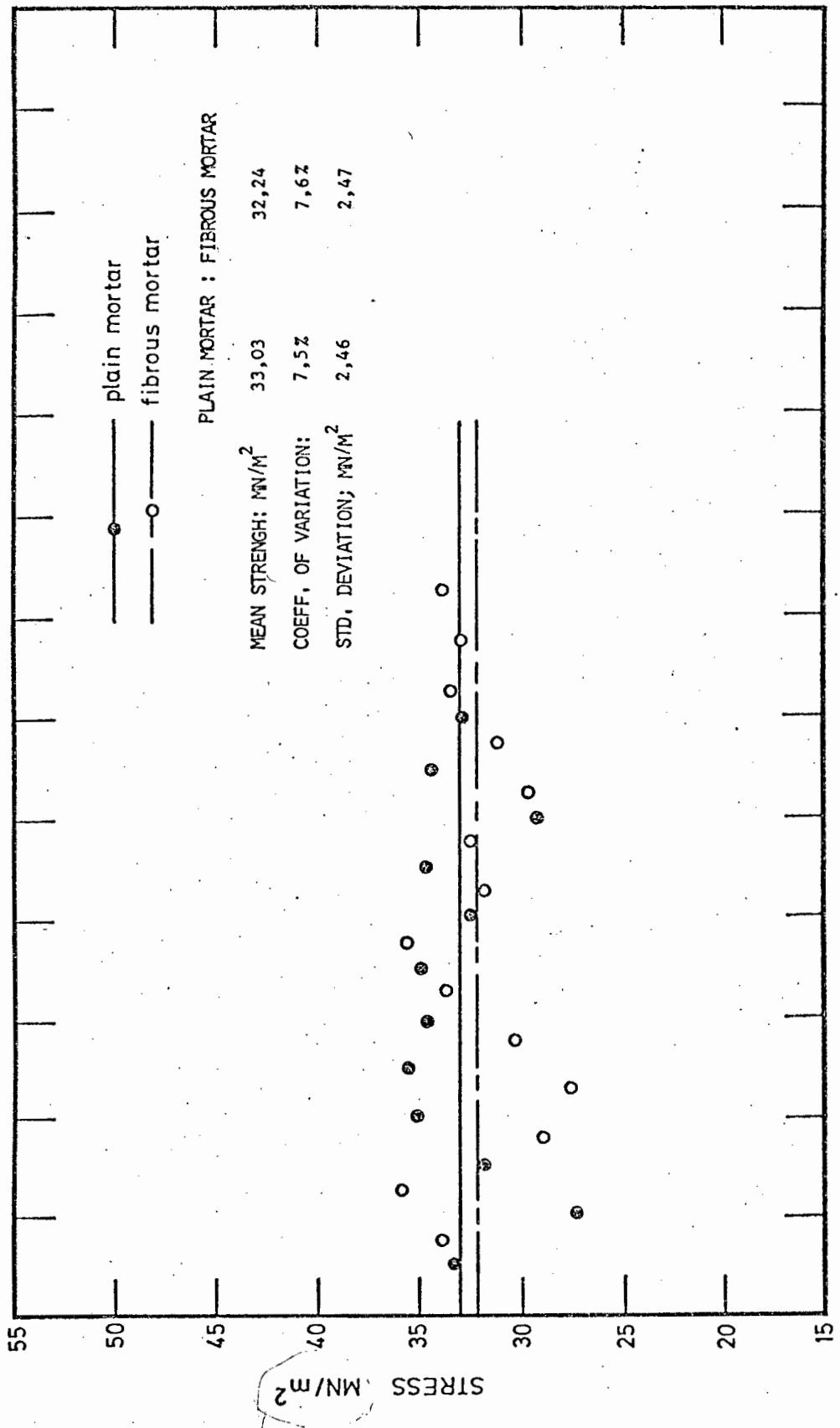

Fig. 4.1: Comparison of Ultimate static compressive strength of Plain and Fibrous Mortar.

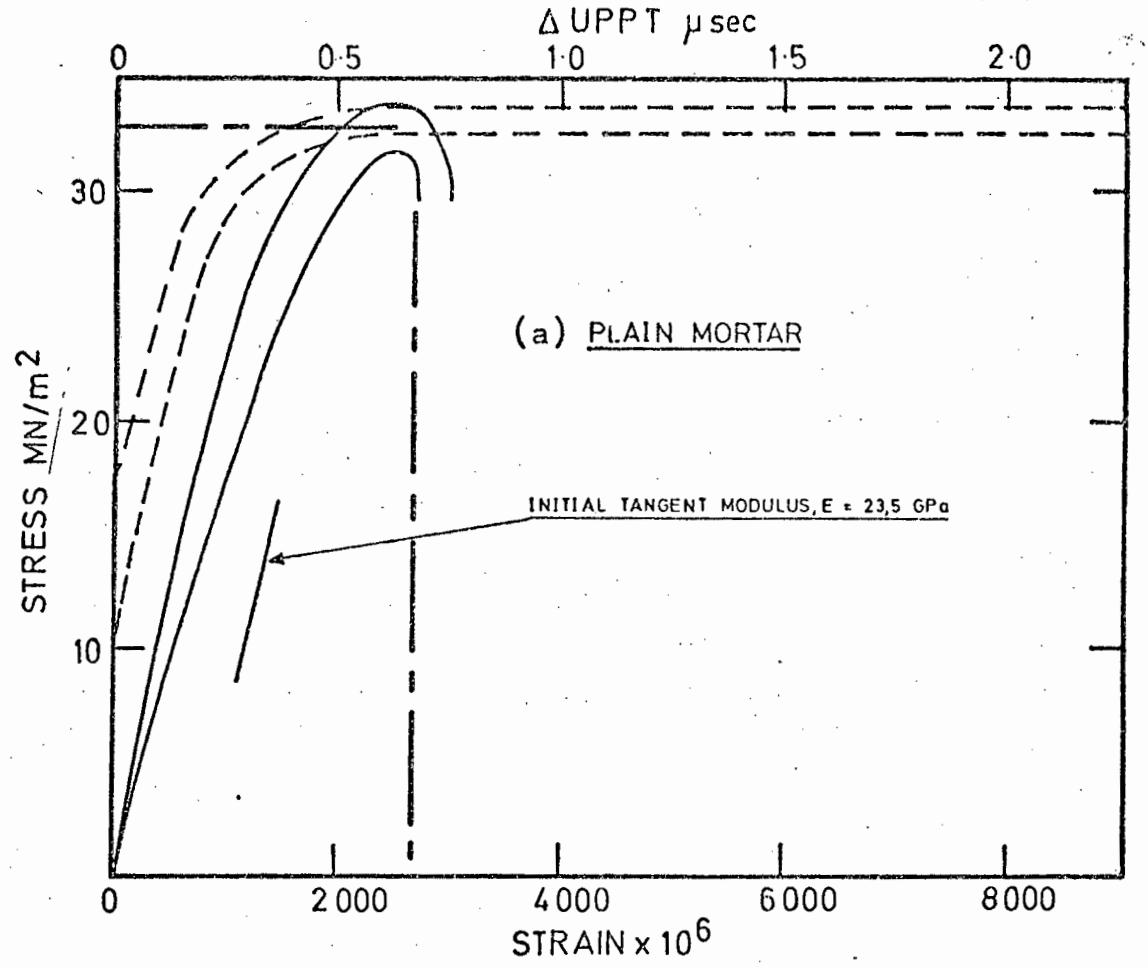

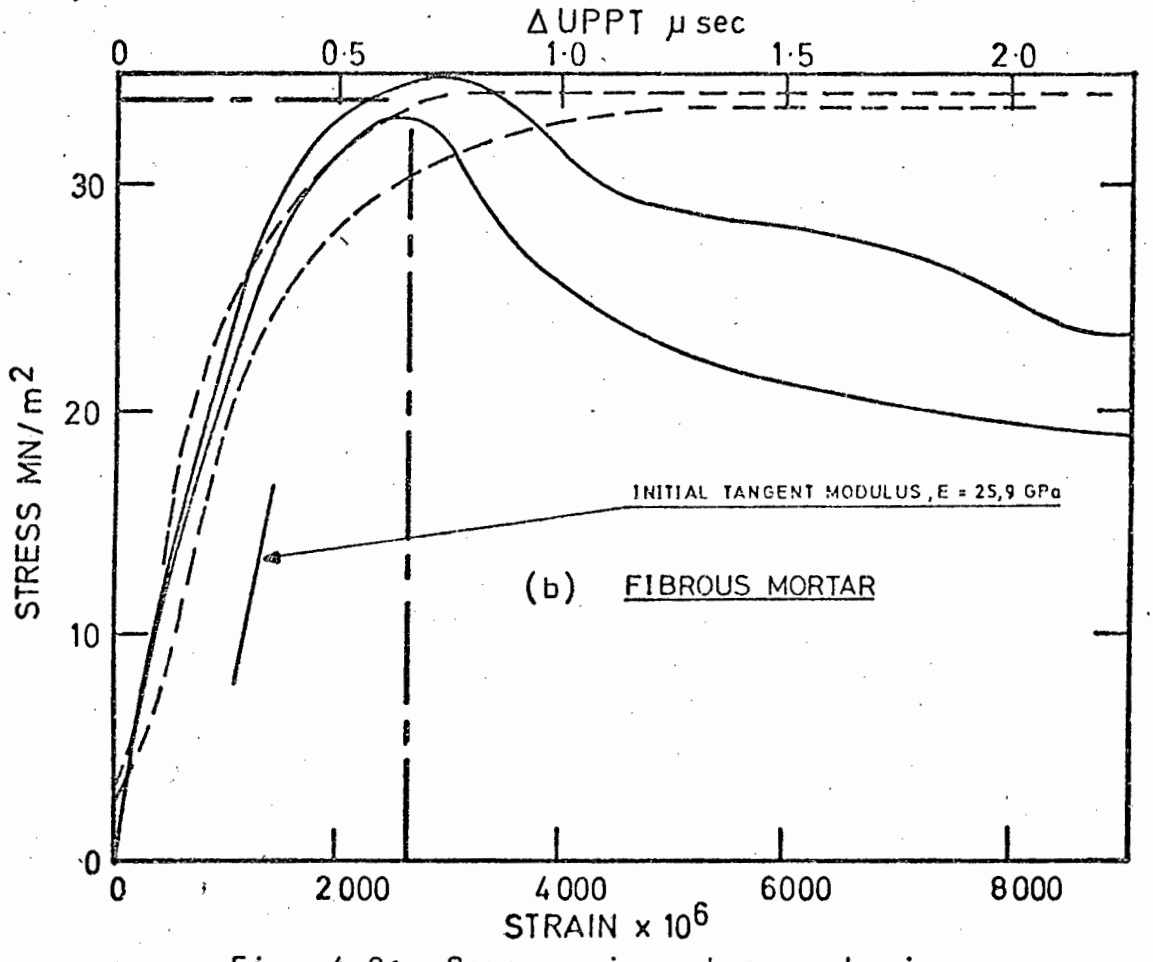

Fig. 4.2: Compressive stress-strain curves with corresponding UPTT measurements for (a) Plain Mortar, and (b) Fibrous Mortar.

(a): Plain mortar.

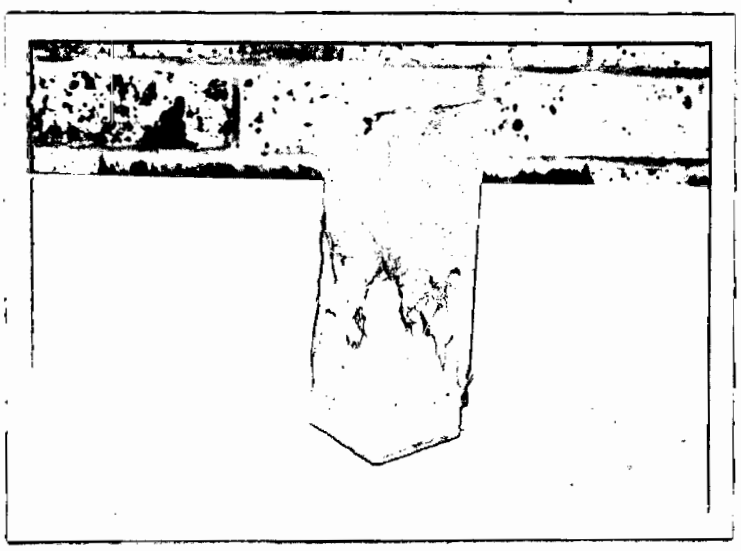

(b): Fibrous mortar.

Fig. 4.3: Comparative difference between compressive failure modes of (a) plain mortar, and (b) steel-fibre reinforced mortar.

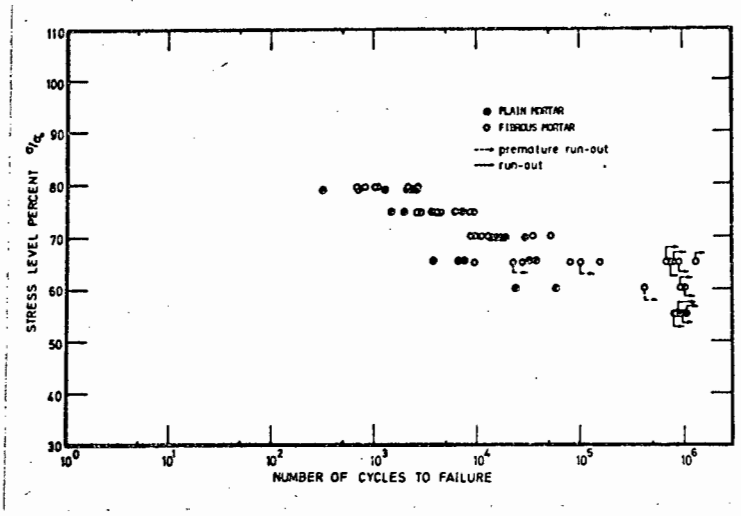

Fig. 4.4(a): S - N data for uniaxial compressive fatigue.

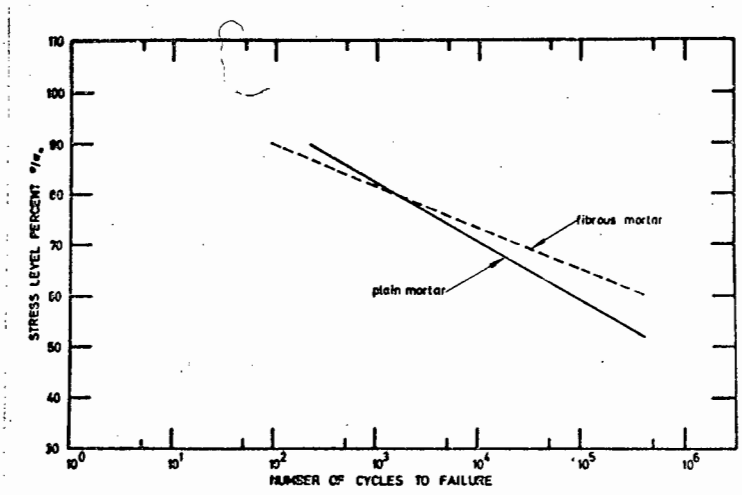

Fig. 4.4(b): 'Best-fit' (average fatigue life at each stress level) S - N curves obtained from data above.

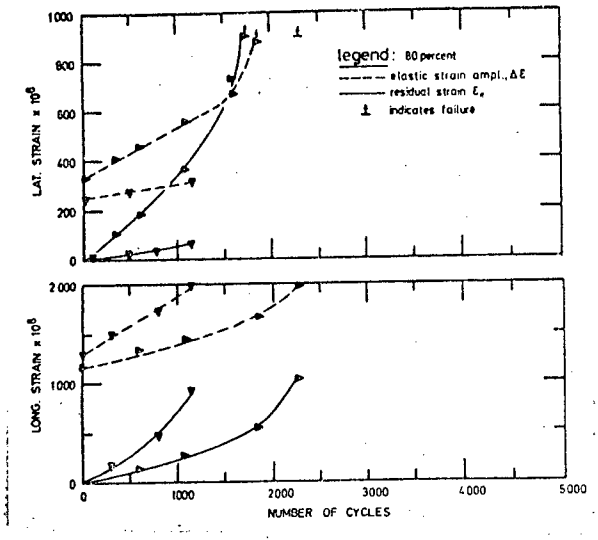

(a): 80% stress level.

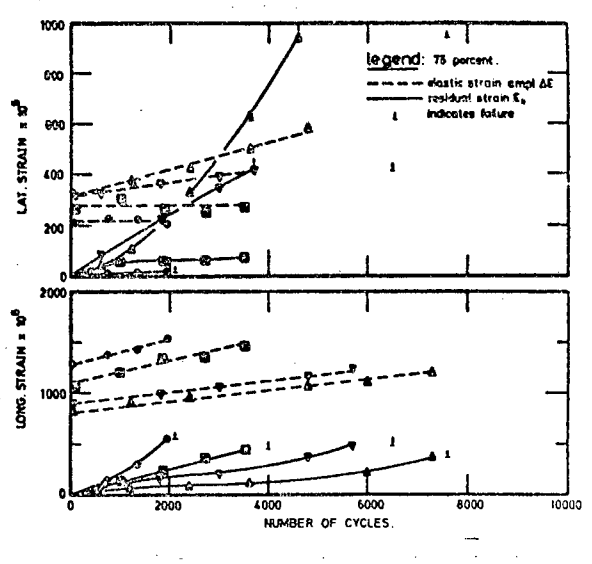

(b): 75% stress level.

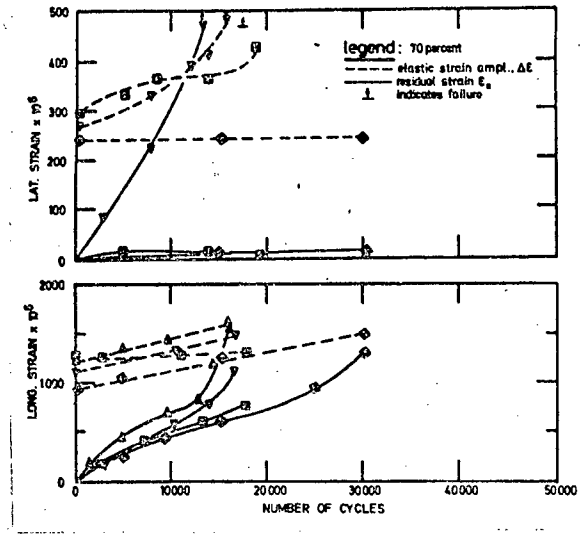

(c): 70% stress level.

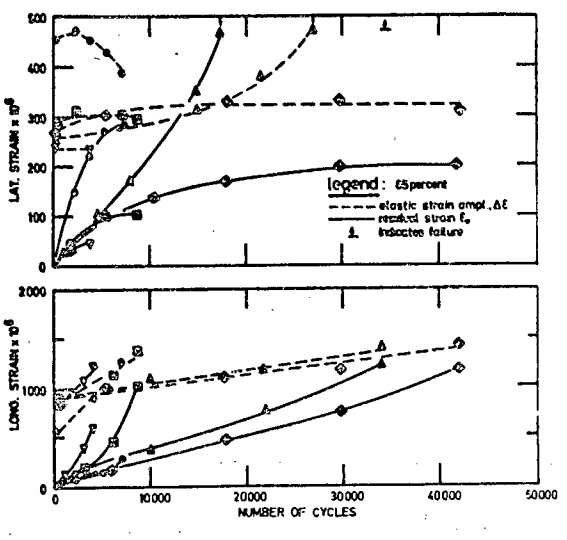

(d): 65% stress level.

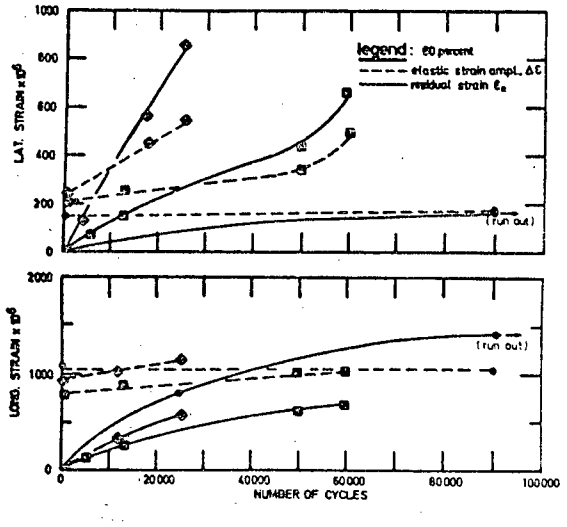

(e): 60% stress level.

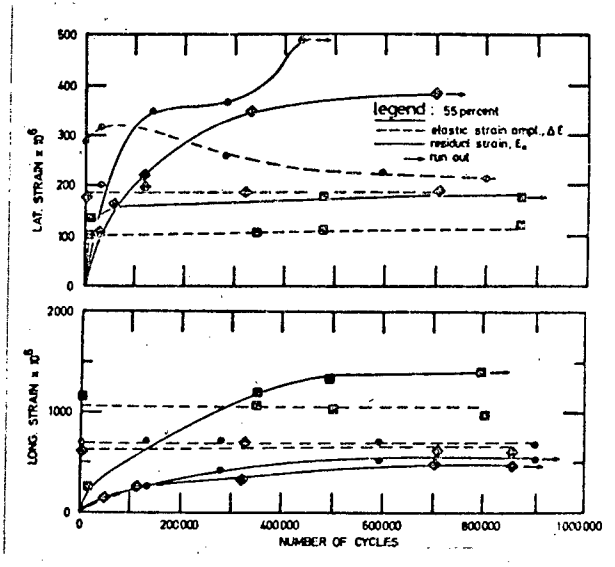

(f): 55% stress level.

Fig. 4.5: Variation in lateral and longitudinal strains, as a function of stress level, with number of cycles to failure - PLAIN MORTAR.

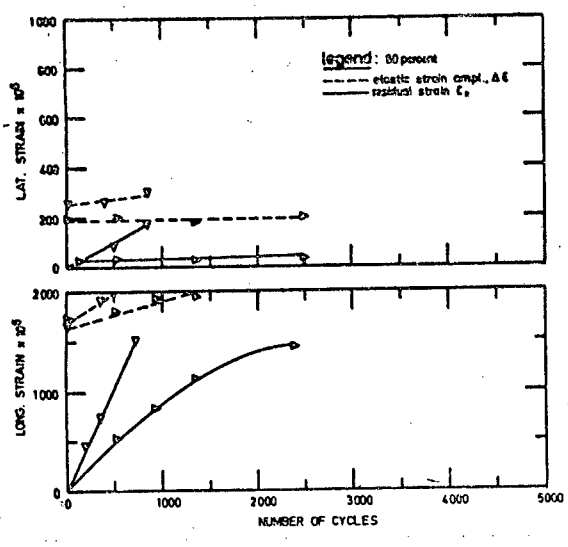

(a): 80% stress level.

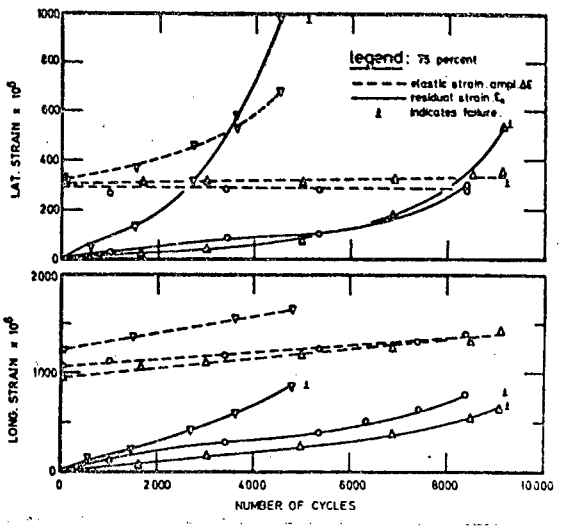

(b): 75% stress level.

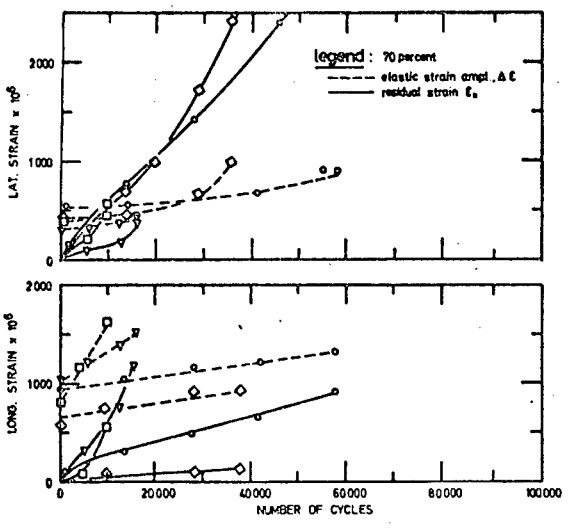

(c): 70% stress level.

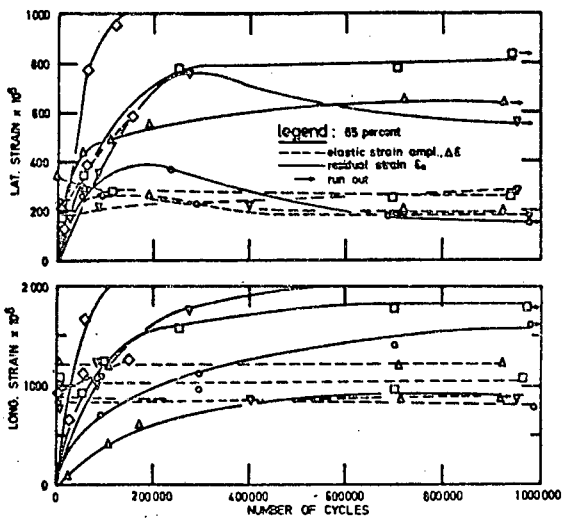

(d): 65% stress level.

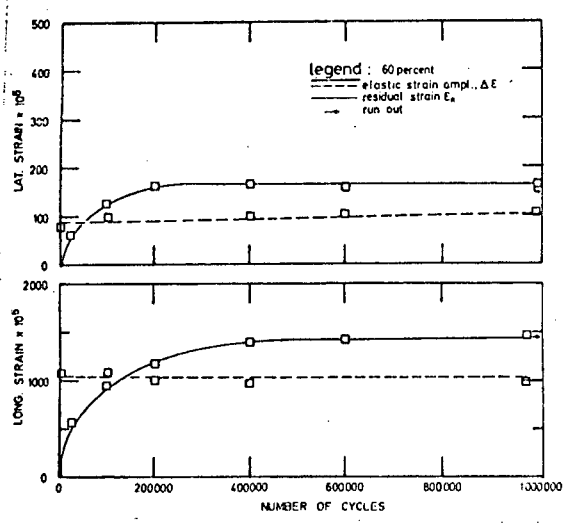

(e): 60% stress level.

Fig. 4.6: Variation in lateral and longitudinal strains, as a function of stress level, with number of cycles to failure - FIBROUS MORTAR.

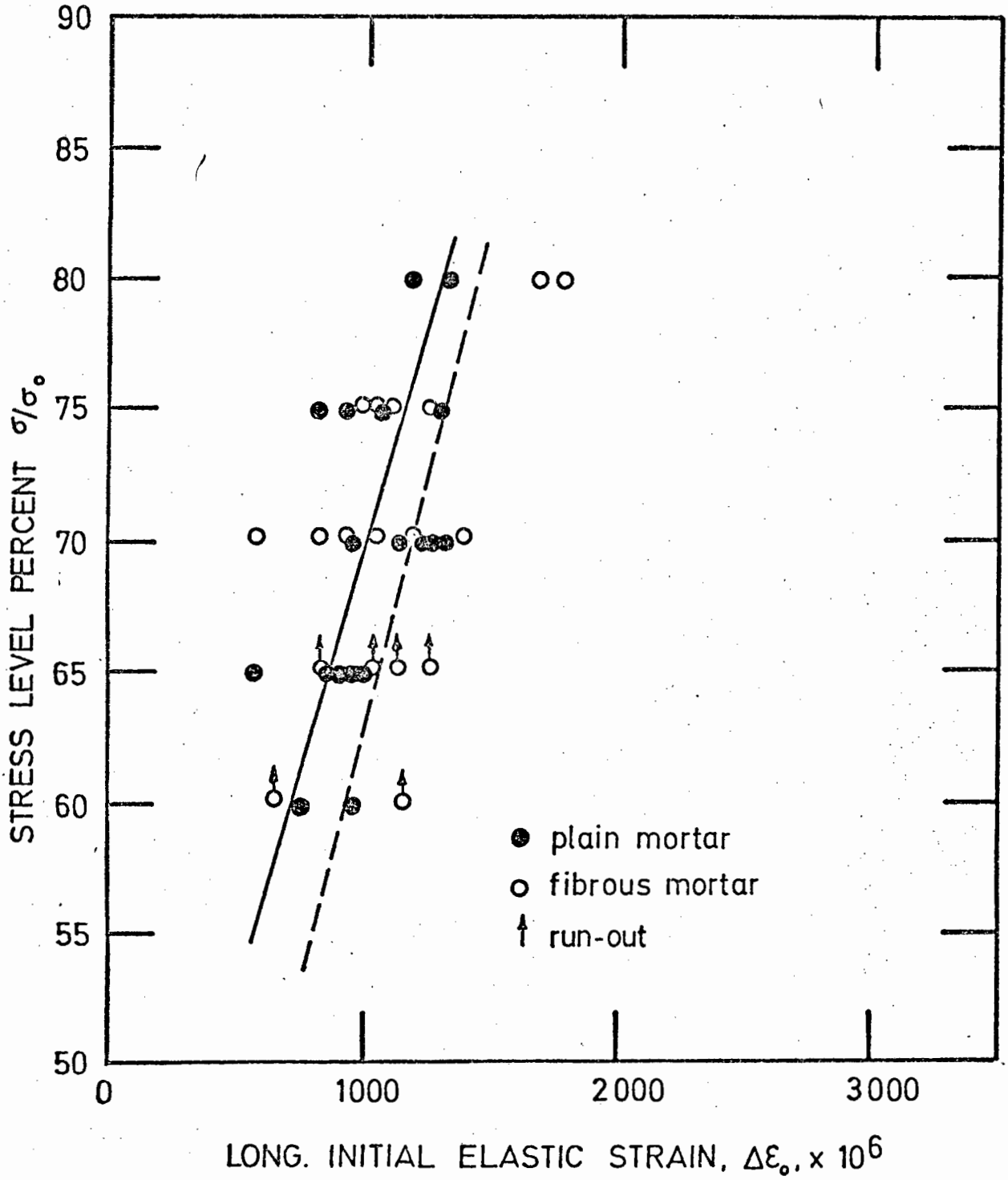

Fig. 4.7: Variations in Initial longitudinal elastic strain amplitude as a function of stress level.

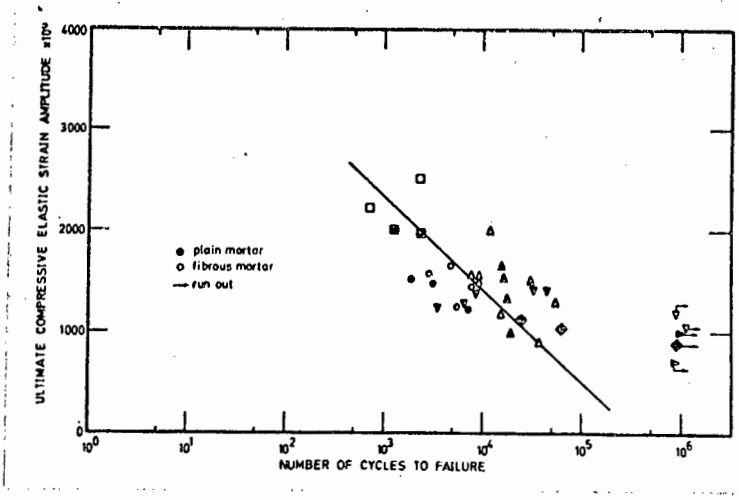

Fig. 4.8: Ultimate longitudinal elastic strain amplitude as a function of fatigue life. (Number of cycles to failure.)

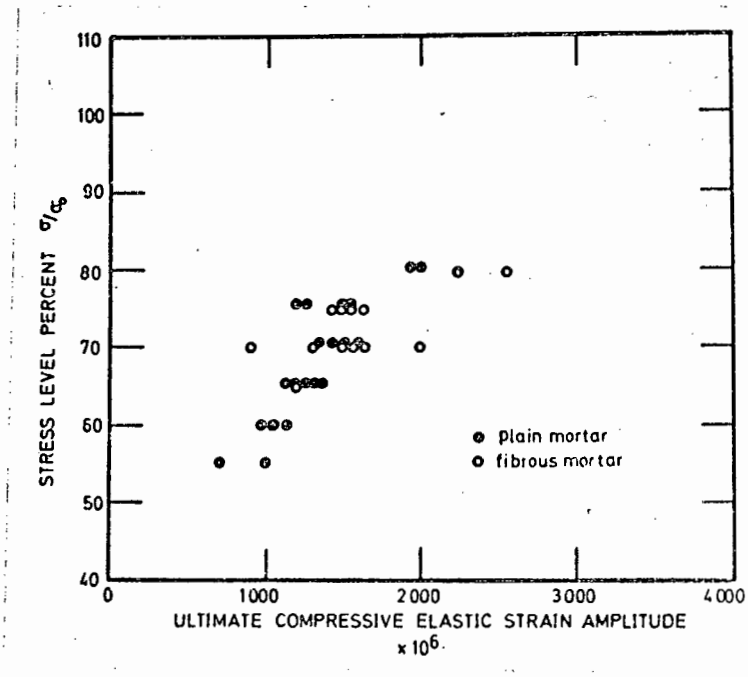

Fig. 4.9: Ultimate longitudinal elastic strain amplitude as a function of stress level.

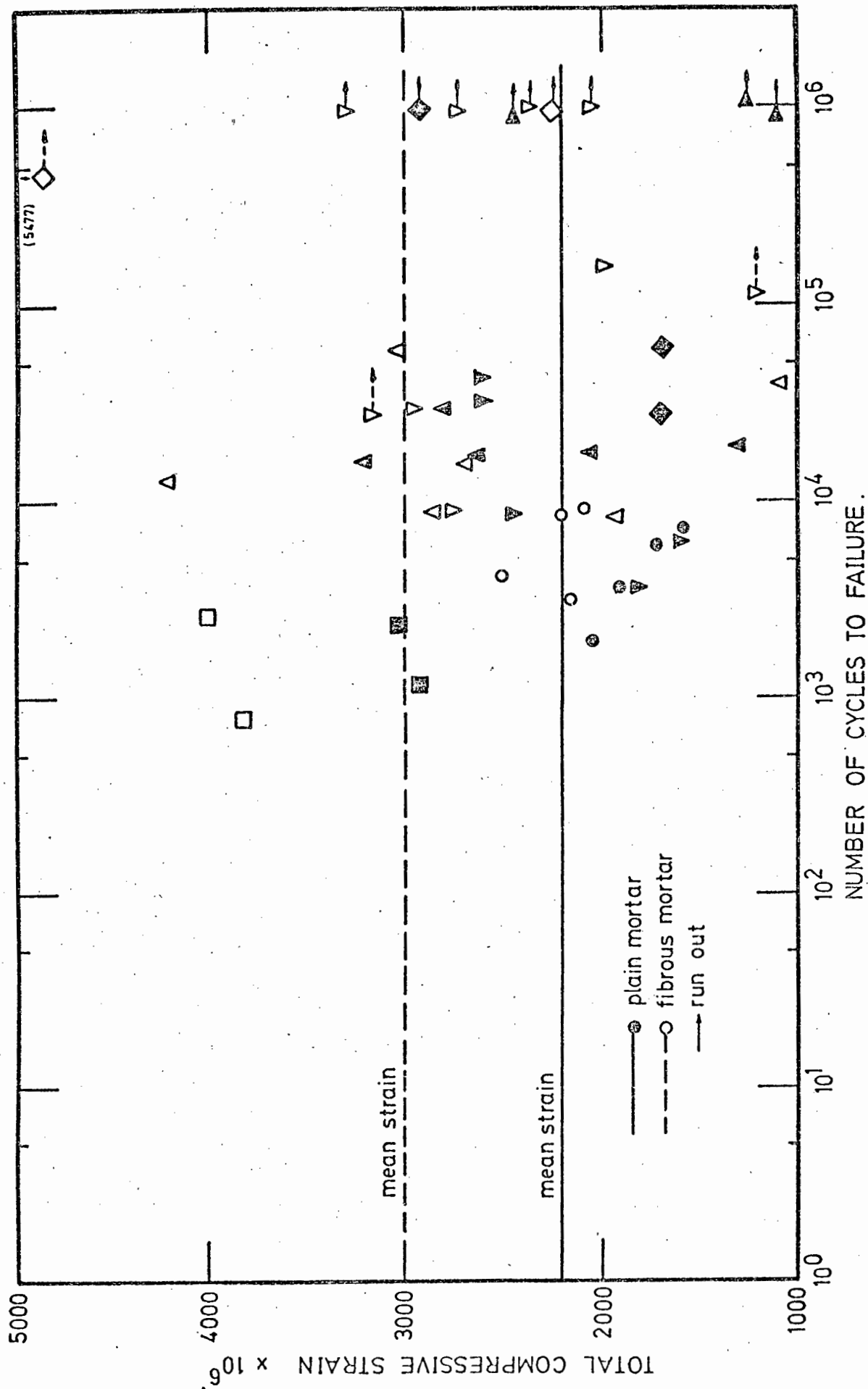

Fig. 4.10: Relationship between Total compressive strains and the number of cycles to failure.

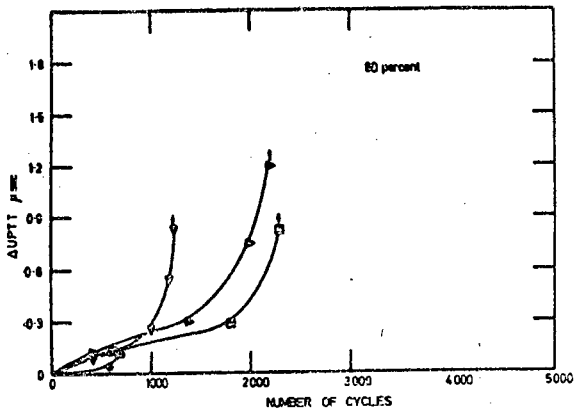

(a): 80% stress level.

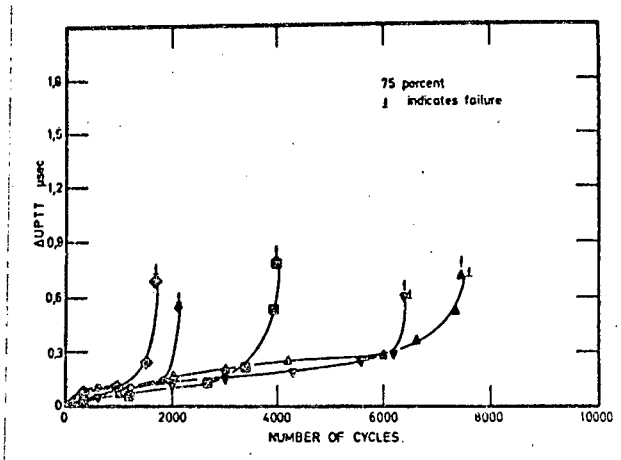

(b): 75% stress level.

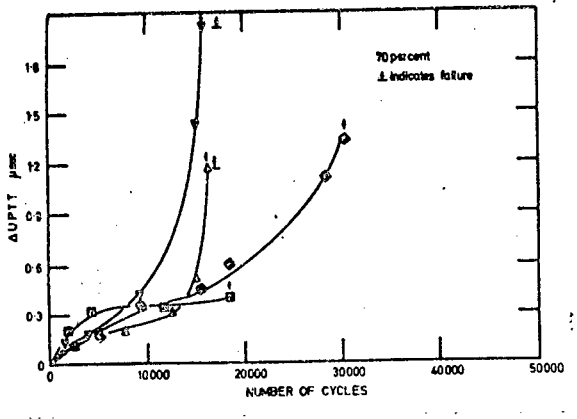

(c): 70% stress level.

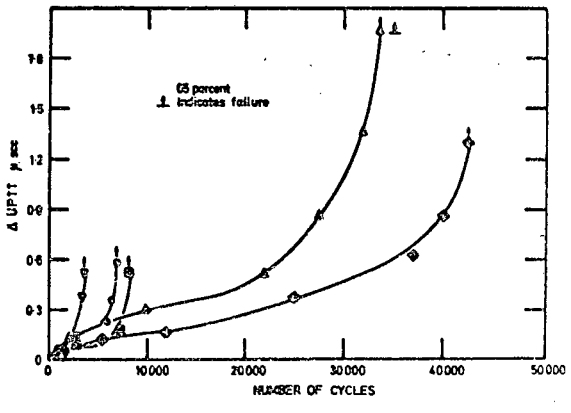

(d): 65% stress level.

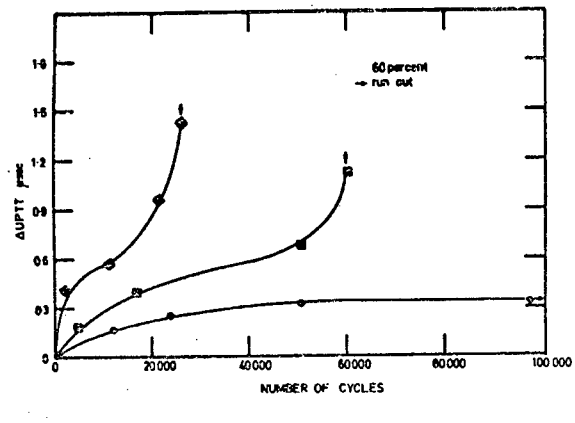

(e): 60% stress level.

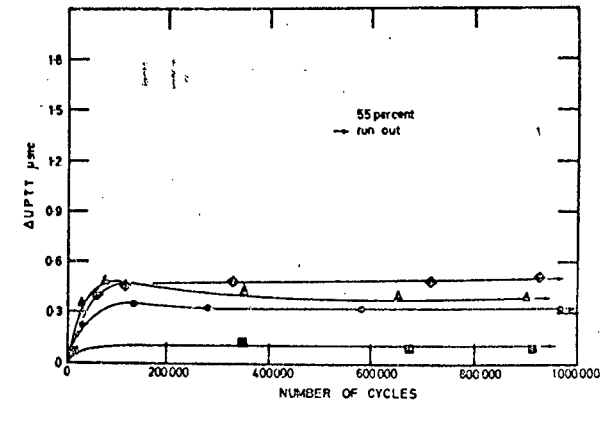

(f): 55% stress level.

Fig. 4.11: Changes in ultrasonic pulse transit times (UPTT), as a function of stress level, with fatigue life - PLAIN MORTAR.

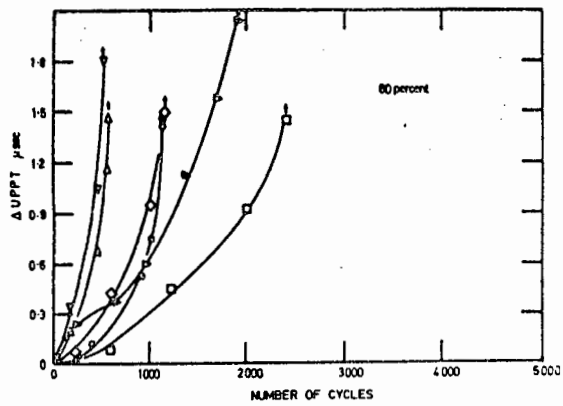

(a): 80% stress level.

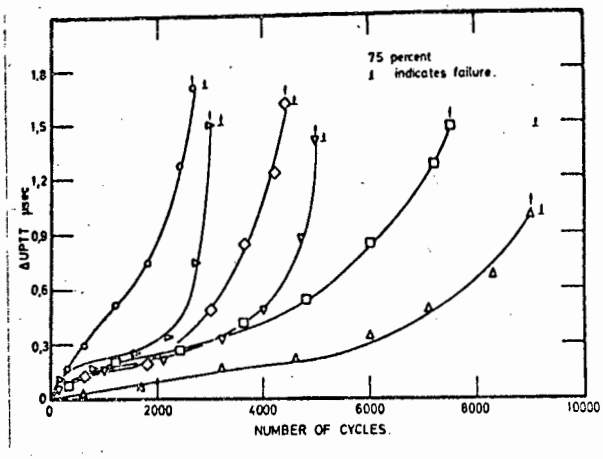

(b): 75% stress level.

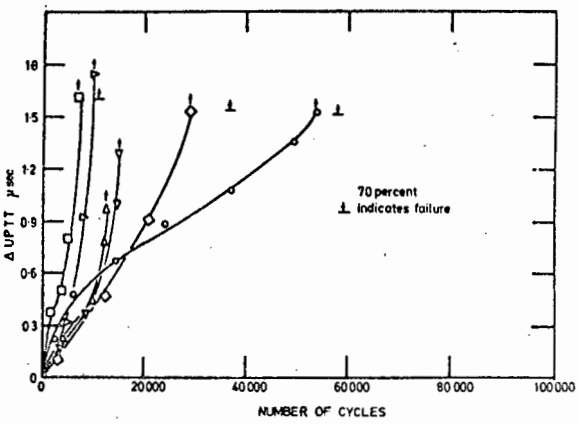

(c): 70% stress level.

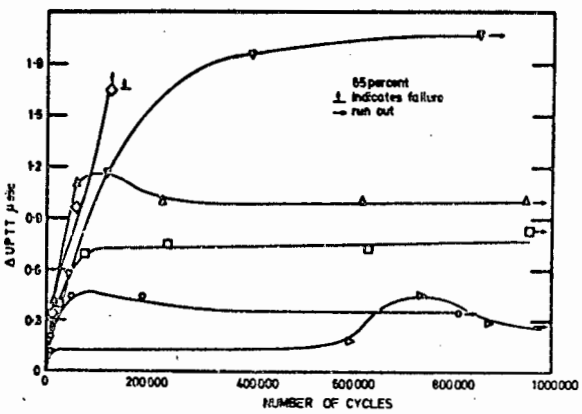

(d): 65% stress level.

Fig. 4.12: Changes in ultrasonic pulse transit times (UPTT), as a function of stress level, with fatigue life - FIBROUS MORTAR.

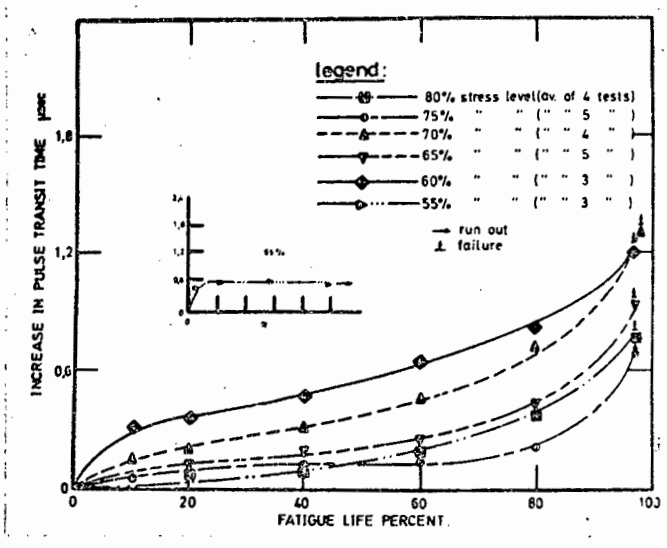

(a): Plain Mortar.

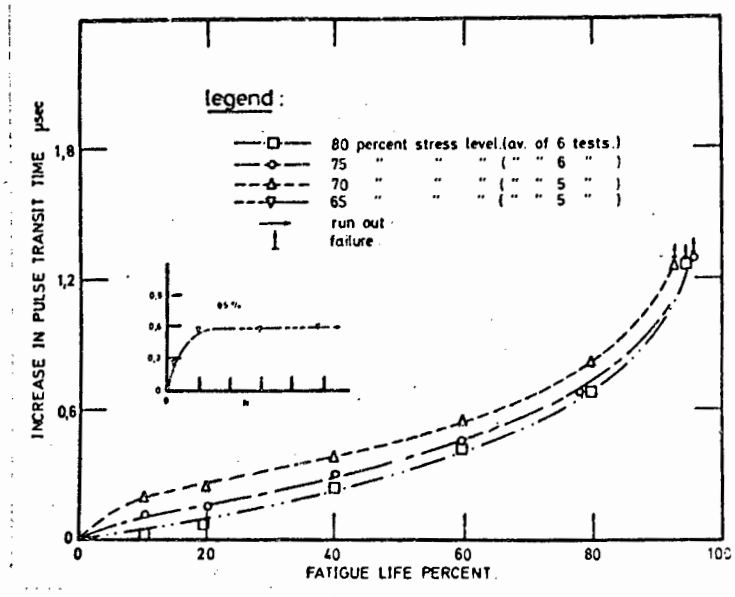

(b): Fibrous Mortar.

Fig. 4.13: Illustrating the variation in incremental changes of ultrasonic pulse transit time, as a function of stress level, with percentage fatigue life.

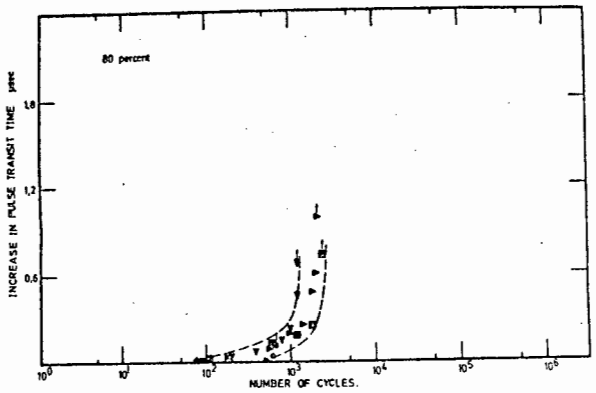

(a): 80% stress level.

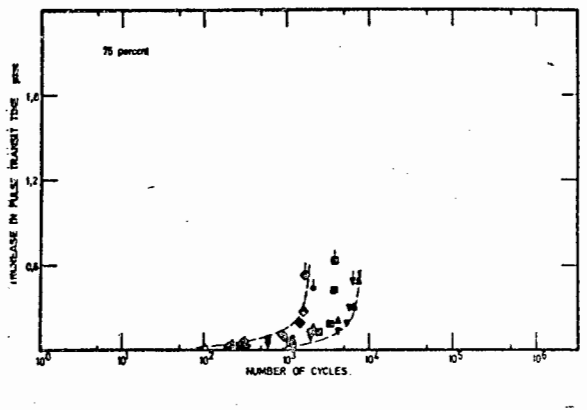

(b): 75% stress level.

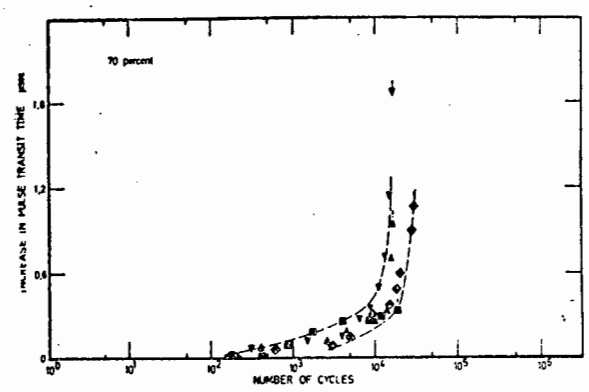

(c): 70% stress level.

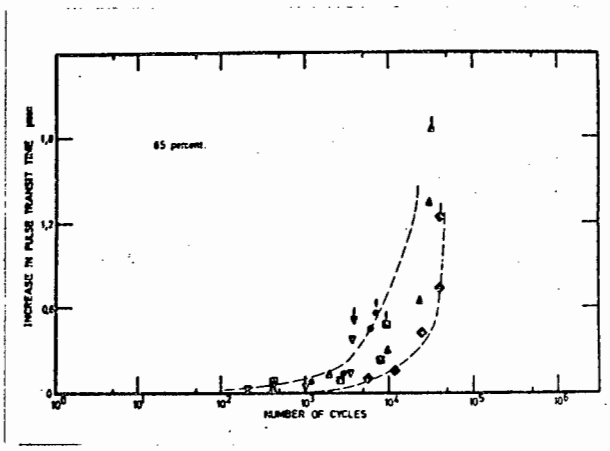

(d): 65% stress level.

Fig. 4.14: Variation in ultrasonic pulse transit times, as a function of stress level, with <u>logarithmic</u> representation of fatigue life - PLAIN MORTAR.

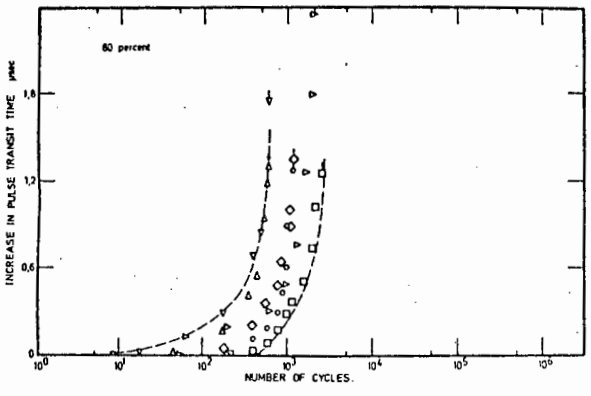

(a): 80% stress level.

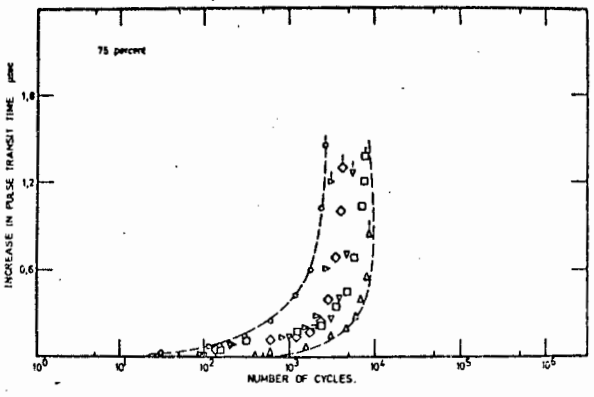

(b): 75% stress level.

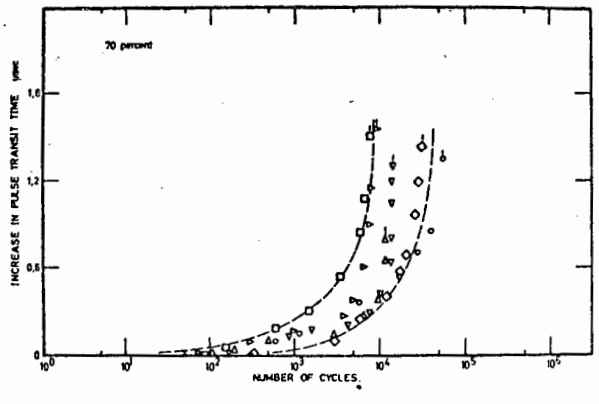

(c): 70% stress level.

Fig. 4.15: Variation in ultrasonic pulse transit times, as a function of stress level, with logarithmic representation of fatigue life - FIBROUS MORTAR.

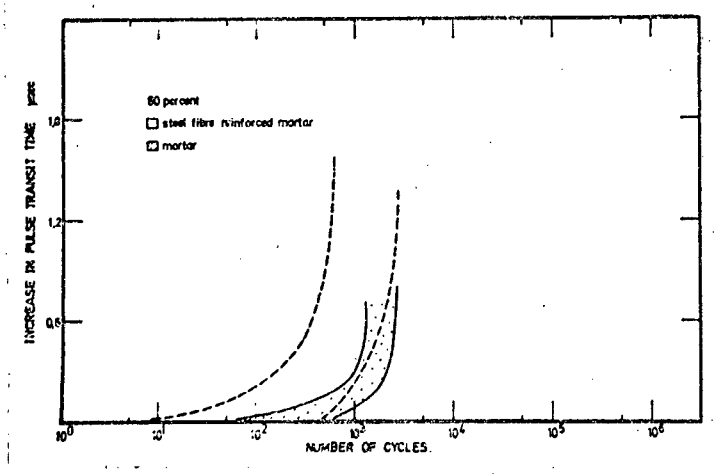

(a): 80% stress level

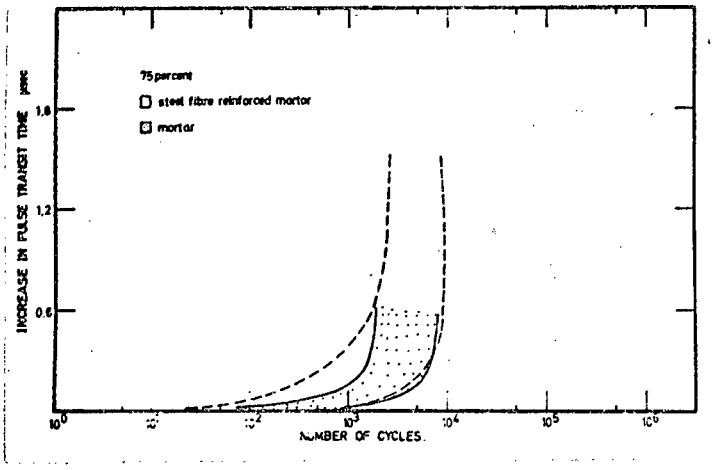

(b): 75% stress level

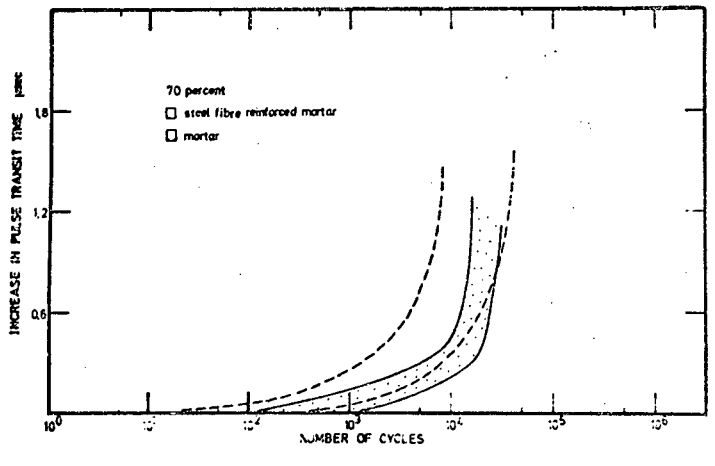

(c): 70% stress level.

Fig. 4.16: Comparison of ultrasonic pulse transit times between PLAIN and FIBROUS MORTAR.

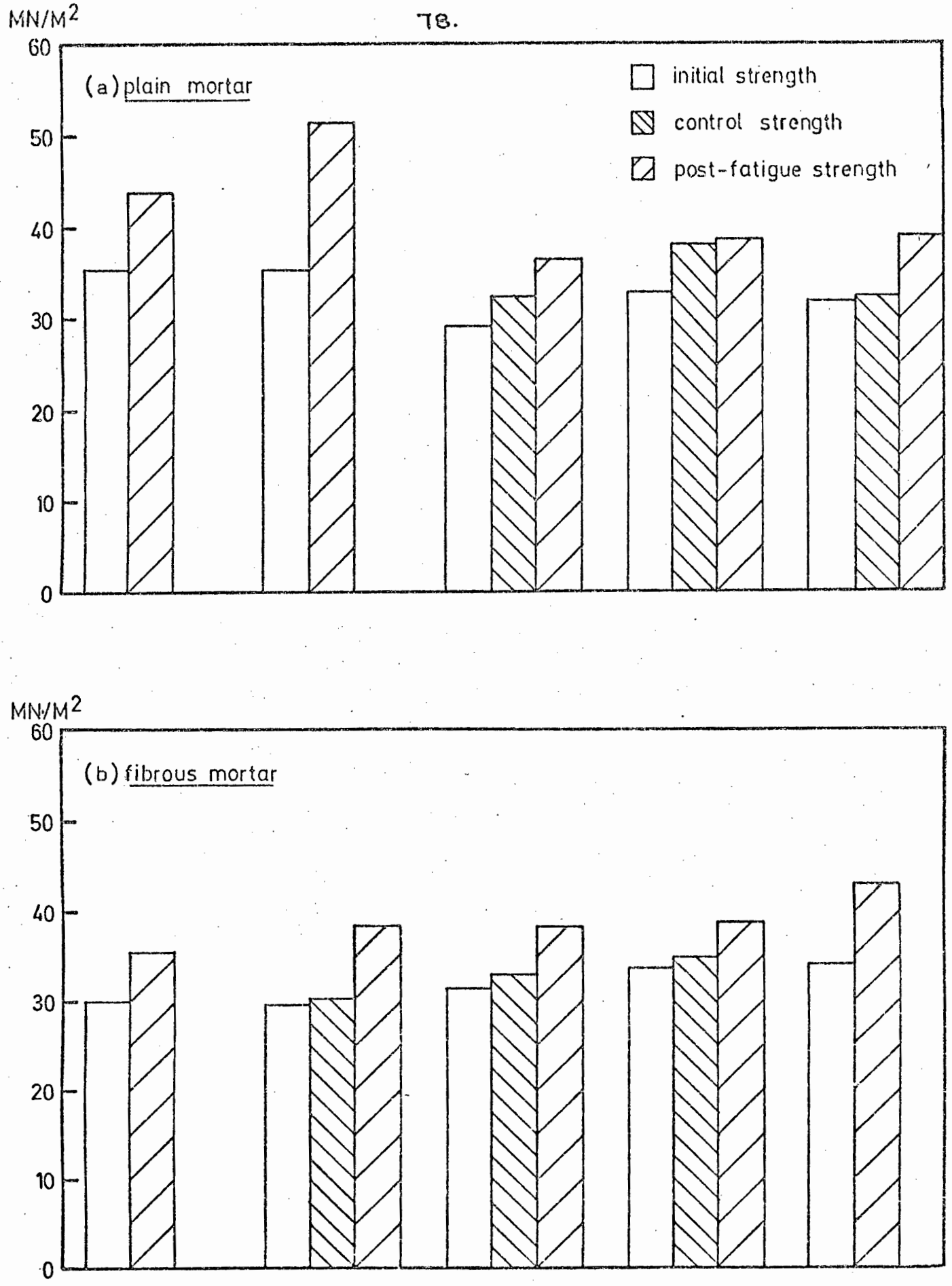

Fig. 4.17: Illustrating the effects of repeated loading on the post-fatigue compressive static strength of (a) Plain Mortar, and (b) Fibrous Mortar.

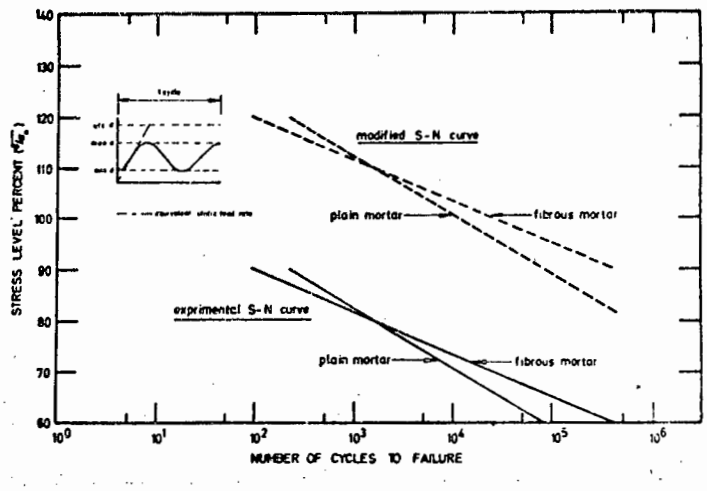

Fig. 4.18: Modified S - N curves.

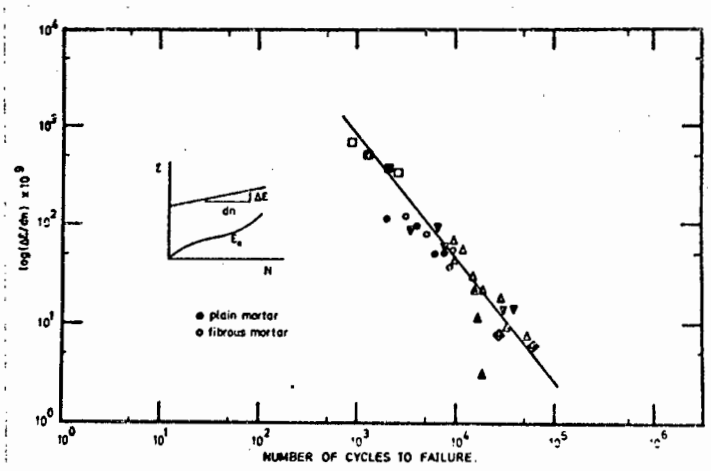

Fig. 4.19: Showing the rate of change in longitudinal elastic strain amplitude with fatigue life.

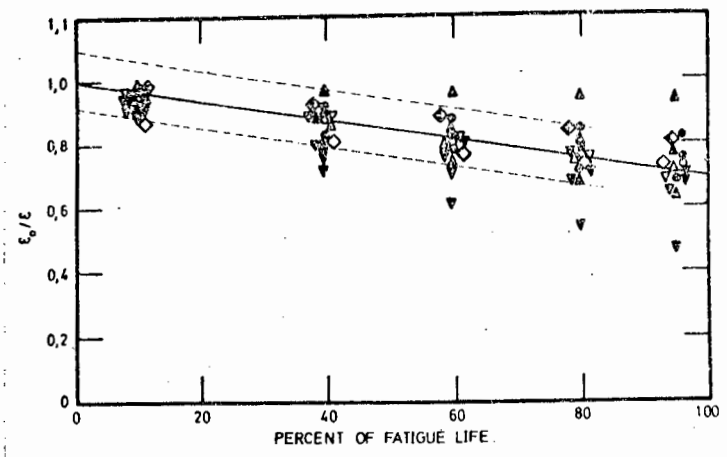

(a): Plain Mortar.

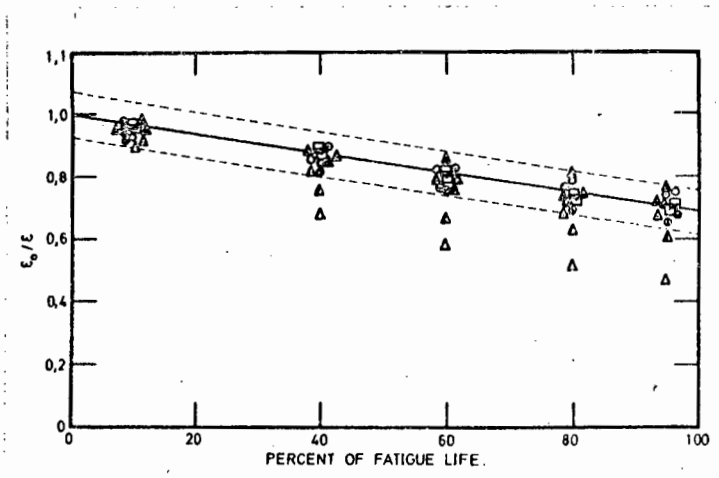

(b): Fibrous Mortar.

Fig. 4.20: Illustrating the increase in longitudinal elastic strain (decrease in elastic modulus) with repeated loading.

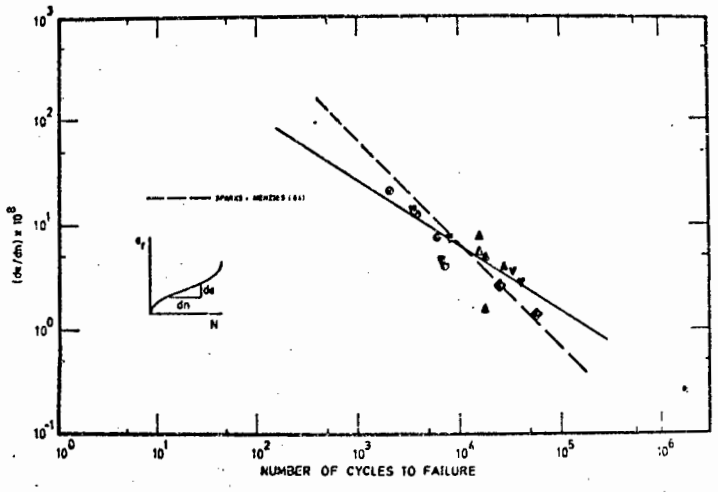

(a): Plain Mortar.

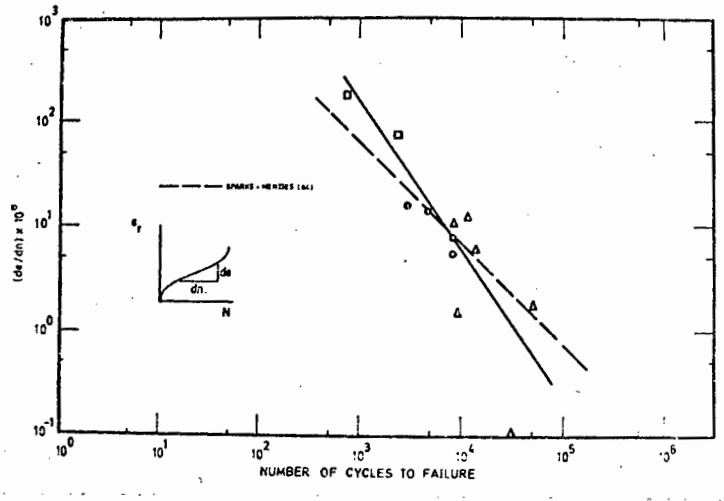

(b): Fibrous Mortar.

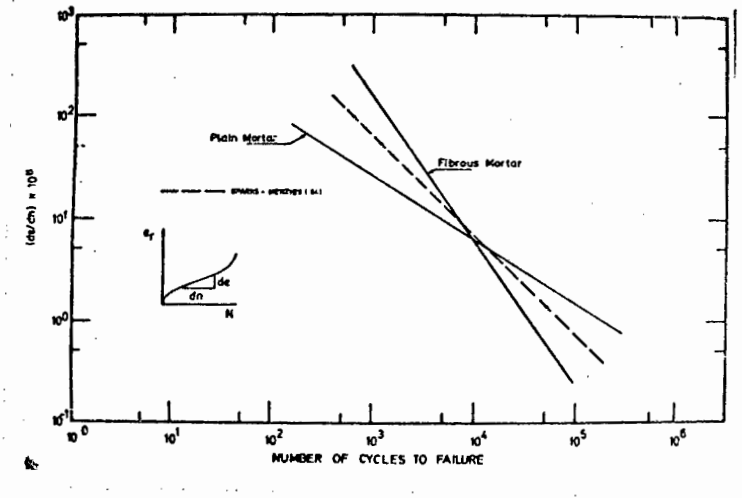

(c): Comparison between plain and fibrous mortar.

Fig. 4.21: Relationship between rate of increase in elastic strain (at specimen half-life) and fatigue life.

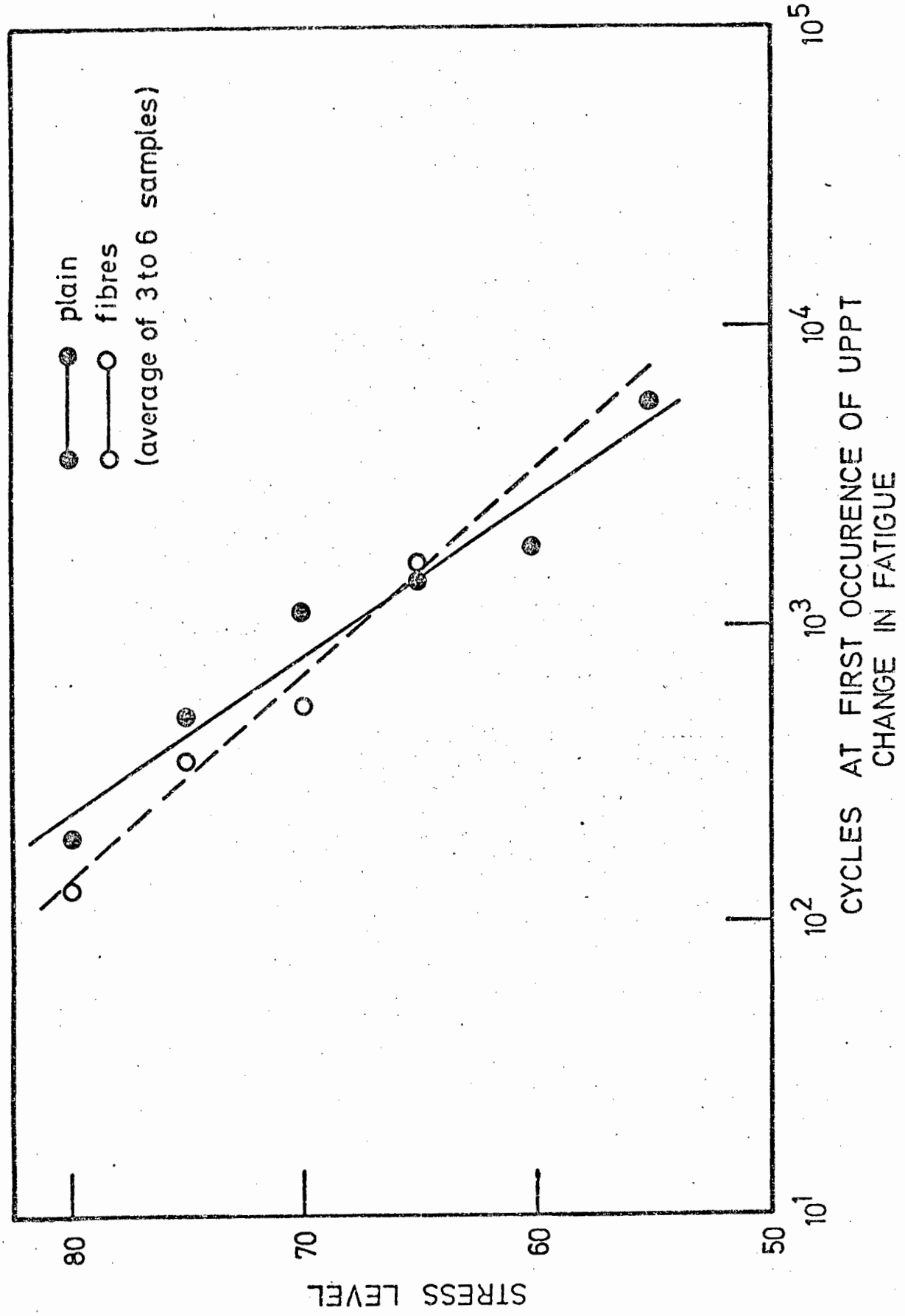

Fig. 4.22: Showing the effects of steel fibre addition on the initiation of UPTT measurements in plain mortar.

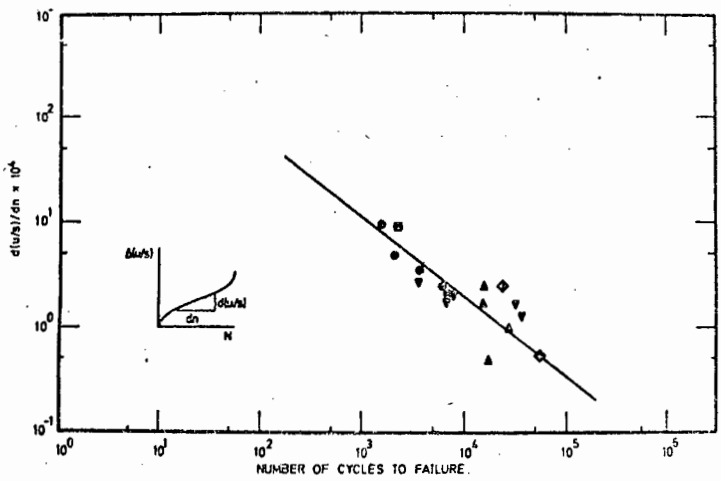

(a): Plain Mortar

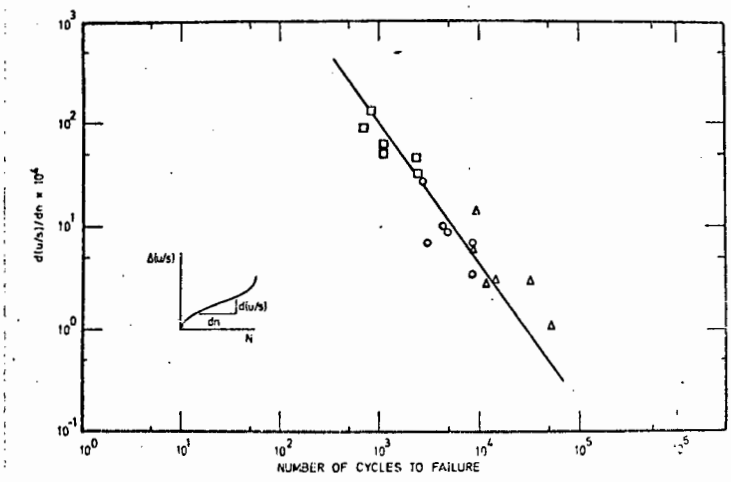

(b): Fibrous Mortar

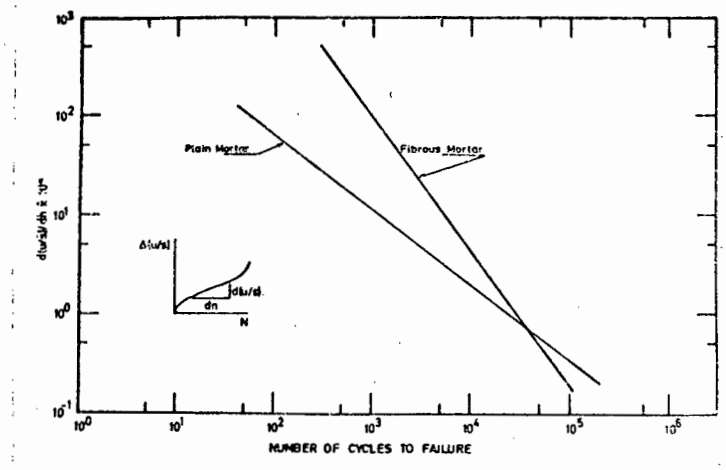

(c): Comparison between plain and fibrous mortar.

Fig. 4.23: Relationship between rate of increase in UPTT (at specimen half-life) and fatigue life.

CHAPTER 5

5. DIRECT TENSILE BEHAVIOUR OF CEMENT-BASED MATERIALS

5.1. INTRODUCTION

It should be evident from the preceding discussion that the compressive failure of cement-based materials can largely be attributed to tensile stresses. Large changes in ultrasonic pulse transit time normal to the direction of the applied compressive load (Chapter 4) are indicative of crack formation parallel to the line of load application. Since there can be no compressive load component normal to the direction of applied load the opening of these cracks must arise due to tensile stresses. Jones (57), in fact, has observed little change in UPTT parallel to the direction of the applied compressive load relative to changes measured normal to that direction. He also concludes, therefore, that failure is due purely to tensile stresses.

In spite of these observations which indicate the importance of tensile crack opening in controlling deformation and failure in cement and concrete, little investigation of failure in tension has been carried out, particularly when compared to the extensive work performed under compressive and flexural loading. An appreciation of the factors specifically affecting the tensile strength (although not taken into account in design considerations) together with an understanding of the corresponding tensile fracture modes and mechanisms could well assist in obtaining an improved overall understanding of the deformation and fracture behaviour of concrete under the more common loading conditions.

Reasons for the paucity of information relating to direct tensile testing include: firstly, the problems involved in obtaining a pure tensile force, free from eccentricity; and secondly, complications arising from secondary stresses induced by the tensile grips. Furthermore, as mentioned previously, cement-based materials contain numerous discontinuities, e.g. capillary pores and voids, which lead to stress concentrations in localised regions within the matrix. These

regions can then undergo microscopic fracture while the nominal applied load in the test specimen is still comparatively low. These discontinuities, or flaws, will vary in size and it is likely that only the few larger ones or the coalescence of several smaller ones will contribute significantly to the failure process. Consequently, tensile failure loads and other tensile characteristics will typically exhibit high variability. It follows that tensile characteristics, more so than compressive or flexural properties, must be described in terms of a statistical probability, particularly in view of the unstable nature of tensile fracture of brittle materials. This is readily appreciated when comparing the coefficient of variation (which describe the relative scatter of results) of the mean static strengths for stable and unstable failure modes, figs. 4.1 and 5.2 respectively.

5.1.1. Indirect Tensile Testing Methods

Various indirect tensile tests have been used extensively to attempt to measure the static tensile properties of cement-based materials. However, each have their limitations. For example, the modulus of rupture, as measured from the flexural test (46) assumes an elastic stress distribution. Welsh (90) has shown this to be an erroneous assumption since the modulus of rupture overestimates the true tensile failure stress.

The cylinder splitting test, or "Brazillian Test" (46), is another indirect tensile test which also falsely assumes that concrete remains elastic up to failure. It is evident, therefore, that the direct tensile test has an advantage of not relying on assumptions concerning the relative proportions of elastic and permanent deformation in order to calculate the failure stress.

Although there is no standard direct tensile test for cementitious materials, a number of tests have been devised for testing specimens statically in direct tension and some of these are discussed in the following section.

Analogous to the indirect methods of static tensile

property determination, the fatigue behaviour of cements in tension has been studied mainly by means of flexural tests on small beams. It is apparent from the literature that fatigue loading in uniaxial tension has thus far remained unresearched. The reason for this is probably associated with experimental difficulties which become even more severe than those arising in static tensile tests.

5.1.2. Direct Static Tensile Test Methods

A number of tests have been proposed for testing specimens in direct tension. As far back as 1865 Grant (91) devised a method for testing briquettes. Many of these tests have been summarised in a RILEM inquiry (52), published in 1963.

The most common techniques that have been investigated prior, and subsequent, to the RILEM inquiry can be divided into four different categories, depending upon the method of clamping the ends of the test specimen to the test rig. Referring to fig. 5.1, these are:

(i) friction grips with the lateral force applied by means of a scissor action (23,53);
(ii) by means of embedded steel bars (92,93);
(iii) glueing end plates to the test specimen (94);
(iv) by means of tapered concrete sections or truncated cones (95).

Elvery and Haroun (95) have discussed all these methods pointing out various drawbacks including: load eccentricity and non-uniformity of stress, (i)-(iv); the central location and good bond of embedded bars, (ii); poor adhestion between steel plates and concrete, (iii); the elaborate specimen preparation and casting techniques required, (iv).

From the literature, therefore, it would seem that there are a number of direct static tensile test methods available, each having their own particular advantage and limitations. It is certainly necessary to have an appreciation of the various factors involved in order to select, or refine, the

method most appropriate to the current comparative investigation.

5.1.3. Experimental Objective

As mentioned in Chapter 1, the inclusion of steel fibres in a cementitious matrix is primarily to inhibit or retard the propagation of tensile cracks which are recognised to be the major contributing factor to concrete failure. One of the aims of this thesis, then, was to develop a fully instrumented tensile test for reliable use under both static and fatigue loading. The technique developed has been described in Chapter 3.

The remaining sections of this chapter discuss the feasibility of such a testing technique with respect to the test results obtained in direct tension (static and fatigue). From these results it is also possible to observe the direct consequences of steel fibre reinforcement within a mortar matrix compared to the relatively more complex situation arising in compression (Chapter 4).

5.2. STATIC PROPERTIES

5.2.1. Experimental Results

5.2.1.(a) Mean Strength: The addition of steel fibres was found to increase the ultimate static tensile strength of mortar from an average value of 3,45 N/mm^2 to an average value of 5,64 N/mm^2, as shown in fig. 5.2, representing an approximate 60% increase in static ultimate tensile strength.

5.2.1.(b) Stress-Strain Behaviour: Typical tensile stress-strain curves are shown in figs. 5.3(a,b) for plain and fibrous mortar, together with corresponding changes in ultrasonic pulse transit time.

In a similar manner to the compressive properties, the steel-fibre reinforced mortar exhibits a far superior load-bearing capacity after the initiation of macro-cracking (herein defined as the limit of proportionality or deviation from linearity, which in this case corresponds to the failure stress of plain mortar). There is, therefore, a substantial increase in toughness of plain mortar with the addition of steel fibres, as measured by the area under the stress-strain curve. The plain mortar fails in a typically brittle manner, fig. 5.3(a), while the fibre reinforced composite results in a 'pseudo-ductile' mode of failure, fig. 5.3(b). This significant increase in energy required for final fracture is also illustrated by comparing relative fracture surfaces, fig. 5.4(a,b), the fibrous mortar exhibiting a greater fracture surface area than the plain mortar. It can also be seen that final fracture of the reinforced composite, fig. 5.3(b), does not result from the fracture of any individual steel fibres, but rather from fibre pull-out; this also contributes to the energy required for final failure.

As would be expected for such low volume fractions of steel fibres, i.e. 2%, the change in elastic modulus with fibre addition is insignificant compared to the fibre composite's greater ability to withstand load, i.e. both toughness and ultimate strength. This observation is consistent with that predicted by a simple law of mixtures (Chapter 2)

as will be shown later.

Deviation from linearity, i.e. initiation of permanent deformation or macro-cracking, in fibre reinforced mortar appears to occur at approximately the same stress-strain as matrix failure (ultimate failure) in unreinforced mortar. The strain corresponding to the maximum observed stress, on the other hand, is substantially increased with the addition of fibres.

The presence of steel fibres also significantly affects the initiation of micro-cracking (defined as the point at which the ultrasonic pulse velocity starts to decrease) which occurs in the early stages of loading. This is illustrated by corresponding changes in ultrasonic pulse transit time (UPTT), figs. 5.3(a,b). However, in contrast to compression failure where fibres induce earlier cracking, pure tensile cracks are initiated at a higher stress-strain in fibrous mortar compared to plain mortar (changes in UPTT being due primarily to micro-cracking).

5.2.2. Discussion

Increases in the direct tensile strength of cement-based materials reinforced with steel fibres have been reported previously (21, 22). These results and others are summarised in table 5.1. The 60% increase in ultimate tensile strength observed in this investigation is of the same order of magnitude as that found by Shah and Rangan (21) who observed a 30% increase in the maximum tensile strength of a mortar containing a 1,25% (by volume) concentration of a 2-dimensional array of aligned steel fibres. These authors found the 30% increase to be consistent with the theory of elasticity and their composite materials analysis (reviewed in Chapter 2). However, the composite materials analysis used by Shah and Rangan would appear to under-estimate the ultimate strength increase observed in this investigation as shown in table 2.1, although the percentage increases are of the same order.

Increases have also been shown to be directly proportional to the product of fibre concentration and aspect ratio (22,67). In these instances, fibre spacing was not found to be the

fundamental governing parameter as proposed by Romualdi and Batson (3), who, it will be recalled, predicted an increase of nearly two-and-a-half times in the direct tensile stress with a fibre spacing of approximately 8 mm (0,3 inches).

Although no cohesive explanation has been offered by the above authors (3, 21, 22, 67), it can be reasonably assumed that they have attributed increases in the static tensile strength due to fibre addition to the partial load carrying capacity and crack-arresting role of the fibres. Certainly, evidence for the fibres acting in this manner can be derived from experimental results obtained in this study such as the delay in the initiation of micro-cracking (as indicated by ultrasonic measurements), the fibrous mortar's extensive increase in toughness (approx. = area under the stress-strain curve) and its greater load-bearing capacity compared to mortar (figs. 5.3 (a,b)).

Figs. 5.3(a) and 5.4(a) suggest that plain mortar fails in a typically brittle manner, failure being due to the rapid propagation of the critical flaw with no crack growth prior to failure. (Cracking prior to failure is generally associated with non-linear stress-strain characteristics.) However, observed increases in ultrasonic pulse transit time, figs. 5.3(a,b), would suggest that micro-cracking is indeed taking place prior to failure, contrary to the previous statement. It could be argued that these increases in transit time, being relatively small, could be due to changes in specimen length under load. If the transit times are due to length changes, $\sim 110\,\mu\varepsilon$ corresponding to a length change of $\sim$0,013 mm (115 mm gauge length), then the increase in UPTT would be of the same order of percentage increase as the change in specimen length. This would represent an increase of $\sim 5{,}5.\ 10^{-4}$ microseconds for the initial incremental transit times used ($\sim$5 μsecs). Actual increases in ultrasonic pulse transit times are in fact four orders of magnitude greater than this value, suggesting that true micro-cracking is indeed taking place prior to failure. The higher stress/strain at the initiation of micro-cracking in fibrous mortar compared to plain mortar (fig. 5.3) can, in fact, be readily explained

in terms of conventional random fibre reinforcement theory, i.e. the steel fibres become load-bearing delaying the formation of microcracks.

Shah and Rangan (21) considered that the limit of proportionality provides a method of measuring the initiation of cracking and concluded, therefore, that fibre additions had no effect on crack initiation in plain mortars. If the same assumptions regarding the limit of proportionality are made from results obtained herein (and UPTT measurements ignored), this conclusion would be valid. Elvery and Samarai (96, 97) also report similar observations to those of Shah and Rangan (21), indicating that plain mortar fails at approximately the same stress at which cracking occurs in the fibrous specimens. These authors, in fact, used ultrasonics for crack monitoring, so the evident difference between their results and those obtained in this study is likely to be a function of the sensitivity of the ultrasonic equipment. (It is perhaps relevant to note that a commercial PUNDIT apparatus, identical to that developed by Elvery, provided significantly less sensitivity when compared to the sophisticated Harwell instrumentation used throughout this study.)

The limit of proportionality, as explained earlier, is defined (in this study) as the point at which macro-cracking (as distinct from micro-cracking) occurs. As mentioned and similar to Shah and Rangan's results (21), the stress/strain at this point is found to be unaffected by fibre additions. As this limit also corresponds to the failure of the mortar matrix it would be reasonable to suggest that in the fibrous composite the load-bearing capacity is transferred almost completely to the steel fibres which act to bridge the matrix macro-cracks. This would be consistent with the work of Aveston et al. (6) who suggested that multiple matrix cracking occurs at the end of the elastic limit (Chapter 2 - fig. 2.3). Thus the additional increase in stress observed after the onset of matrix cracking will arise due to the stresses maintained by the uniform, but randomly oriented fibres, bridging the newly formed fracture surfaces (the fibres being subjected to tensile and bonding stresses due to their 3-dimensional

randomness). Final failure results from fibre pull-out at a strain far in excess of the failure strain of plain mortar.

Chen and Carson (67) have also observed significant increases in the failure strain of plain concrete with the addition of 2% by volume steel fibres, as have Johnston and Coleman (22). Chen and Carson, however, claim large increases in elastic modulus which contradicts the marginal increase observed in this present, or other (21, 26, 43), investigation (table 5.1). From figs. 5.3(a,b) the increase in elastic modulus with fibre addition is only about 10% which compares favourably with that predicted by the law of mixtures (Chapter 2 - equation 2.5).

5.2.3. Conclusions

The results obtained in this thesis concerning the effects of fibre additions on the direct static tensile properties of plain mortar are as follows:

(1) The modulus of elasticity is only marginally increased with fibre addition, not reflecting the fibrous composite's greater capability to resist deformation and maintain higher loads.

(2) The initiation of micro-cracking, as measured by ultrasonic pulse transit times, is delayed with the addition of steel fibres, as anticipated from conventional random fibre reinforcement theory.

(3) The stress/strain at which macro or multiple matrix cracking is initiated in fibrous mortar, as indicated by a deviation from linearity in the stress-strain curve, corresponds to the stress-strain at failure of plain mortar. Both mixes behave in a nominally elastic manner up to this point.

(4) The ability of the steel fibres to maintain load and inhibit the propagation of cracking is clearly illustrated by the fibrous mortar's higher maximum static tensile stress, substantially increased toughness, and the ductile failure mode compared to plain mortar.

5.3. FATIGUE BEHAVIOUR

Although the concept is hardly unique no information at all is available in the literature concerning the fatigue performance of cement-based materials under direct tensile loading. It was initially intended, therefore, to carry out a comprehensive, comparative study of the tensile fatigue properties of plain and fibrous mortar along the lines of that undertaken in compression. However, because of significant experimental difficulties encountered in developing the testing technique, the time factor precluded such an extensive investigation and tests were only carried out at a limited number of different stress levels. Nevertheless, some interesting results have been obtained, so that certainly the feasibility of such a testing technique can be justified.

5.3.1. Experimental Results

5.3.1.(a) S - N Curve: Fatigue data can be represented using an S - N curve, as previously described. Fig. 5.5(a) presents the results of fatigue tests for both plain and fibrous mortar with the corresponding, best-fit S_f - N curves shown in fig. 5.5(b) (obtained from average fatigue lives at each stress level).

As anticipated in testing cement-based materials in direct tension, there appears to be a greater variation in test results compared to those obtained in uniaxial compression (cf: fig. 4.4(a)). However, certain comparative characteristics are clearly evident:

(1) The fatigue properties of the fibre reinforced mortar are significantly different from those of the plain mortar; in particular, the fatigue life of fibrous mortar is considerably in excess of that of plain mortar at equivalent stress levels (fig. 5.5(b)).

(2) Both systems exhibit linear decreasing relationships between the cyclic stress amplitude and the corresponding number of cycles to failure.

(3) Although at this point in time insufficient data is available to permit unequivocal conclusions, it would appear that fibrous mortar has an endurance limit at run-out

of approximately 1 million cycles at approximately 65-70% of the ultimate static tensile strength. At the 70% stress level for plain mortar there was no evidence of run-out.

5.3.1.(b) Strain Results: Typical strain data for unreinforced and fibre-reinforced mortar, respectively, are shown in figs. 5.6(a-c) and 5.7(a-d) for the various stress levels tested. These strains correspond to deformational changes taking place parallel to the applied stress, i.e. longitudinal strains.

In plain mortar there is neither a change in the elastic strain amplitude $\Delta\varepsilon$, nor an accumulation of residual strain (figs. 5.6(a-c)). This is in direct contrast to mortar reinforced with steel fibres where large changes in both elastic strain amplitude and residual strain occur during fatigue (figs. 5.7(a-d)).

At corresponding stress levels it can be observed that the initial strain amplitude, $\Delta\varepsilon_o$, is greater in fibrous mortar than in plain mortar. (For example, compare figs. 5.6(a) and 5.7(c)). For both plain and fibrous mortar there appear to be only small differences between the average initial strain amplitude at the various stress levels although these do decrease with decreasing stress level, as expected. However, at the stress levels tested, it should be noted that, firstly the considerable variation in $\Delta\varepsilon_o$ at a given stress level (e.g. see fig. 5.6(a)); and secondly, the fact that $\Delta\varepsilon_o$ for plain mortar in some cases exceeds the strain corresponding to the limit of proportionality in static tests (fig. 5.3(a)),(suggesting changes in elastic modulus), both confirm comments made earlier concerning the variability of tensile properties of plain mortar. The presence of randomly distributed flaws of varying size in the mortar substantially affect the observed modulus and tensile strength for a given mix (the coefficient of variation in the latter being as high as 15% for plain mortar, cf. 8 % for corresponding compressive strength).

The larger initial strain amplitudes exhibited by the fibrous mortar (of the order of 200 $\mu\varepsilon$ compared to 100 $\mu\varepsilon$ for

plain mortar) appears to contradict the earlier observation that the addition of fibres has negligible effect upon the elastic modulus of plain mortar in direct tension (5.2.1.(b) - figs. 5.3(a,b)). However, the stress levels at which fibrous mortar was tested were greater than the ultimate static failure strength of plain mortar and certainly beyond the limit of proportionality of the static stress-strain curve for fibrous mortar. Since the initial strains were correspondingly beyond the limit of proportionality, the measured $\Delta\varepsilon_o$ is not purely an elastic value in the case of fibrous mortar.

It is also evident from figs. 5.7(a-d) that, for the fibre reinforced matrix, in several tests observed increases in elastic and residual strain are similar to those characteristic of stable compressive failure, i.e. the curve can be considered in terms of three distinct regions (cf: fig. 4.5(b)).

At this point in time it is not possible to ascertain whether fatigue failure is governed by a limiting strain criteria. Certainly from the results obtained in this investigation there is no evidence to suggest that there should be some critical failure strain (either elastic or residual strain or a summation of both these components). Due to the extreme variability that will be obtained in direct tension, much more data is required to enable any statistically valid conclusions to be drawn.

5.3.1.(c) Ultrasonic Pulse transit time measurements:
Changes in ultrasonic pulse transit times during fatigue of plain mortar were found to be correspondingly smaller than in compression (cf. figs. 5.8(a-c) and 4.11 (a-f)). The largest change at tensile failure was approximately 0,6 μsec (fig. 5.8(c)) whereas changes at the point of failure in compression were as high as 1,2 μsec. Nevertheless, the fact that there even are small changes in UPTT in tension would indicate the occurrence of sub-critical micro-cracking. This would be consistent with the strain and UPTT data obtained under static loading (of plain mortar), where the corresponding changes are also small. Small increases in

UPTT (0,06 μsec) were also observed to occur in the initial loading to mean load prior to fatigue. Furthermore, similar to strain data for plain mortar (fig. 5.6(a-c)), no rapid changes in UPTT prior to fatigue failure were observed.

In contrast to these results, the changes in UPTT during fatigue of fibrous specimens were observed to increase quite substantially (fig. 5.9).

It has been mentioned previously that the sensitivity of ultrasonic pulse velocity measuring equipment is likely to be a contributory factor in obtaining UPTT results. Thus, high sensitivity may allow changes in UPTT to be measured at very low stress/strain but will limit the maximum value in UPTT that can be measured (this value usually being comparatively small for increasing low stress sensitivity). On the other hand, low sensitivity will allow a larger overall maximum value in UPTT to be measured but at the risk of losing information at the low stress/strain end. At the time of testing, the ultrasonic equipment used did not have a switch facility to enable variable sensitivity selection during a test in order to accommodate the maximum change in UPTT that may occur.

Throughout most of the testing programme, therefore, an integrating capacitor giving a 40 μsec full scale was used, (i.e. comparatively high sensitivity as shown in comparison to other work (5.2.2.)). From all the results obtained in compression together with those obtained in tension of plain mortar, there was certainly no reason to suspect that UPTT changes in fibrous mortar in the tensile fatigue tests would exceed the maximum integrating capacitor of the ultrasonic equipment. However, changes in UPTT observed for the fibrous mortar were certainly considerably in excess of 40 μsecs for <u>all</u> stress levels at which tests were carried out. Furthermore, these increases were found to be cyclic in nature, i.e. the value changed depending on the point in the loading cycle, the maximum values of UPTT being associated with the maximum applied cyclic tensile load (fig. 5.9). This observation was confirmed by carrying out low cycle fatigue tests (0.1 Hz) and monitoring both the load cycle and the cyclic waveform of the

UPTT, both these outputs being 'in-phase'.

In the initial stages of fatigue loading of fibrous mortar, the UPTT was observed to increase very rapidly. (This is as expected since the maximum cyclic tensile load is beyond the limit of proportionality at which macro-, or multiple, cracking is initiated, as described earlier.) However, this rapid increase in UPTT was preceded by only small increases in UPTT (fig. 5.9) with correspondingly smaller cyclic amplitudes in UPTT. This is in contrast to the instantaneous increases in ultrasonic pulse transit times measured in compressive fatigue (e.g. fig. 4.11(f)). At some point there typically occurred a large rapid jump in UPTT, the maximum value of which was often in excess of 40 μsecs. Triggering of the integrating capacitor would thus be erratic. This erratic behaviour could be partially alleviated or reduced by adjusting the amplifier gain control of the Harwell system. However, this in turn results in a changed zero or base level with which the relative changes in UPTT are compared, although the actual sensitivity is left unchanged. (Thus the change in UPTT for 'unit' increase in extent of cracking is left unaltered.) Values recorded in this way therefore become somewhat open to interpretation, since it is still unclear whether such marked increases in UPTT correspond to actual, non-uniform cracking or instrumentation associated effects.

It is because of these yet unclear observations that only a 'diagrammatic' illustration of the sequence of events occurring during the fatigue loading of fibrous specimens is shown (fig. 5.9).

5.3.2. Discussion

It is evident from the S - N curves that the addition of steel fibres considerably influences the mechanisms of tensile fatigue failure of plain mortar; certainly reasonably large increases in fatigue life result. Batson et al. (76) and Romualdi (75) have reported large increases in the fatigue life of plain concrete with fibre addition when testing beams in flexure (which may be considered as effecting a tensile mode of failure). However, these authors represented their

fatigue stress level as a percentage of the first cracking strength (measured as the strength at the limit of proportionality), reporting fatigue strength at run-out (2 million cycles) of 83% (76) and 95% (75) for fibrous concrete compared to a value of 55% for plain mortar. Although no data is available for plain mortar at run-out from this investigation, the observed 65-70% fatigue strength (defined in terms of the ultimate static tensile stress) at 1 million cycles (run-out) for fibrous mortar corresponds to a fatigue strength (defined in terms of the stress at the limit of proportionality) of approximately 114%! It may be argued that this value is only an 'apparent' increase for, as in compression, the static loading rate is much lower than the equivalent fatigue loading rate. Further, if the limit of proportionality was determined at a loading rate equivalent to the fatigue loading rate (i.e. corresponding to failure in $\frac{1}{4}$ cycle, i.e. approximately 0,025 sec at 10 Hz) this percentage fatigue strength could well decrease because of the increase in stress corresponding to the limit of proportionality (cf: increase in ultimate compressive static strength with increasing rate of load application (58, 59)). However, further discussion on this point at the present time is not possible because of the lack of experimental information on the effect of strain rate on the tensile stress-strain characteristics both from this investigation and the available literature.

It should be noted that, as mentioned earlier, the large increases in both strain and UPTT of fibrous mortar during fatigue were observed to take place at all stress levels including those which do not produce failure. Although run-out (1 million cycles) was observed in the fibrous mortar to take place at a fatigue strength of 65-70% of ultimate static strength, it is quite probable that due to these former observations failure could take place at, say, 1,5 million cycles. Nevertheless, the significant difference from plain mortar is noted.

The increases observed by Batson et al. (76) and Romualdi (75) were explained in terms of their earlier crack-arresting mechanism (3). Certainly, there is no reason to doubt that the increases observed in this thesis also arise

due to the arrest of cracks and continued increase in load-bearing capacity due to the presence of the steel fibres.

Further evidence for these mechanisms can be found in the strain and ultrasonic pulse transit time measurements (figs. 5.7 and 5.9) as follows: In plain mortar in tension strains are observed to remain generally constant until failure when the specimen fractures catastrophically. Similarly, UPTT is found to change by only a small amount, although this does indicate that microcracking is taking place. (The coalescence of these cracks could be responsible for the typically catastrophic nature of the failure process.)

With the addition of steel fibres, however, large increases in strain and UPTT are observed indicating far more extensive cracking is taking place during fatigue. Since the increases in strain and UPTT are significantly greater than in plain mortar it is not unreasonable to suggest that multiple matrix cracking has taken place with the steel fibres acting to inhibit further crack propagation, thereby prolonging failure. It might be suggested that the extensive cracking exhibited by the fibrous mortar, in tension, arises from the fact that the fibres are acting as crack initiators, as in compression. However, it has been shown that these cracks must be due purely to the matrix properties and not to fibre additions, viz: operating stress levels are all beyond the limit of proportionality.

Fig. 5.10 shows a fibrous specimen immediately prior to failure. (The test was interrupted in order to photograph the test specimen.) An extensive network of cracks is quite visible on the specimen surface with the steel fibres obviously still maintaining a significant proportion of the load.

With reference to fig. 5.9, the sudden, large increases in UPTT could be attributed to sudden, extensive macro-crack propagation which is subsequently arrested before leading to overall failure. However, as mentioned previously, this phenomenon could also be due to electronic effects. Because of the time factor, further tests to investigate this behaviour were not possible.

Further evidence for the steel fibres' ability to maintain load during fatigue, after extensive cracking has taken place, is illustrated by the typically cyclic nature of the UPTT measurements, the maximum transit time corresponding with the maximum tensile load. It seems probable that this cyclic nature of changes in UPTT is due to the opening and closing of cracks. It is also noted that no such observations were made during the tensile fatigue of plain mortar. (Neither was this noted in compressive fatigue.)

5.3.3. Conclusions

(1) Data obtained in this investigation, although it cannot be considered conclusive, would indicate that the method developed for testing tensile specimens in uniaxial direct tension is a reliable and accurate technique for fatigue testing.

(2) The addition of steel fibres, contrary to results obtained in compressive fatigue, significantly increases the fatigue life of plain mortar. However, as in compressive fatigue, the results obtained in tension fatigue for both plain and fibrous mortar may be influenced both by the operating frequency and the loading rate chosen in determining a static strength level (from which fatigue strength is expressed as a percentage).

(3) Initial observations would appear to suggest a fatigue strength at run-out (1 million cycles) of 65-70% for fibrous mortar, based on the maximum static strength. When based on the static limit of proportionality, this value is of the order of 114%. It is noted large increases in strain and UPTT occur suggesting possible failure in excess of 1 million cycles. Nevertheless, the significant difference between fibrous and plain mortar is still clearly evident.

(4) The increases in the load-bearing capacity and resistance to crack growth in fatigue of mortar containing steel fibres, when compared with plain mortar, is indicated by the substantial increases in fatigue life and both strain

and ultrasonic pulse transit time measurements (these latter measurements primarily recording the extent of cracking).

(5) In fibrous mortar large cyclic variations in ultrasonic transit times are found, which imply the opening and closing of the matrix macro-cracks while the fibres themselves maintain load.

	Initiation in Cracking	Limit of Proportion-ality	Modulus of Elasticity	Failure Strain	Ultimate tensile load	Toughness
Decrease						
No signifi-cant change	21, 43, 97	21, 97, AUTHOR	21, 26, 43, AUTHOR		43	
Increase	AUTHOR		67	21, 22, 43, 67, AUTHOR	3, 21, 67, 75, 116, AUTHOR	21, 22, 43, 67, AUTHOR

TABLE 5.1

Influence of Steel-fibre addition on the Static Tensile Properties of Plain cement-based materials

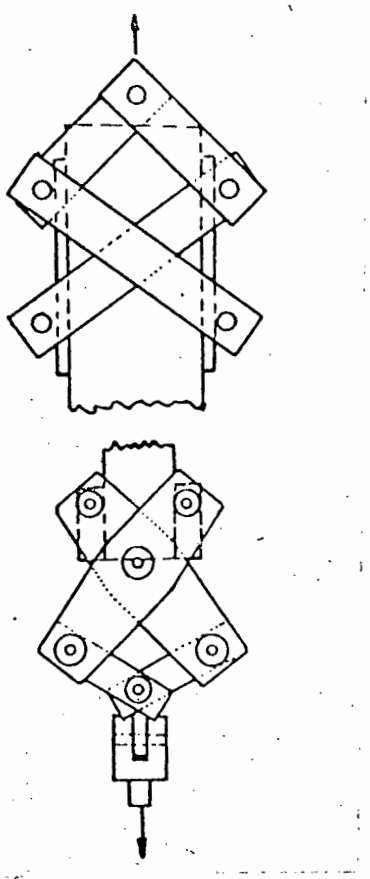

(i): (23, 53)

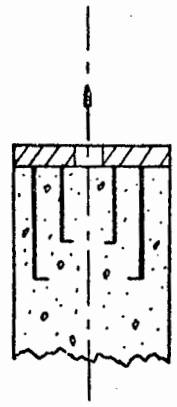

(ii): (92, 93)

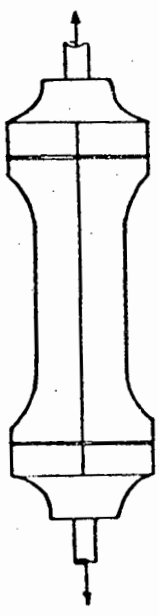

(iii): (94)

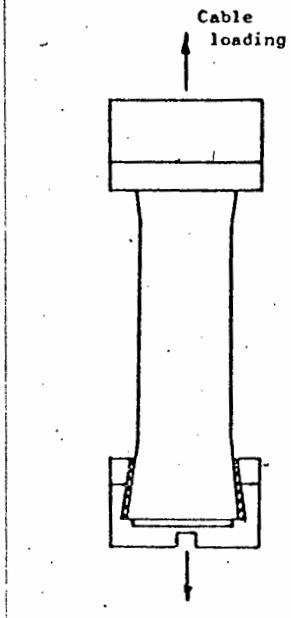

(iv): (95)

Fig. 5.1: Different methods for direct static tensile testing of cement-based materials.

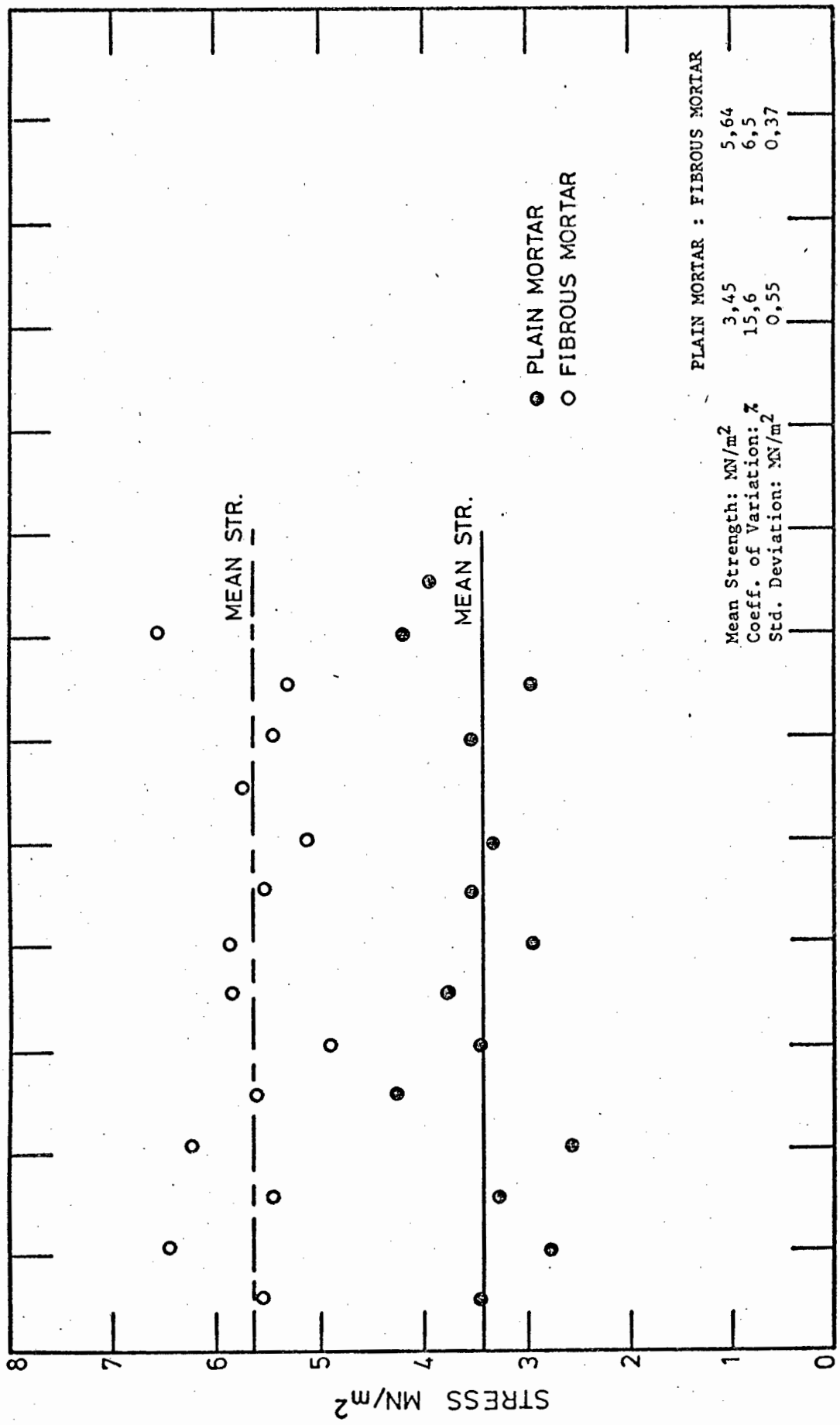

Fig. 5.2: Comparison of Ultimate static tensile strength of Plain and Fibrous Mortar.

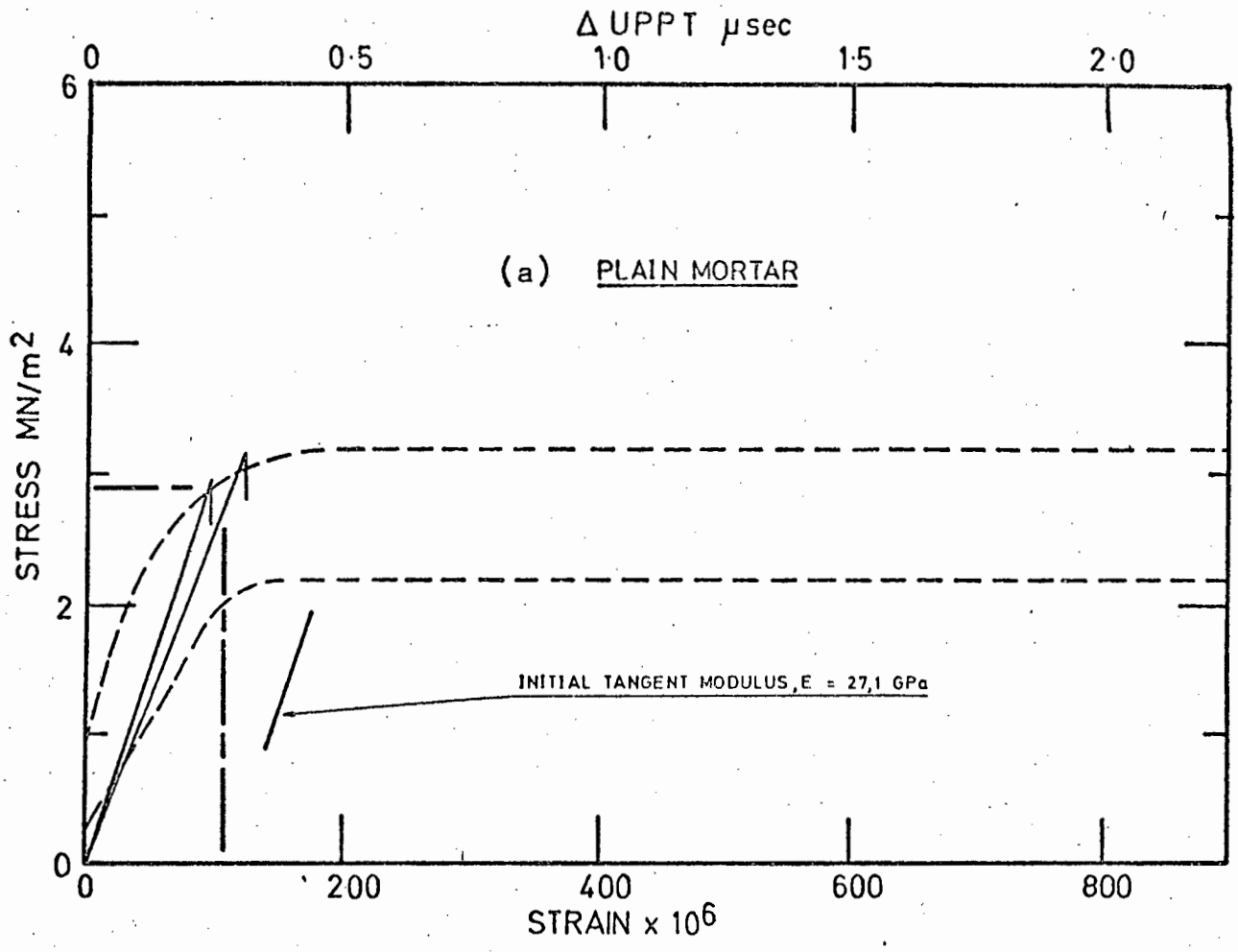

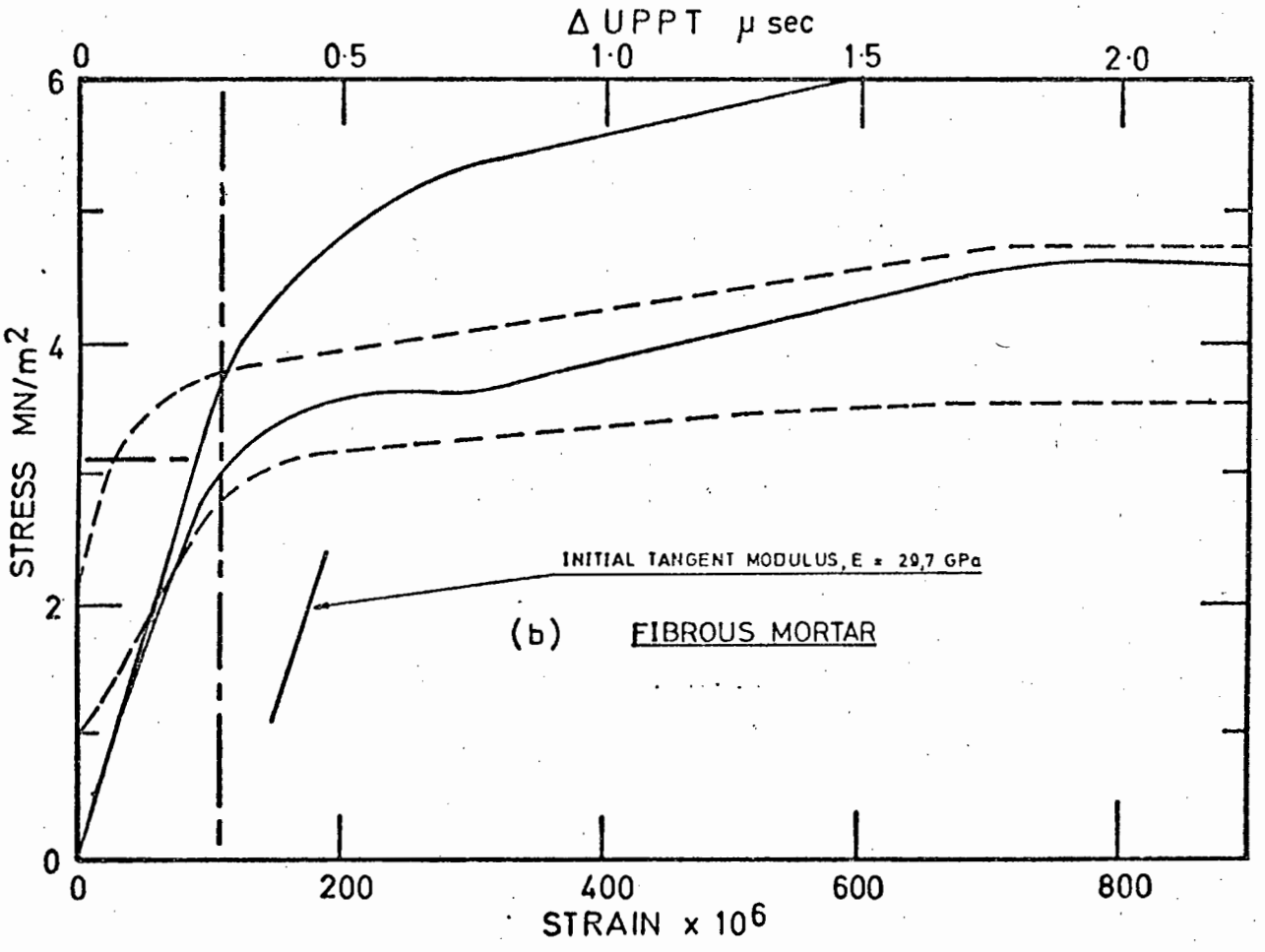

Fig. 5.3: Tensile stress-strain curves with corresponding UPTT measurements of (a) Plain Mortar, and (b) Fibrous Mortar.

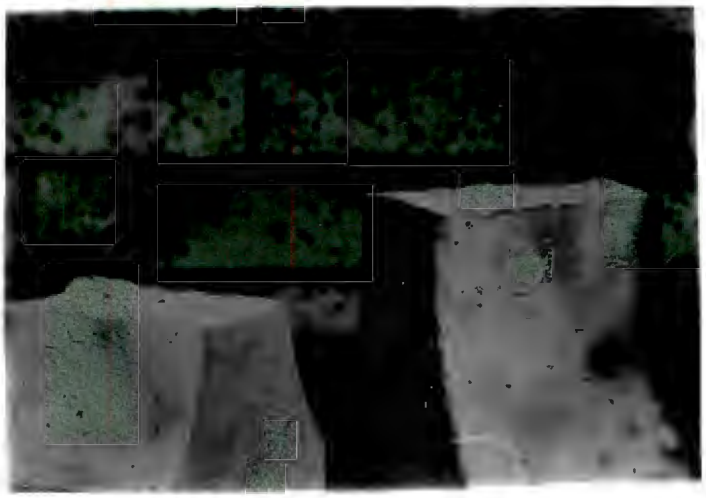

(a): Plain mortar.

(b): Fibrous mortar.

Fig. 5.4: Comparative difference between tensile failure modes of (a) plain mortar, and (b) steel-fibre reinforced mortar.

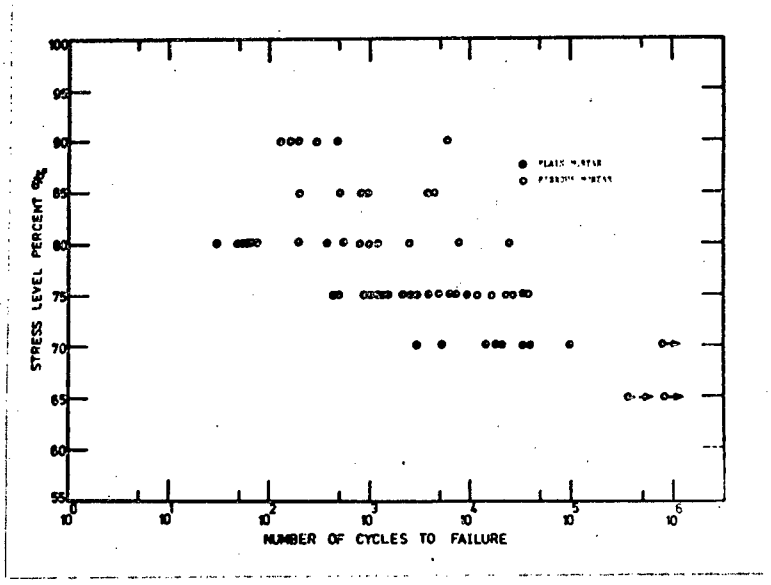

Fig. 5.5(a): S - N data for uniaxial tensile fatigue.

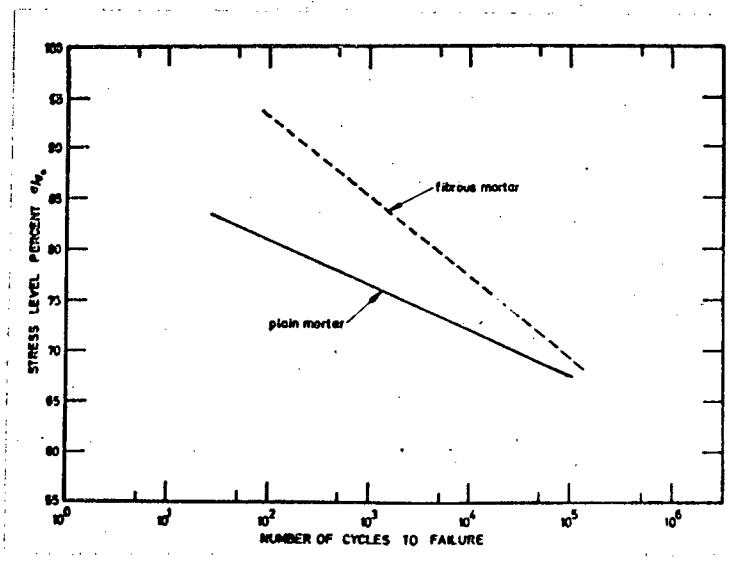

Fig. 5.5(b): 'Best-fit' (average fatigue life at each stress level) S - N curves obtained from data above.

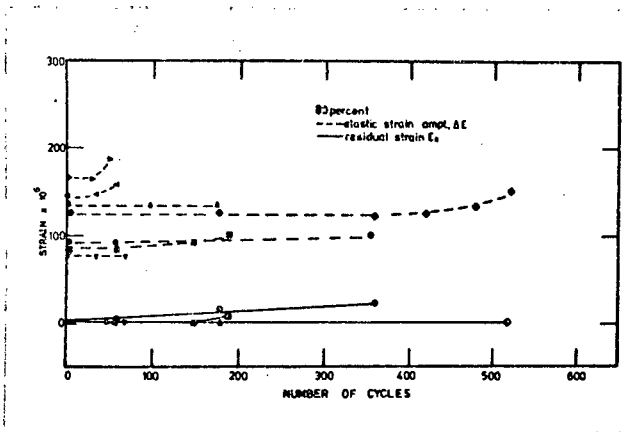

(a): 80% stress level

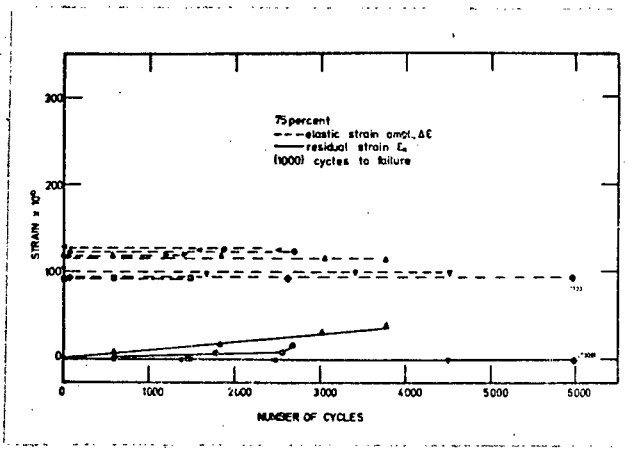

(b): 75% stress level

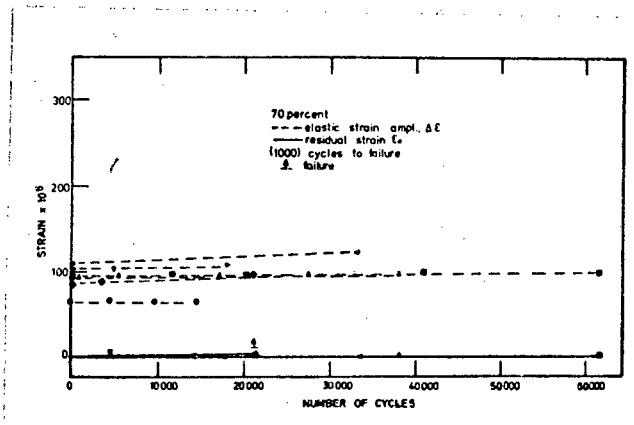

(c): 70% stress level.

Fig. 5.6: Variations in tensile strains, as a function of stress level, with number of cycles to failure - PLAIN MORTAR.

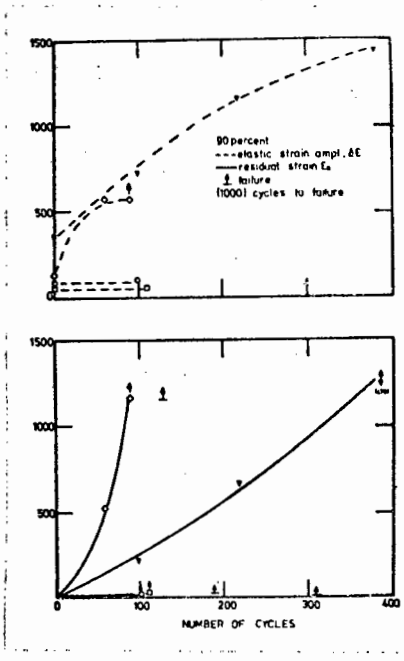

(a): 90% stress level

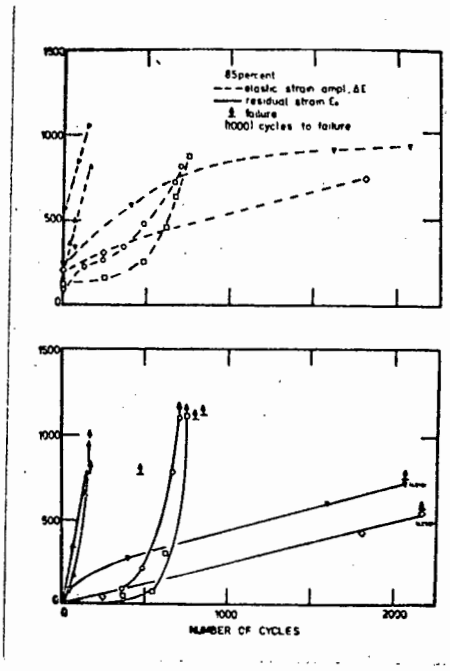

(b): 85% stress level.

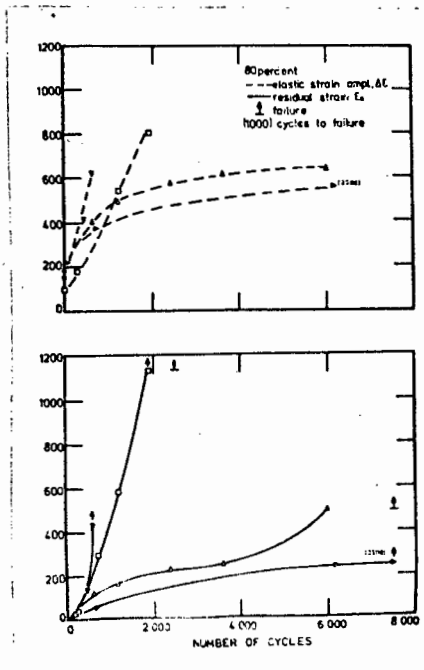

(c): 80% stress level

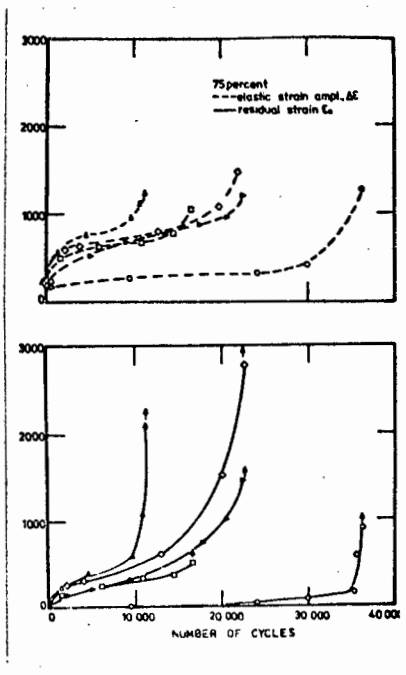

(d): 75% stress level.

Fig. 5.7: Variations in tensile strains, as a function of stress level, with number of cycles to failure - FIBROUS MORTAR.

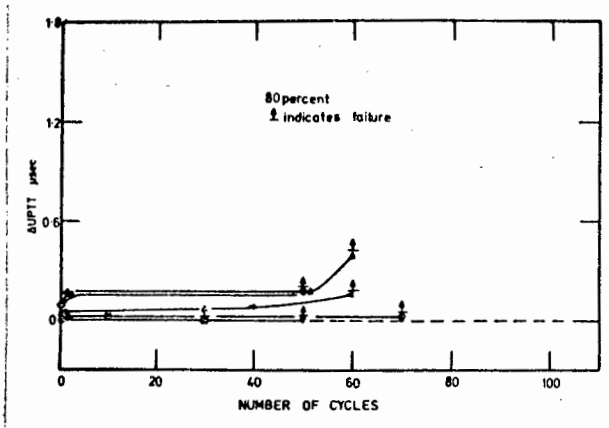

(a): 80% stress level

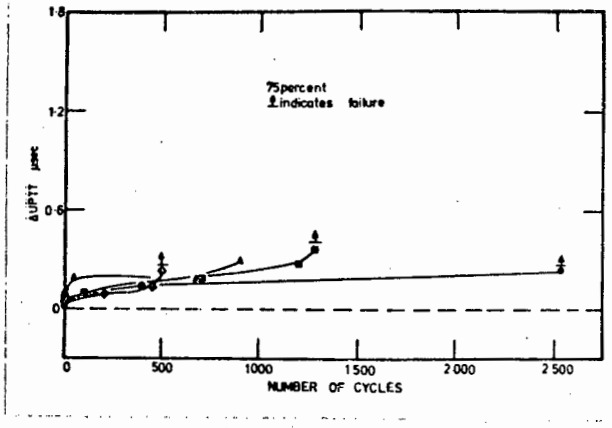

(b): 75% stress level

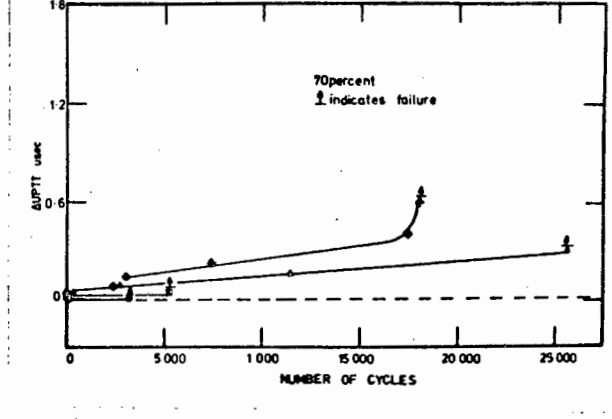

(c): 70% stress level.

Fig. 5.8: Changes in ultrasonic pulse transit times, as a function of stress level, with fatigue life - PLAIN MORTAR.

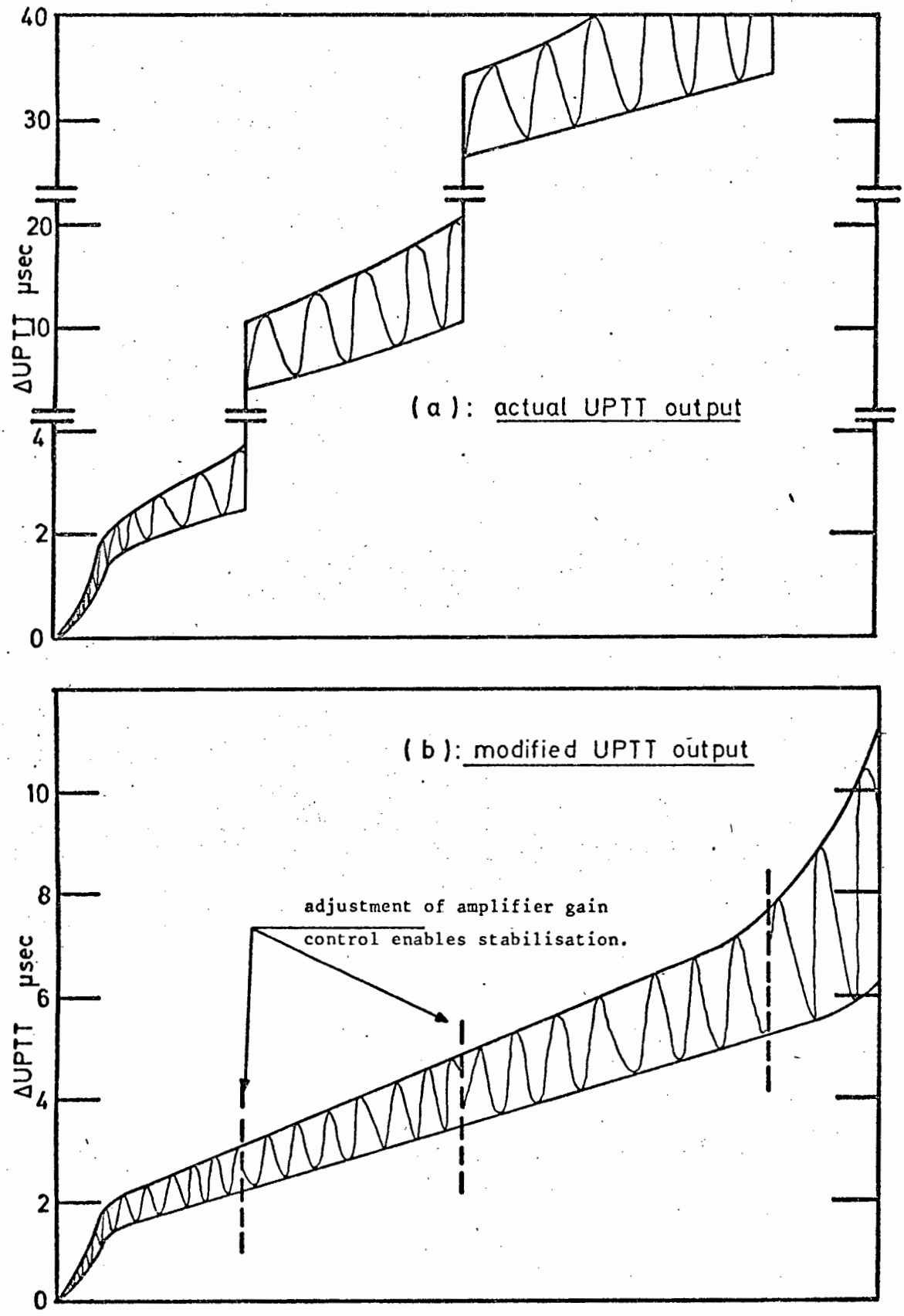

Fig. 5.9: Idealised representation of UPTT measurements during fatigue of FIBROUS MORTAR.

Fig. 5.10: Fibre reinforced tensile specimen immediately prior to final fatigue failure. (Test was stopped at this point.)

CHAPTER 6

6. FIBRE-MATRIX INTERACTION PHENOMENA

6.1. INTRODUCTION

The mechanical properties of any fibre reinforced cement composite will be dependent upon stress transfer between the fibre and the matrix; this in turn depends upon the mechanical properties of the interface (24, 26, 98).

It should now be apparent from the preceding sections that theoretical analysis and experimental tests ultimately relate to the bond between the fibre and matrix; composite failure is generally attributed to debonding between the fibre and matrix resulting in fibre pull-out. Consequently, the strength of the fibre is not generally fully utilised.

A substantial amount of analytical work has been reported in the literature for calculating the bond strength from composite stress-strain behaviour (reference to which is made in Chapter 2). Most experimental investigations have used conventional or modified pull-out techniques to assess variables such as fibre orientation, fibre roughness, fibre-matrix contact pressure, curing methods, age, etc. which are thought to influence bond strength. It is generally considered that measurement of the bond strength will provide some direct indication of the bulk composite properties. Unfortunately, at present, little or no conclusive correlation has been found between analytical calculations and experimental data; also, neither method has led to an adequate understanding of the mechanism of the stress transfer in fibre reinforced cement systems.

It is evident from the literature that little effort has been devoted to obtaining a qualitative assessment of the failure mechanism between the steel fibre and the matrix, although the morphology of plain and fibre reinforced

cement systems has been extensively studied (98 - 103).

6.2. PREVIOUS WORK

Majumdar (98) has discussed the interface and interfacial reactions of glass-fibre reinforced cements (GRC). He shows the interfacial contact zone to be quite complex, therefore inhibiting any description in terms of simple parameters. Unlike most glass fibres, steel remains relatively stable in alkaline environments and the bond is reportedly almost entirely mechanical (36) i.e. of a frictional nature. In GRC, for example, the bond strength may be attributed to chemical as well as mechanical bonding (26, 98). However, it has been suggested (26) that in steel fibre reinforced cements Fe^{+} diffusion takes place across the interface zone into the cement matrix; other studies (36), however, show that this is not the case.

Various wire treatments have been investigated (36, 37) with a view to increasing the bond strength between fibre and matrix. Some of the results obtained in these investigations are summarised in table 6.1. It can be seen that although there may be an increase in actual bond strength with various treatments, the corresponding increases in 'tensile' (flexural) strength have been only marginal.

The effects of air or wet curing have also been found to have an important influence upon the interfacial bond, although results available appear to be contradictory (see table 6.1) (37, 104).

Tattersall and Urbanowicz (37) investigated, on a limited scale, the effects of applied pressure during casting and found as much as a fivefold increase in pull-out bond strength for fibres in cement paste. Pinchin and Tabor (105) similarly found that the application of pressure both

immediately subsequent to debonding and after wire movement of 1.0 mm resulted in pull-out load increases of between approximately 1.7 and 3.8, depending upon the stage of pull-out and fibre treatment, i.e. surface roughness.

Several authors (105,107) have found that although smooth wires may have smaller initial debonding loads, they have a better post-debonding interfacial shear traction than that of rough wire. Pinchin (105) suggests the mechanical interaction between the cement matrix and asperities on the rough wire cause the increased debonding load; since compaction is accentuated by the presence of these asperities, further interaction will cause a more rapid decrease in frictional stress transfer than that compared to an entirely smooth wire. Pinchin (106) also observed composite failure to initiate within the matrix adjacent to the fibre interface, whereas failure has generally been reported to occur at the interface itself (26, 37, 38).

Pull-out loads (or equivalent bond strength) associated with fibre groups rather than single fibres has also been investigated. Naaman and Shah (108), for example, found that the bond associated with a group of randomly oriented fibres decreases when the number of fibres pulling out simultaneously from the same area increases. These results, they suggest, explain why the addition of fibres to a concrete matrix with highly improved bond properties does not lead to an equivalent improvement in composite properties. Although this appears to be a reasonable assumption, these authors do not suggest any mechanism which would assist in explaining this phenomenon, other than that the interaction between neighbouring fibres must play some significant role.

From this short review it is clear that little work has been carried out specific to the interfacial zone, and that the mechanism of failure of the fibre-matrix interface remains to be clarified. Scanning Electron Microscopy (SEM) studies have recently been completed by Pinchin (109, 110). However, Pinchin fails to examine the interaction between the fibre and matrix at initial debonding, only

examining the tensile fracture surfaces of the steel-fibre itself and corresponding cement trough at various stages of pull-out. The object of this study was to examine the nature of the fibre-matrix interface at the point of de-bonding, using SEM, and perhaps gain a better understanding of the actual mechanisms leading to failure in steel fibre reinforced cements.

6.3. EXPERIMENTAL DETAILS

Factors such as fibre orientation, fibre roughness, matrix mix, curing methods, fibre coating (33) contributing to the nature and strength of the interfacial bond itself were not specifically examined, primarily because of the scope and depth that such a study would necessitate.

The initial investigation involved a study of the fracture surfaces of the fibre-matrix interface from static tests in uniaxial compression. The catastrophic nature of fatigue failure prevented any specific work on fatigue surfaces. However, previous work described in this thesis would tend to suggest that an examination of static failure should at least give a reasonable indication of the corresponding effects which will occur during fatigue.

In order to examine the initial debonding process, single fibre pull-out tests were carried out during which load-extension curves were monitored; this substantially facilitated examination of the resulting interfacial zone. Initially it was attempted to polish specimens to expose the fibre-matrix interface prior to the application of a pull-out load. However, it will be shown that this technique was not successful. It was, therefore, decided to first apply the pull-out load and subsequently expose the interface by simple tensile fracture across the interfacial plane, as illustrated in fig. 6.4. It was using this latter experimental technique, then, that investigations were primarily carried out.

Pull-out specimens were 15x15x60 mm prisms cast horizontally in sets of three. Each prism had a single steel wire, identical to those used throughout the thesis, centrally embedded 15 mm into the longitudinal face of the prism (fig. 6.1). The standard mix was used in these tests (water:cement:sand; 1:2:4, by weight), but all mixing was done by hand.

After casting, specimens were compacted on a small vibrating table for 2 minutes. The curing procedure to age 7 days was the same as that previously described. Tattersall and Urbanowicz (37) have noted that curing specimens under water may lead to rusting of the exposed wire. However, by coating such wires, before submerging specimens in the water solution, with a thin film of grease appeared to prevent this rusting action.

All pull-out tests were carried out on a Hounsfield Tensometer, fitted with a motor drive. Automatic monitoring of the load-extension curve (a typical curve is illustrated in fig. 6.2) enabled the application of load to be stopped at any predetermined load (usually the debonding or pull-out load) or pull-out distance (wire movement relative to the cement matrix) after initial debonding. A very low cross-head speed of 0,4 mm/min was used so that at the initial debonding load, for example, the test could be stopped almost instantaneously without further pull-out occurring, and therefore without disrupting the interfacial zone. The method used for applying the load is shown diagrammatically in fig.6.3(a), the general apparatus illustrated in fig. 6.3(b). Since precise bond strength measurements were not being made it was considered unnecessary to incorporate sophisticated alignment rigs and universal joints for load application; alignment of pull-out direction was carried out visually.

After the required pull-out criteria (initial debonding load, for example) had been reached, the fibre-matrix interface was exposed, one fracture surface containing the embedded steel-fibre, the other the corresponding

fibre mould or cement trough (fig. 6.4).

Fracture surfaces were mounted onto standard SEM aluminium stubs and then vacuum dried. Prior to microscopic examination the specimens and stubs were coated with a thin layer of vacuum-deposited gold-palladium. Specimens were stored in vacua. SEM studies were carried out using a Cambridge Stereoscan S180.

A LINK Energy Dispersion X-Ray analysis (EDXA) system was used in conjunction with SEM for studying the material composition of selected areas of the fracture surfaces. Stucke and Majumdar (99, 111) and also Diamond et al (100) have noted the difficulties involved in obtaining quantitative results by EDXA methods, particularly on rough surfaces. Such factors as spurious excitation (i.e. back-scattered electrons), spurious adsorption (i.e. differential absorption or shielding of the different kinds of X-rays by projecting surfaces on the specimen in the line-of-sight to the X-ray detector), take-off and incidence angles, and lateral spread of electrons, may lead to inaccurate results without an understanding of such techniques. Semi-quantitative results, however, have been obtained with good reproducibility on a comparative basis (99, 109, 112). Such a comparative technique was also adopted for the present study by undertaking line scan analyses parallel to the fibre-matrix interface. The peak height counts and area integrals (fig. 6.14) of the Ca-kα, Si-k and Fe-k X-ray intensities were determined in the region of, and adjacent to, the interface as well as within the bulk matrix. The peak-to-background count ratios were found to be relatively high and, therefore, since the background counts were insignificant, they were not taken into account. Average Ca/Si integral area ratios were compared between the selected areas at, and adjacent to, the interface and the corresponding standard bulk matrix Ca/Si ratio. Table 6.2 gives the energy ranges within which the elemental area counts were determined.

6.4 EXPERIMENTAL RESULTS AND DISCUSSION

6.4.1. SEM Studies

A typical fracture surface of a fibre embedded within the cement matrix after initial debonding and a corresponding cement trough are illustrated in figs. 6.5(a) and (b) respectively. Several features on these surfaces are apparent. At the matrix-fibre contact zone it appears that in certain places the bond is still intact, whereas in other areas the bond has been broken. Cement has been left adhering to the steel-fibre surface which is consistent with the observations of Pinchin (109, 110) who explained this as a result of tensile fracture taking place at both the actual interface and within bulk cement matrix.

The discontinuous nature of the interfacial bond is clearly evident from the cement trough where large voids, also observed by Pinchin (109), are present within the trough and interface. Voids within the trough may have been caused either by the removal of matrix material from the interfacial zone by the steel-fibre (109), or by the inability of the matrix particles to compact closely and continuously around the steel-fibre (102), and thereby provide voids at the actual interface during manufacture (33). On the latter point, it has been suggested that air entrainment is higher in the vicinity of the interface due to inertia effects of steel-fibre vibrating the small surrounding volume of cement matrix during vibration compaction (109, 113).

It would appear, however, that these large voids found within the cement trough in fig. 6.5(b) are, firstly, substantially larger than typical voids, and secondly would seem to correspond to particles of adhering cement similar to those shown in fig. 6.5(a). In accordance with Pinchin (109, 110), whose results are based on observations of the fibre surface at various stages of pull-out, it would seem reasonable to suggest that tensile fracture (to expose the

fibre) has resulted in failure within the bulk cement matrix as well as the interface itself.

Closer examination of similar fracture surfaces of the interfacial zone and matrix adjacent to the interface has shown that, at initial debonding, composite failure also appears to be due to extensive matrix cracking adjacent to the interface as well as interfacial bond failure (figs. 6.6 (a-d)). (Control specimens have shown that these cracking systems are solely due to pull-out load, as indicated later.) Matrix cracking is also evident within, and adjacent to, the cement trough, as shown in figs. 6.7(a)and (b).

Another feature of the fractographs are that the steel fibres show clearly defined striation marks (figs.6.6(b-d)); these marks are also present within the cement trough (fig.6.7(a)). Pinchin (110), using electropolished stainless wires, found similar striations to be an adhering thin layer of cement on the fibre due to pull out; removal of this film of adhering cement resulted in the disappearance of the striations. Pinchin (110) notes that Maage attributed similar striations to mechanical working of the steel fibres and to the removal of metal from the wire surface during pull-out. However, this would appear to be an unlikely explanation (110). The striation marks found in this investigation appear to be due to a manufacturing treatment of the steel fibres, as indicated by the 'virgin' fibre shown in fig. 6.8.

In figs.6.6(b)and6.6(c)the areas marked (c) show remarkable similarity to the Portlandite ($Ca(OH)_2$ or ~~COH~~ CH) morphology reported by other authors (98, 101, 102, 109). Fig. 6.6(d)also shows the 'platey' Portlandite morphology previously observed elsewhere (101, 103, 114). (Some areas, such as that shown in fig.6.6(a), were not so obvious for morphology identification.) It is generally acknowledged (101, 102, 103, 109) that an important feature of calcium hydroxide formation (a hydrolytic product resulting from the hydration of the calcium silicate phases) is that it grows within and subsequently fills much of the available

void space (for example, water filled voids, entrapped air voids). It is quite likely, therefore, that these areas (c) are indeed calcium hydroxide which fill the initial concentration of voids, resulting from vibration compaction, in the vicinity of the steel wire. Pinchin (109) observed an enrichment of CH at the steel-fibre-matrix interface, also suggesting that the fibre surface provides a centre for nucleation of CH. The area (s) in fig.6.6(b)seen adhering to the fibre is of different morphology to the surrounding area, probably composed of the stronger calcium silicate hydrate (CSH) phase (44, 101, 102, 114).

From figs. 6.6(a-d)and 6.7(b),therefore, matrix cracking (within 30 μm from the interface) occurs within the probably weaker CH (c) phase (114) with transverse cracking completing the locus of failure between the matrix cracks and the bond cracks.

Fig. 6.9(a) is a micrograph of a fracture surface obtained from a static compressive test specimen. The observations made from single fibre pull-out specimens at initial debonding are consistent with the failure mode of this specimen, i.e. some matrix failure within 30 μm from the interface has occurred with bond remaining essentially intact; the overall fracture path consists of regions of matrix and interfacial failure. This can also be seen in fig. 6.9(b) which shows a cement trough from another static compression test.

Although failure has, thus far, been shown to occur within two zones (i.e. the interface and matrix adjacent to the interface) it may be argued that bond failure is the first to occur, giving rise to subsequent matrix failure. However, it was found that bond failure never occurred discreetly but was always associated with matrix failure whereas matrix failure was found to occur without corresponding bond failure (figs. 6.10-11).

Fig. 6.10(a) shows a fibre embedded within the mortar matrix after having been stressed to the initial debonding

load. Similar to fig. 6.5(a), a thin layer of adhering cement on the fibre surface is evident; however, in contrast to fig. 6.5(a), the interfacial bond is still intact along the length shown. The central area indicated, enlarged in fig. 6.10(b), shows extensive matrix cracking with an intact fibre-matrix bond. Similar areas are shown in figs.6.11(a-c). The role of the platey Portlandite (COH) (regions (c)) is again in evidence in fig.6.11(b), with matrix failure occurring within 35 μm from the interface.

Further evidence of matrix cracking taking place preferentially to bond cracking is shown in fig. 6.12(a). This is from a polished specimen prior to the application of a fibre load. It seems quite possible that these cracks either are caused by the polishing process (the main reason the polishing technique was not adopted) or by the restraints imposed by the stiffer fibre upon volume changes that occur within the matrix during curing. Nevertheless, cracking, or failure, takes place preferentially at the weakest zone (within COH enrichment areas, for example). Fig. 6.12(b) also shows a further example of extensive matrix cracking without fibre debonding.

In concluding this section, in order to justify the results discussed above, it should be noted that control tensile fracture surfaces of the embedded fibre were also examined (these specimens having not been subjected to any form of applied pull-out stress). These specimens (figs. 6.13(a,b)) show relatively undisturbed material at, and adjacent to, the fibre and interface in comparison with pull-out specimens.

6.4.2. Chemical Analysis

Point scan microanalysis of the cement hydrate may not be entirely accurate because the diameter of the area from which X-rays are produced in SEM can be ~1.5 μm (the electron voltages used in this study being in the range 10-30 kV) and many crystals within the cement hydrate may

be larger than this. Line scan analysis was therefore chosen in order to provide an average of an infinite number of points, thereby reducing the inaccuracies due to localised sampling. The relative magnitudes of the Ca/Si integral ratios for lines at, and away from, the wire-matrix interface should thus give a comparative indication of the relative proportions of $CaOH_2$ and CSH present along the line sampled.

A typical line scan elemental distribution is shown in fig. 6.14. A typical area over which such an analysis was carried out is shown in fig.6.15(a) with the corresponding plot of the Ca/Si integral area ratios. Figs. 6.15(b-d) show the respective elemental distribution maps. Although these are only semi-quantitative measurements they also give an indication of the comparative proportions of the important elements present. The Fe-k distribution shown in fig. 6.15(d) is not considered to be a true reflection of Fe^+ migration into the matrix since it has been shown (100) that the effective diameter/depth of X-ray generation can be of the order of 2-3μm, thereby detecting the wire at probe areas in the immediate vicinity (within 2-3μm) of the interface. Since significant Fe^+ counts are registered on the fibre surface, however, the thin layer of adhering cement must be at least 2-3μm thick in places.

Similar line scan analyses were also carried out on cement trough specimens, (fig.6.16(a)). Figs. 6.16(b-d) show the respective elemental distribution maps. The Fe^+ concentration illustrated in fig. 6.16(d) is not nearly as significant as that suggested in fig. 6.15(d). In fact the Fe-k integral count expressed as a percentage of the summation of Ca-Kα and Si-k integral counts was ~3-4% as would be expected from the chemical composition of cements (115). It may be concluded, therefore, that any chemical bonding that may be present is insignificant compared to the mechanical bonding and that the high Fe-k integral observed in fig. 6.15(d) is due to X-ray penetration.

A plot of the integral area ratios for Ca-Kα and

Si-k as a function of distance from the interface from the two types of specimens discussed above, is shown in fig. 6.17. From this, a number of observations can be made, as follows:

1. There is a Ca^{++} - enriched zone within ~ 5-60 μm away from the actual interface with a concentration ~ 30 μm from the interface; this indicates an abundance of CH relative to CSH. Pinchin (109) observed CH enrichment within ~ 10 μm from the interface, using X-ray diffration, of material removed by a drill 20 μm larger than the fibre diameter from the hole left by the pulled-out fibre. He suggests that this enrichment arises from CH nucleation at the fibre surface and subsequent filling of voids which occur preferentially in the vicinity of the wire, the latter being consistent with observations presented earlier in this chapter concerning CH formation close to the interface. It is possible that had Pinchin analysed material > 10 μm from the interface, he would have found an even greater CH enrichment.

2. The thin layer of cement which adheres to the steel wire shows a normal composition of hydration products relative to the bulk material (Ca/Si ~ 2.0-3.0) - Pinchin (109) only measured the relative ratios in the trough regions (assumed to be in direct contact with the fibre) suggesting a progressively increasing Ca/Si ratio right up to the actual interface.

Hydration of the calcium silicates results in the formation of CH (101), with the CH occupying void spaces not already occupied by CSH. Therefore, the formation of CSH must occur before CH can be produced. Hence, it would seem more reasonable to suggest that nucleation of the CSH phase takes place at the fibre surface rather than CH, as suggested by Pinchin and others (109). Since CSH has the finest particle size of the solid phases present in the cement paste (111), therefore being able to compact more readily around the wire, the formation of CH at the actual interface might be expected to be inhibited. These observations are, therefore, consistent with those made

earlier with respect to initial debonding resulting from initial matrix cracking ~30 μm from the interface, with subsequent failure (pull-out) taking place within the bulk matrix or cement immediate (2-3 μm) to the interface and the interface itself because of 'mechanical' damage within the surface cement regions during the pull-out process.

3. In comparison to analyses taken on the fibre surface, a higher concentration of $\overline{C\bar{O}H}$ is found within the cement trough (fig. 6.17), hitherto matrix, possibly caused by the normal composition hydrate in the immediate vicinity of the fibre being pulled away with the fibre thus exposing this relatively weaker $\overline{C\bar{O}H}$ zone. This would appear to justify the proposal made above i.e. final pull-out occurs within the immediate vicinity of the fibre interface.

Pinchin (109) carried out hardness tests near the fibre (to within ~200 μm) and found the hardness to decrease rapidly from within 750 μm to 150 μm of the interface compared to the bulk material. This decrease he attributes to the increase in porosity. However, he suggests that the $\overline{C\bar{O}H}$ enrichment near the fibre interface (i.e. within ~10 μm) would cause the hardness to increase because of the filling of voids in this regime by $\overline{C\bar{O}H}$. It seems questionable, however, that only the voids within the immediate vicinity of the interface become filled with $\overline{C\bar{O}H}$ and not the voids up to and exceeding ~200 μm from the interface.

6.5. SUMMARY

The results and discussions of the preceding sections may be summarised with reference to fig. 6.18.

1. Due to vibration compaction excessive voids relative to the bulk matrix are formed within the immediate vicinity of the interface. Calcium silicate hydrates are nucleated first at the fibre interface and because of their fineness prevent the formation of calcium hydroxides at the interface. Calcium hydroxides fill up the voids adjacent to the inter-

I doubt this!

face. The CSH thus forms a strong core immediately surrounding the fibre with a secondary, weaker core of ~~CSH~~ CH around the CSH.

2. When the fibre is stressed, initial failure (corresponding to the initial debonding load) occurs within the weaker secondary core (within ~ 30μm from the interface).

3. As fibre pull-out proceeds a 'stick-slip' behaviour results (see fig. 6.2) with the stress transfer from matrix to fibre becoming increasingly reduced due to the 'mechanically' disrupted interface. At final failure interfacial (within 2-3 μm from the interface) bond failure occurs; a very strong CSH core is left adhering to the steel fibre. ?

It becomes clear, therefore, that before strengthening cement matrices with reinforcement (fibres or otherwise) the properties of the cement matrix itself must be more fully investigated. Aveston (6) notes that for the stress transfer to be fully effective the shear stress of the cement material will have to be in excess of 200 N/mm^2. However, if fibres are to be incorporated effectively into a cement matrix for properties other than strength (for example, energy absorption i.e. impact loading), increasing the cement-fibre contact zone and frictional force between the two may result in improved properties since it has been shown that 'bonding' is purely mechanical in nature.

Agreed

has this been shown without doubt, I wonder?

(1) Cleaning Fibres:	
(a) $Na(OH)_2$ (36)	50% increase in bond strength (37); 10% increase in flexural strength (36)
(b) acetone (36)	
(c) trichloroethylene (37)	
(2) Surface Roughening:	
(a) Rusting:	2 x increase in bond (37); 20% increase in flexure strength (36)
(b) Heating to 600°C	4,7 x increase in bond (37); 3,3 x increase in flexural strength (36)
(c) Dilute hydrochloric acid (36)	60% increase in bond (37); no increase in flexural strength.
(d) Conc. nitric acid (37)	
(3) Surface Coating:	
(a) Galvanising:	5,2 x increase in bond (37); 30% increase in flexural strength (36)
(b) Epoxy and cement:	5,7 x increase in bond (37); no report on strength.
(4) Mechanical treatment:	
(a) Crimped: >	9,2 x increase in bond (37); 2,7 increase in flexural strength (36)
(b) Hooked end: >	10,8 x increase in bond (37); no report in strength changes.
(5) Effect of Curing:	
(a) Normal curing (90% R.H.):	1,05 x increase in bond (37)
(b) Laboratory atmosphere:	0,6 x increase in bond strength (37); bond stress at 25°C 11,00 MPa (104)
(c) Under water:	1,8 x increase in bond strength (37); bond strength at 25°C 5,54 MPa (104).

TABLE 6.1.

Influence of various wire treatments on fibre-matrix bond strength.

Element	Energy Range (KeV)
Calcium / Ca-kα	3,44 - 3,90
Silicon / Si-k	1,60 - 1,94
Iron / Fe-k	6,18 - 6,58

TABLE 6.2.

Energy Ranges used for
Elemental Integral (Area) Counts

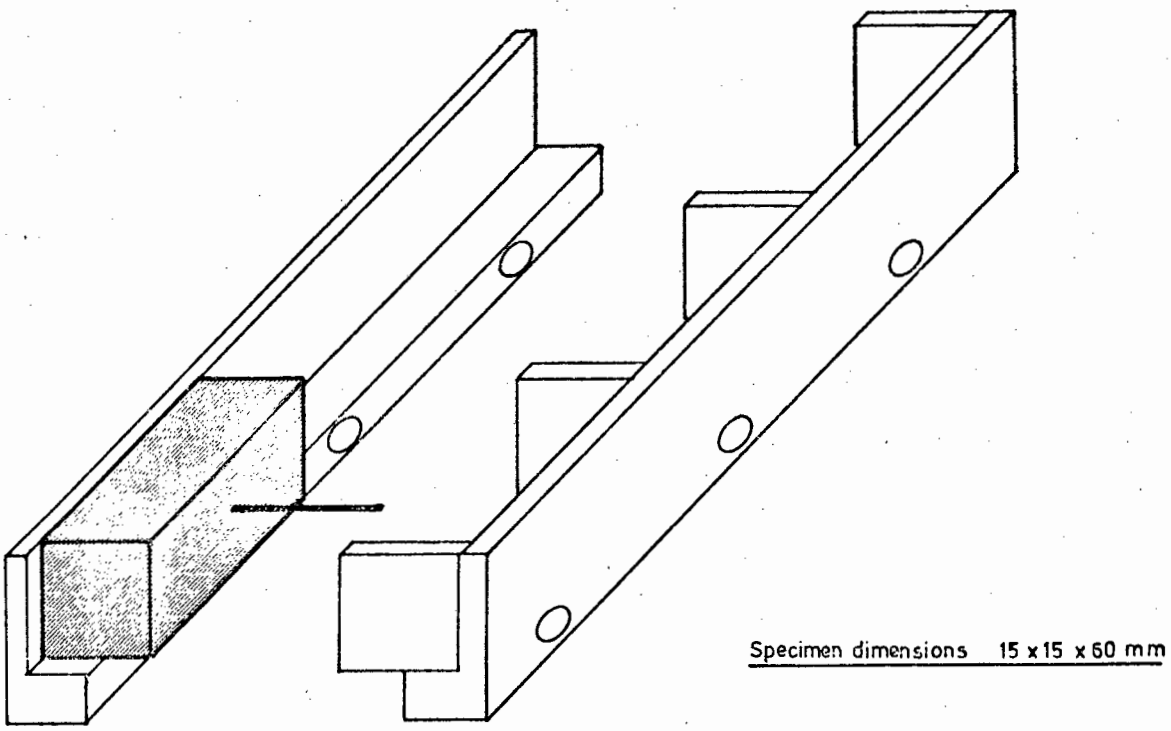

Fig. 6.1: Diagrammatic illustration of pull-out specimen and mould.

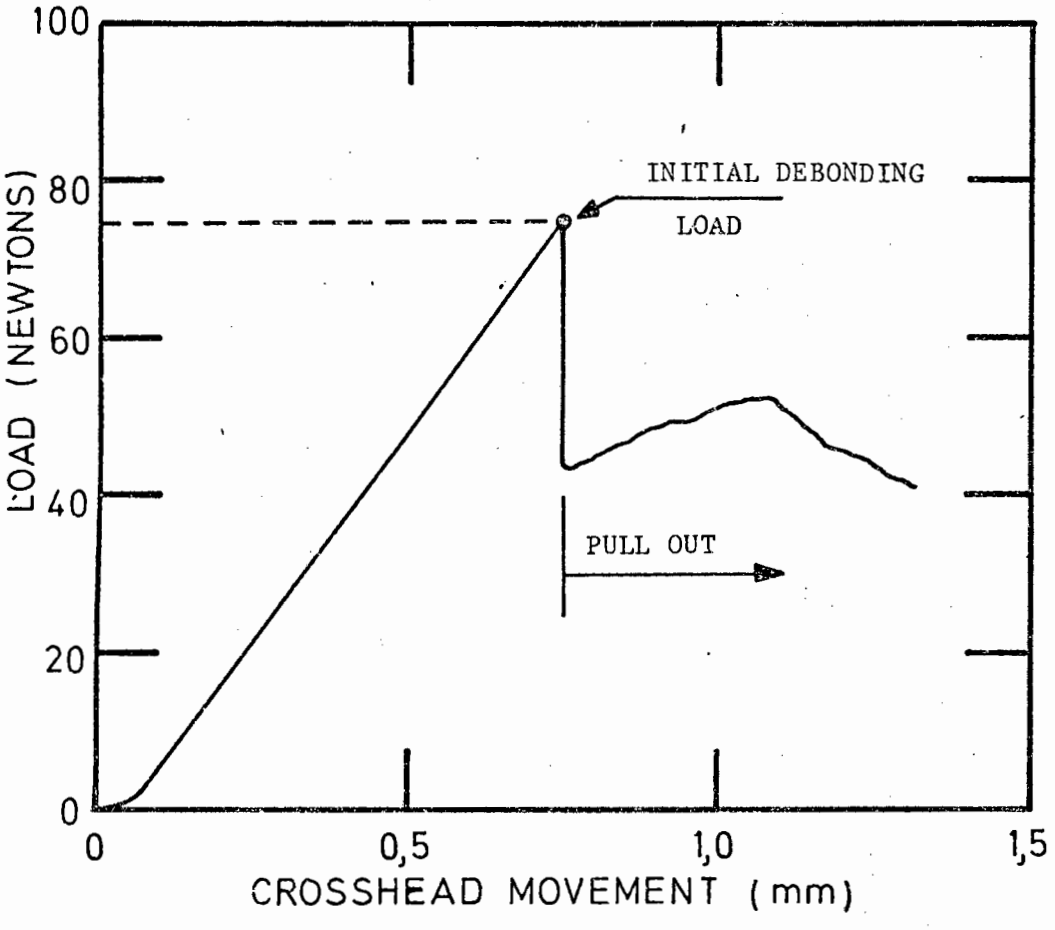

Fig. 6.2: Typical load-extension Curve

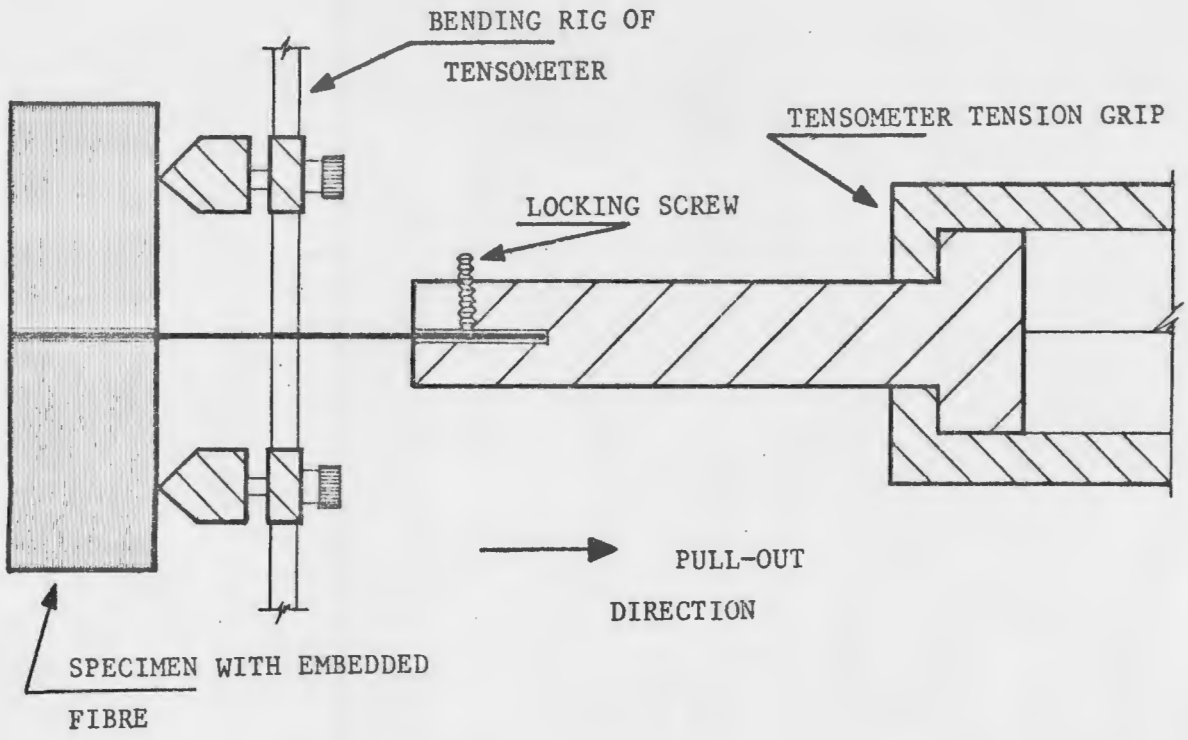

(a): Showing method of applying pull-out load to embedded steel fibre.

(b): Hounsfield Tensometer used for pull-out tests.

Fig. 6.3: Apparatus for applying pull-out load to embedded steel fibre.

Fig. 6.4: Tensile fracture surface exposing embedded steel fibre.

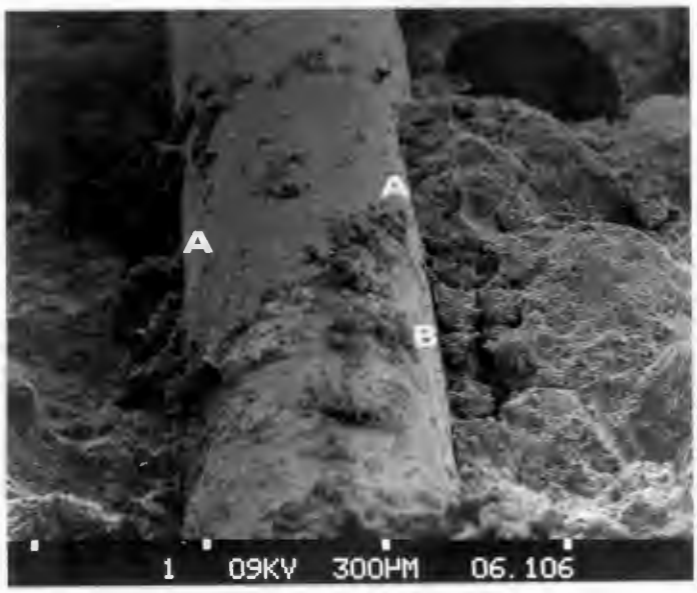

(a): Embedded steel fibre with evidence of adhering cement at fibre surface (A = intact bond; B = bond failure)

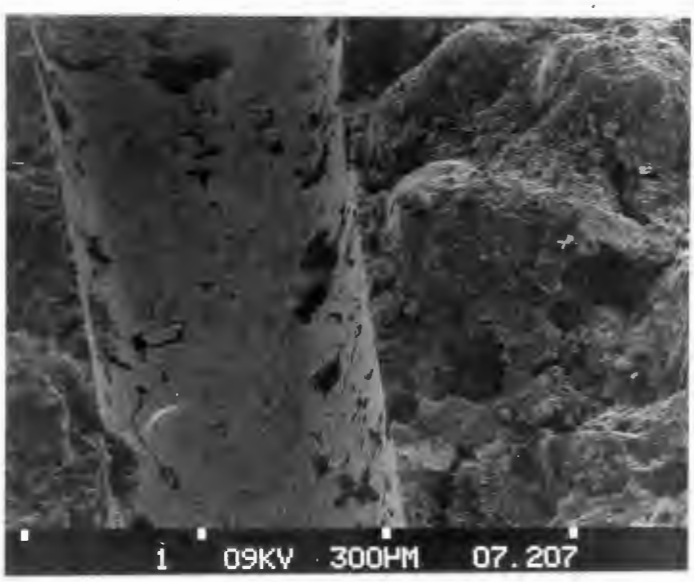

(b): Fibre mould (cement trough) showing large voids contained within trough and at interface.

Fig. 6.5: Typical embedded steel fibre with corresponding cement trough.

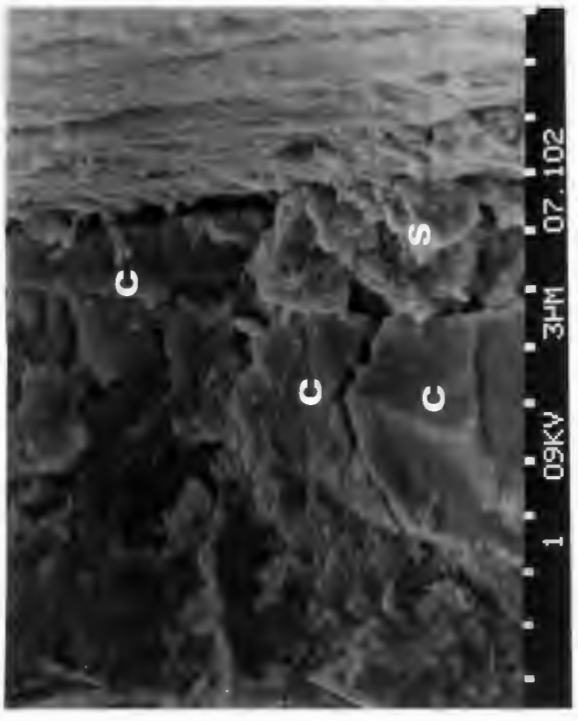

(b): C$\cancel{O}$H evident near interface with CSH adhering to fibre. Striations are also evident on fibre surface.

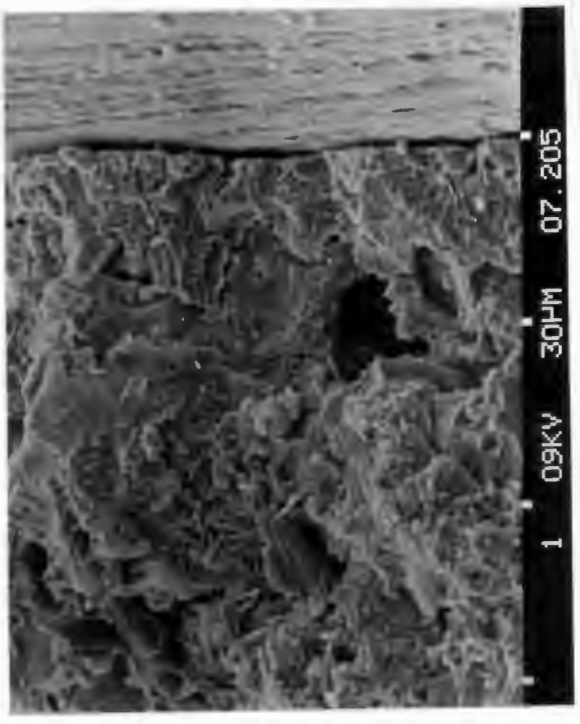

(d): Platey Portlandite (C$\cancel{O}$H) found adjacent to fibre-matrix interface. Striations found on fibre surface.

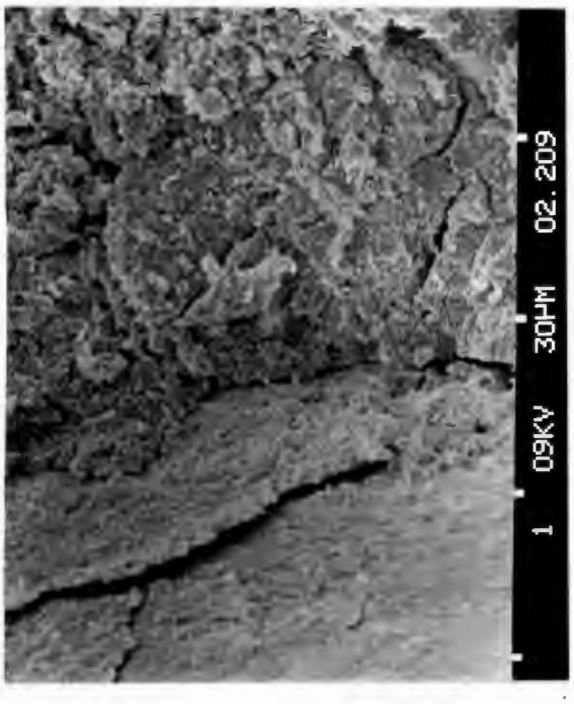

(a): Bond failure and matrix failure adjacent to interface.

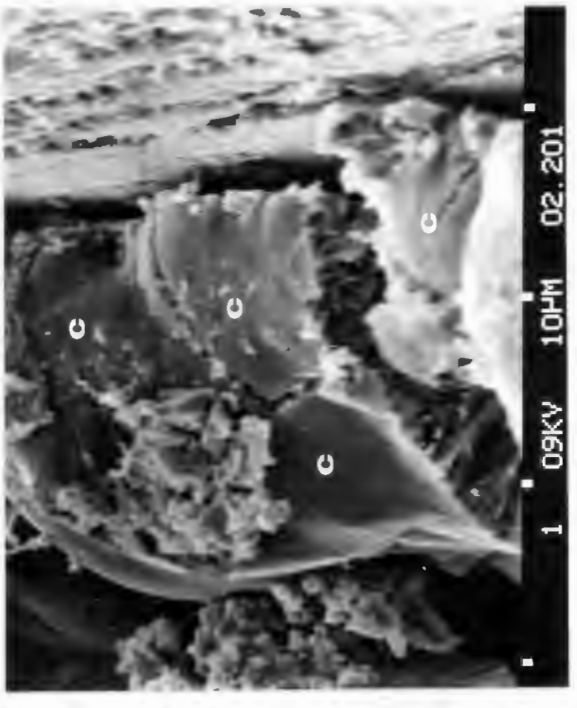

(c): C$\cancel{O}$H present adjacent to interface. Striation marks on fibre surface.

Fig. 6.6: Showing Matrix and Bond failure at the fibre-matrix interfacial region after initial debonding (C = C$\cancel{O}$H; S = CSH).

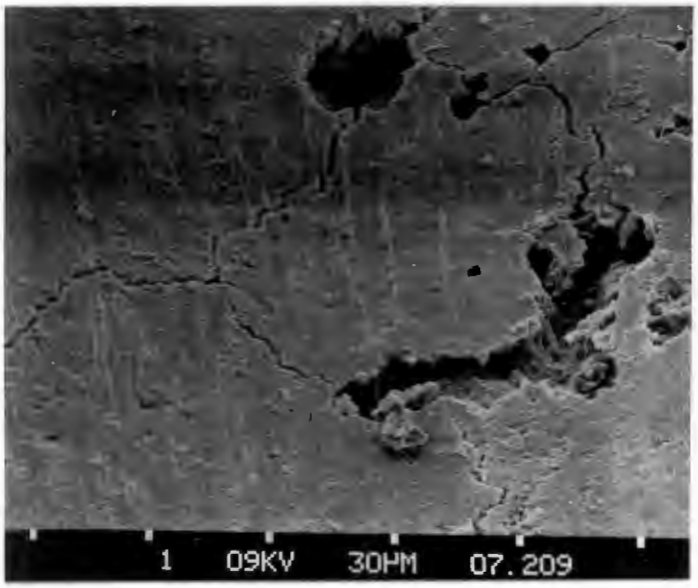

(a): Striation marks are seen in the cement trough. Large voids are also present.

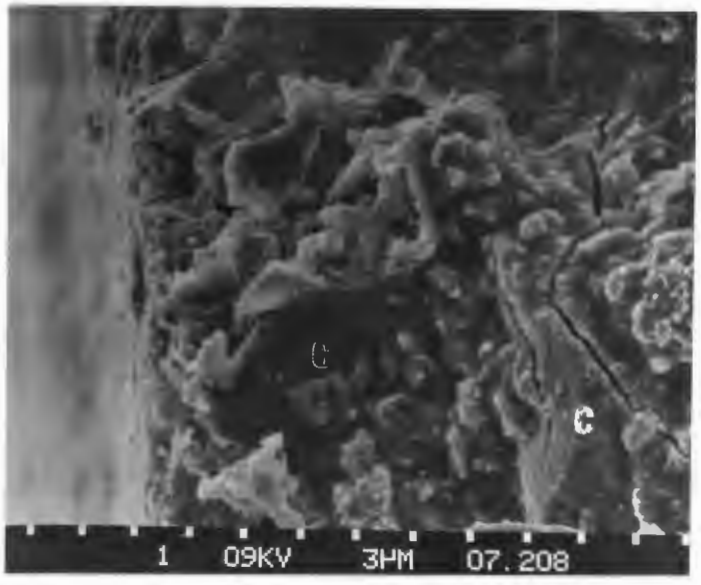

(b): Matrix cracking taking place adjacent to the interface shown on extreme left.

Fig. 6.7: Scanning electron fractographs of (a) cement trough; (b) interface adjacent to cement trough, after initial debonding.

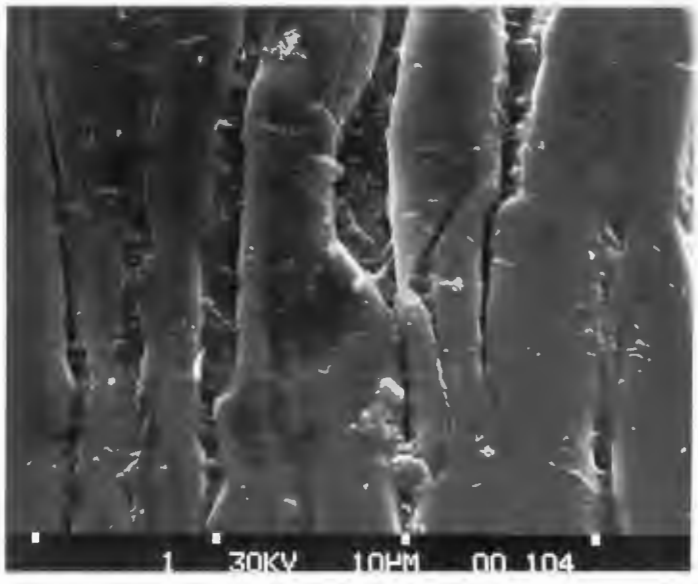

Fig. 6.8: Virgin Duoform steel-fibre.

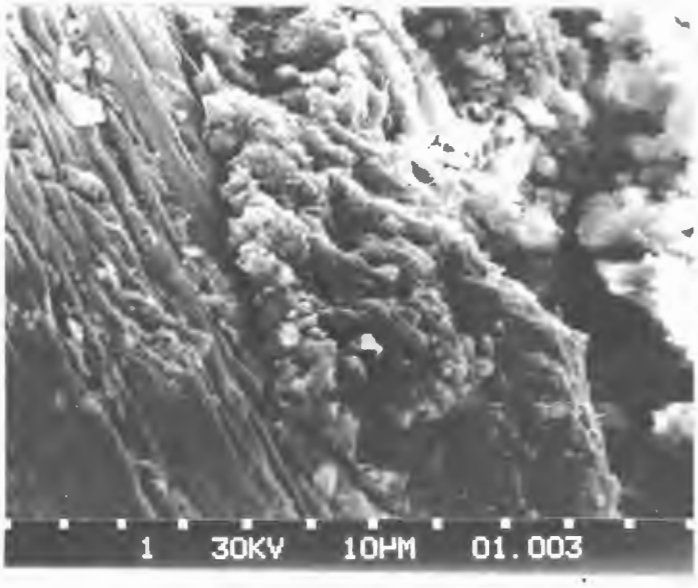

Fig. 6.9:

(a): Static compressive fracture surface containing embedded fibre shows bond failure, matrix cracking adjacent to interface and adhering cement to fibre surface.

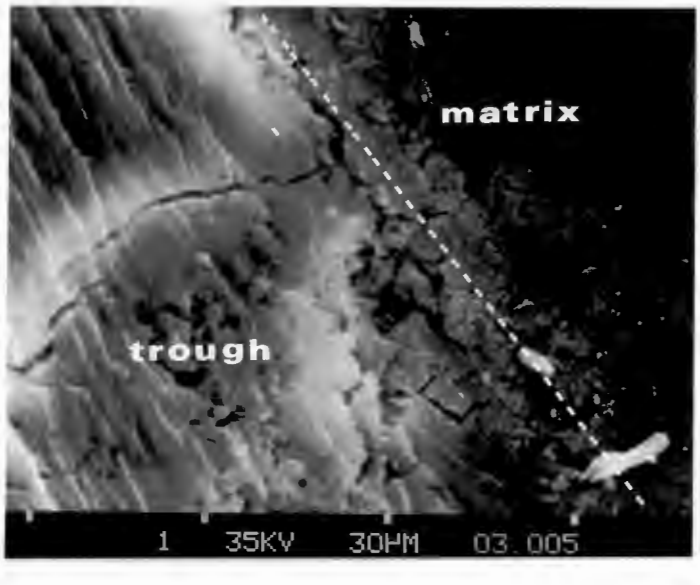

(b): Corresponding cement trough -(dotted line indicates matrix-fibre interface) with extensive microcracking.

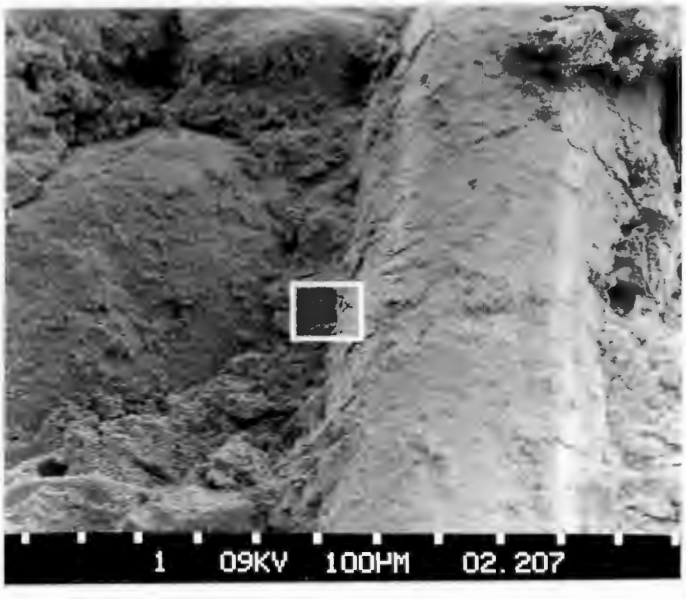

(a): Thin layer of cement adhering to fibre surface. Interfacial bond is still intact along this length of fibre.

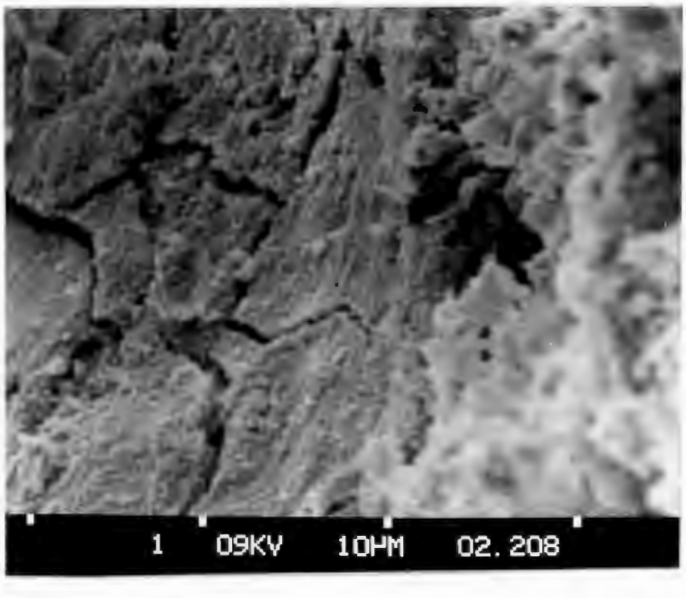

(b): Central area in (a) enlarged shows extensive matrix cracking with intact bond.

Fig. 6.10: Embedded steel fibre after having been stressed to initial debonding load.

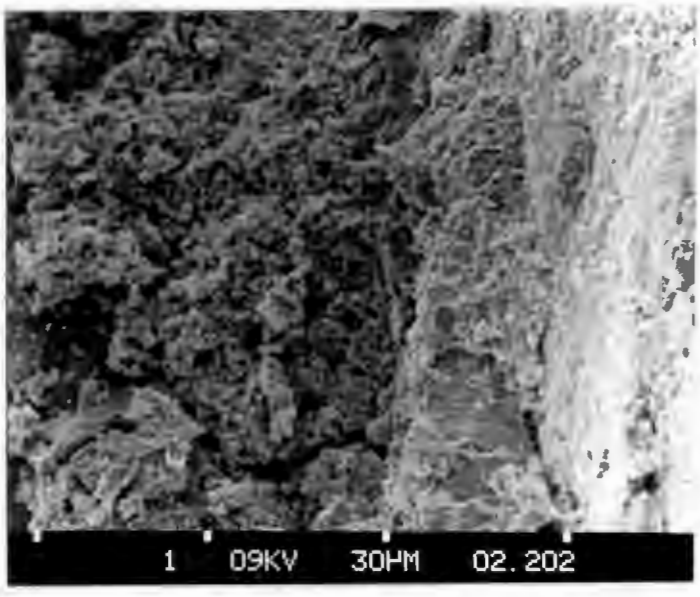

(a):

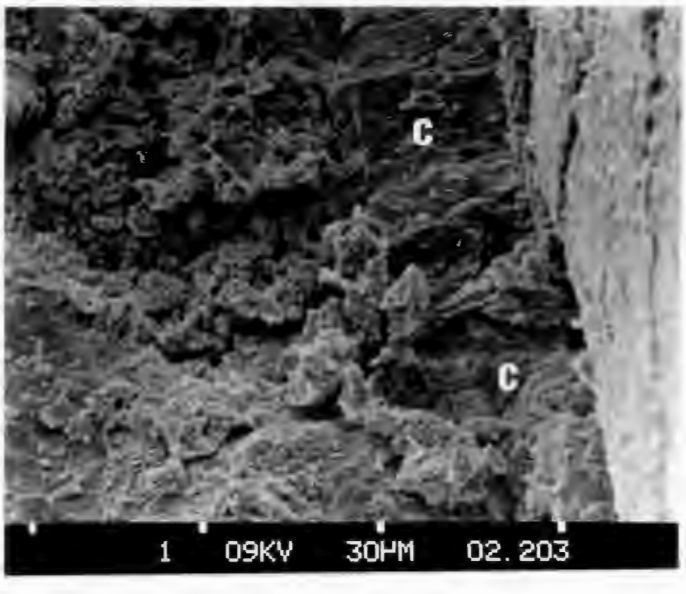

(b):

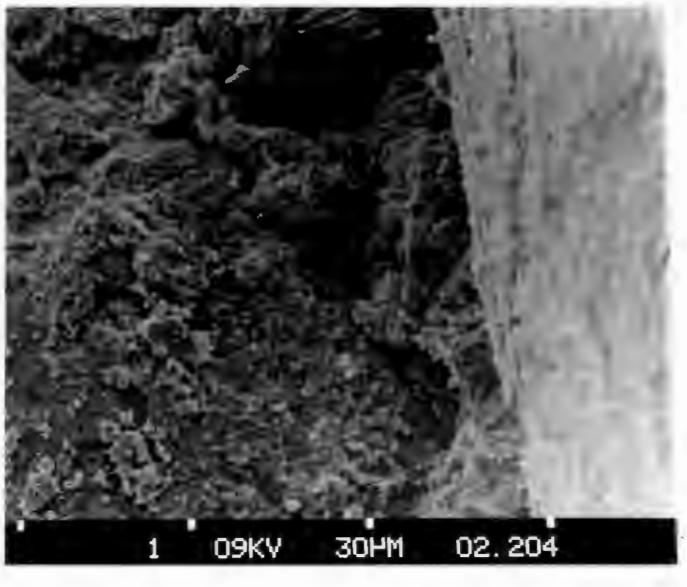

(c):

Fig. 6.11: Fractographs after initial debonding showing intact bond but extensive matrix cracking (C=COH).

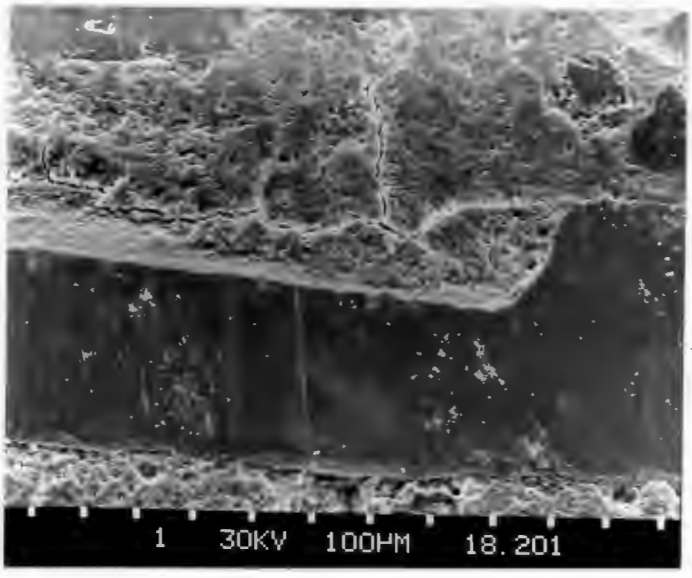

(a): Preferential matrix cracking adjacent to fibre interface rather than at the interface.

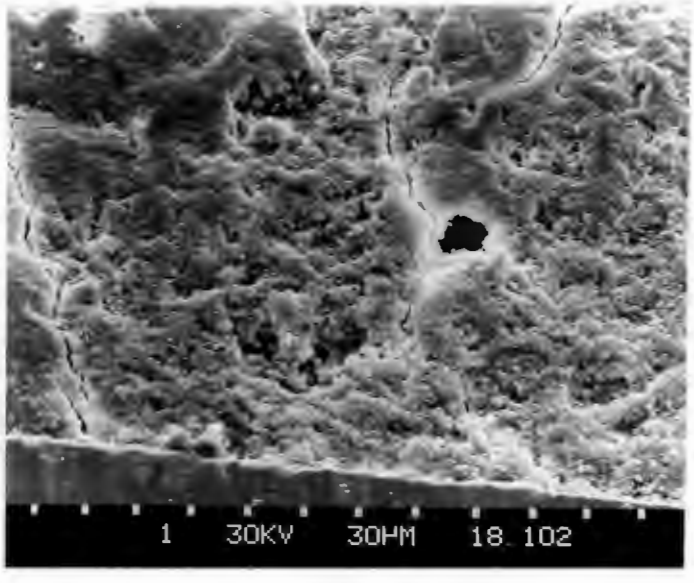

(b): Polishing leads to extensive matrix cracking.

Fig. 6.12: Polished specimens before application of pull-out load.

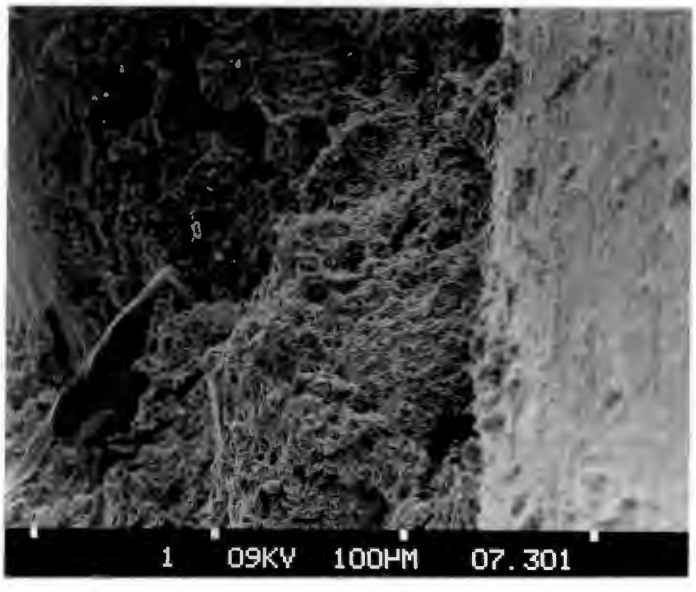

(a): Showing no evidence of bond or matrix cracking.

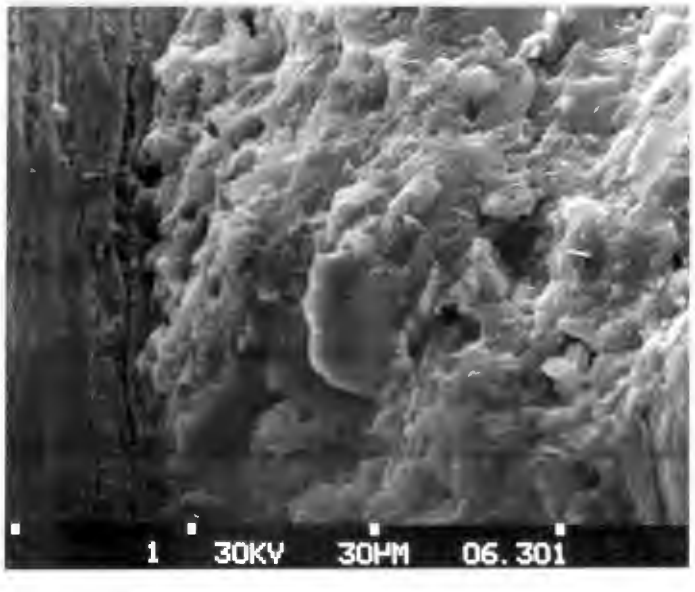

(b): Higher magnification confirms relatively stable interfacial region.

Fig. 6.13: Tensile fracture surfaces of control specimens - no load has been applied to the steel fibre.

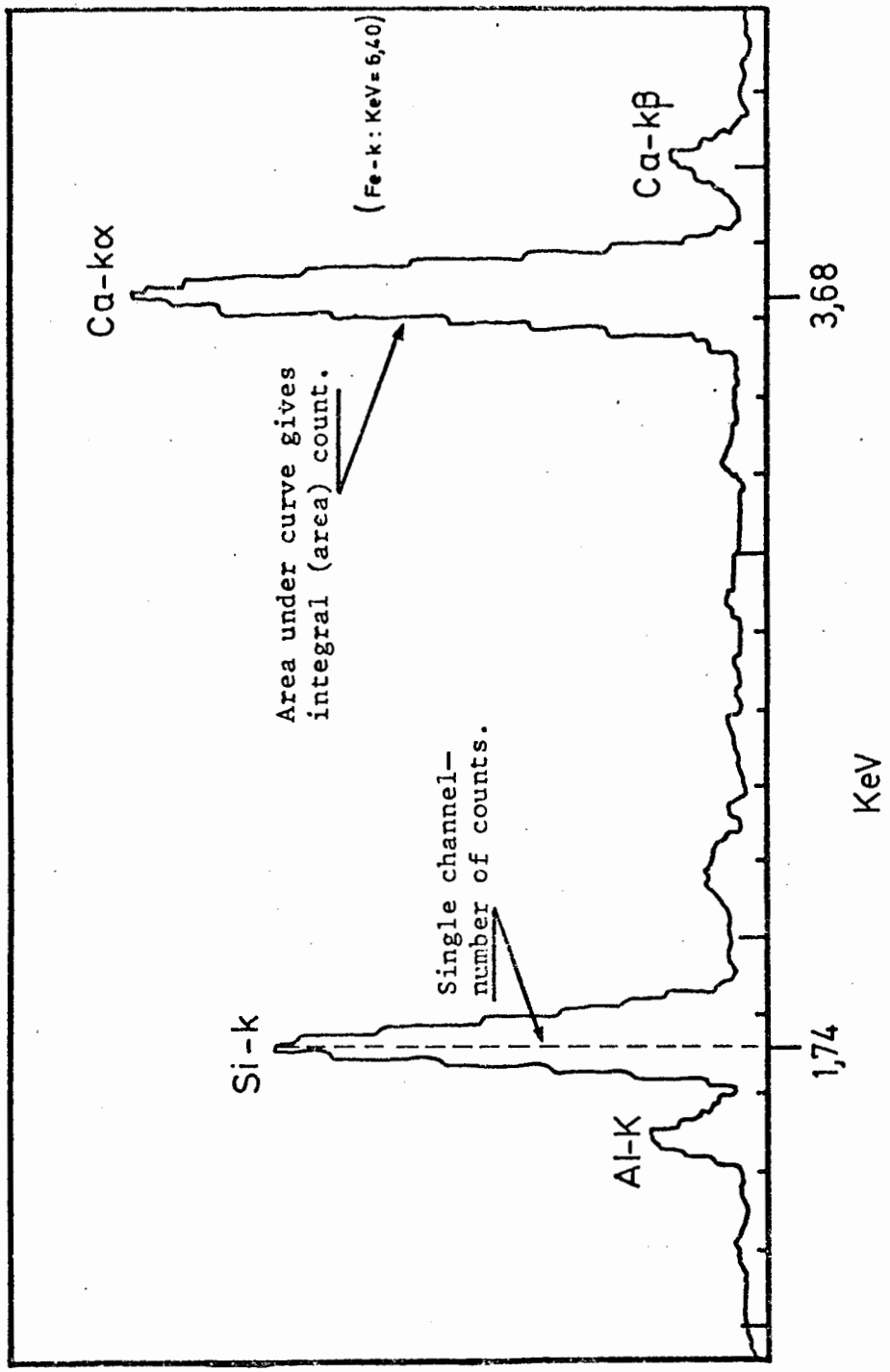

Fig. 6.14: Typical diagrammatic illustration of Elemental Distribution curve (EDXA).

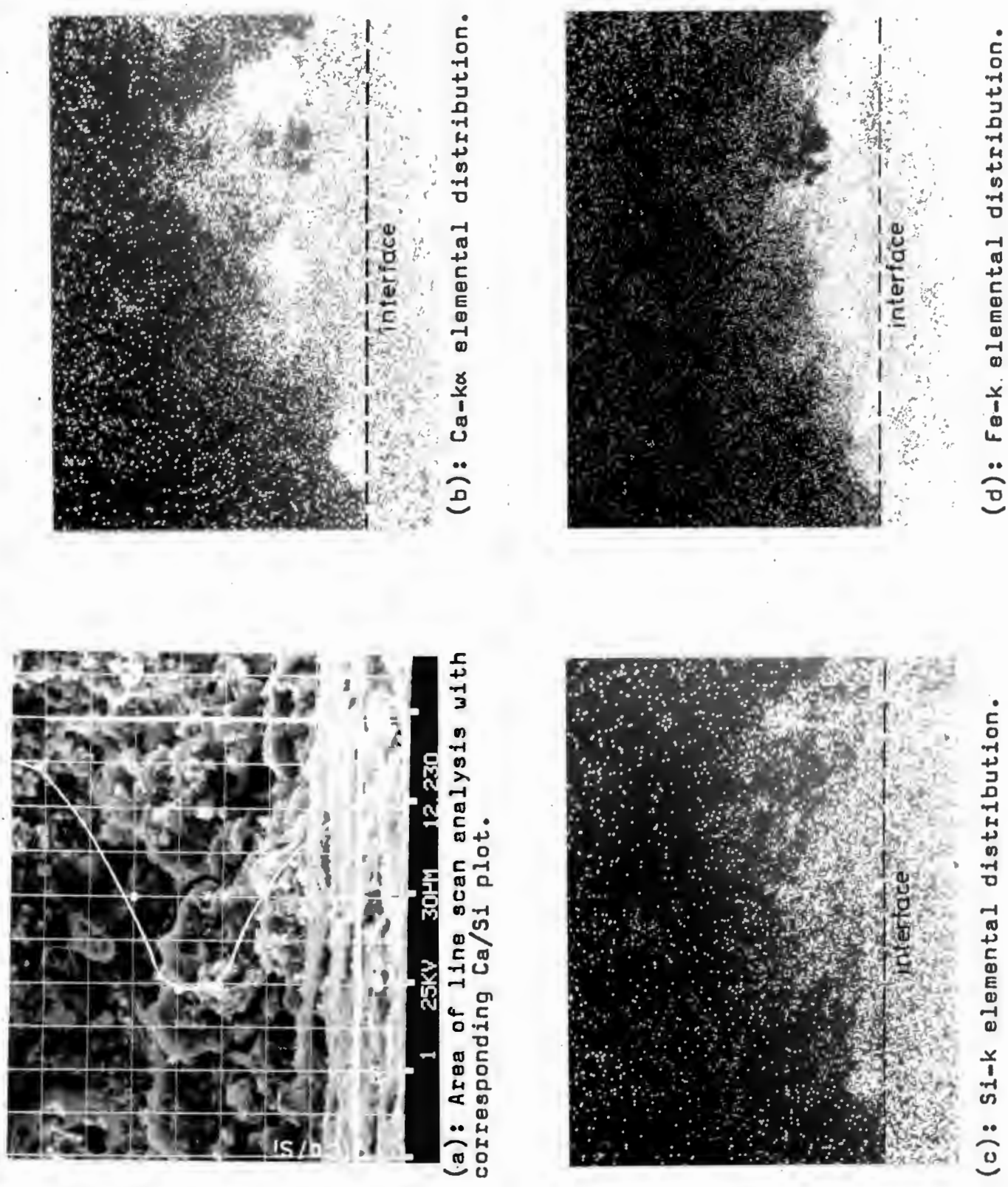

Fig. 6.15: Typical fibre-matrix specimen used for line scan EDX analysis with corresponding elemental distribution maps. (Line scan done at intervals equivalent to grid system.) *Dotted line indicates interface.*

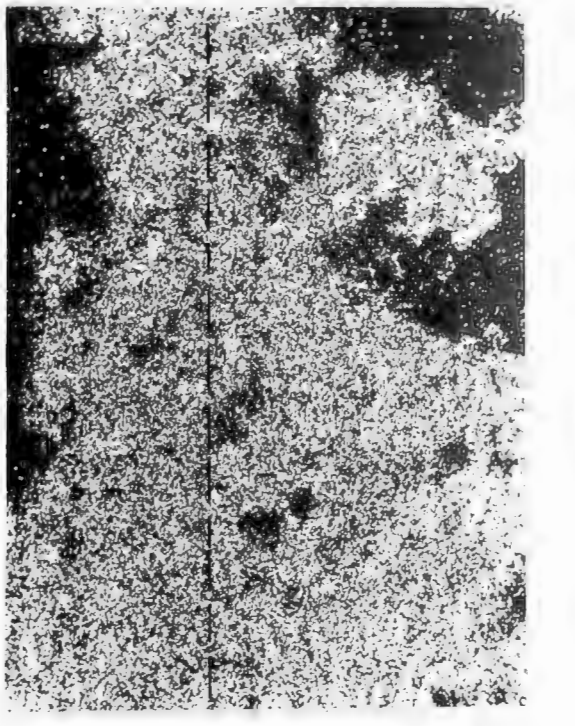

(b): Ca-kα elemental distribution.

(d): Fe-k elemental distribution.

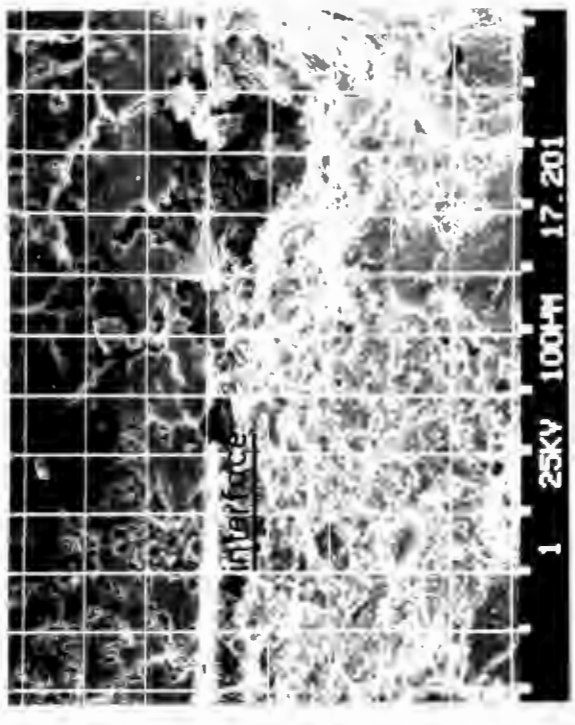

(a): Area of line scan analysis.

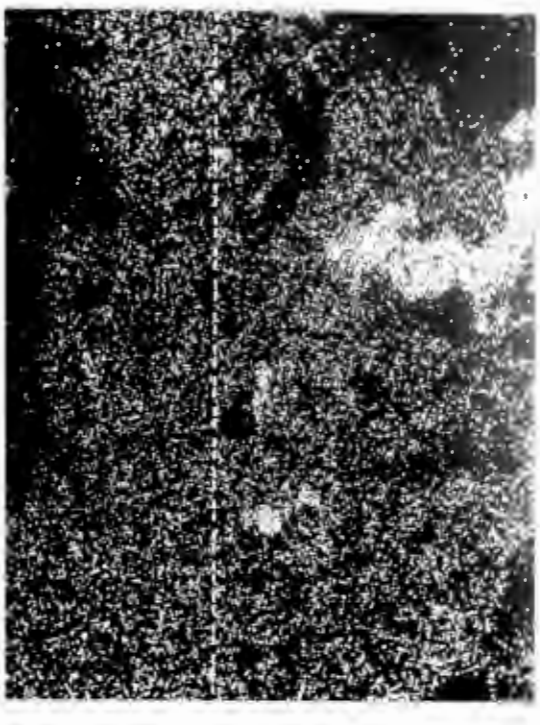

(c): Si-k elemental distribution.

Fig. 6.16: Typical cement-trough specimen used for line scan EDX analysis with corresponding elemental distribution map. (Line scan done at intervals equivalent to grid system.) *Dotted line indicates interface.*

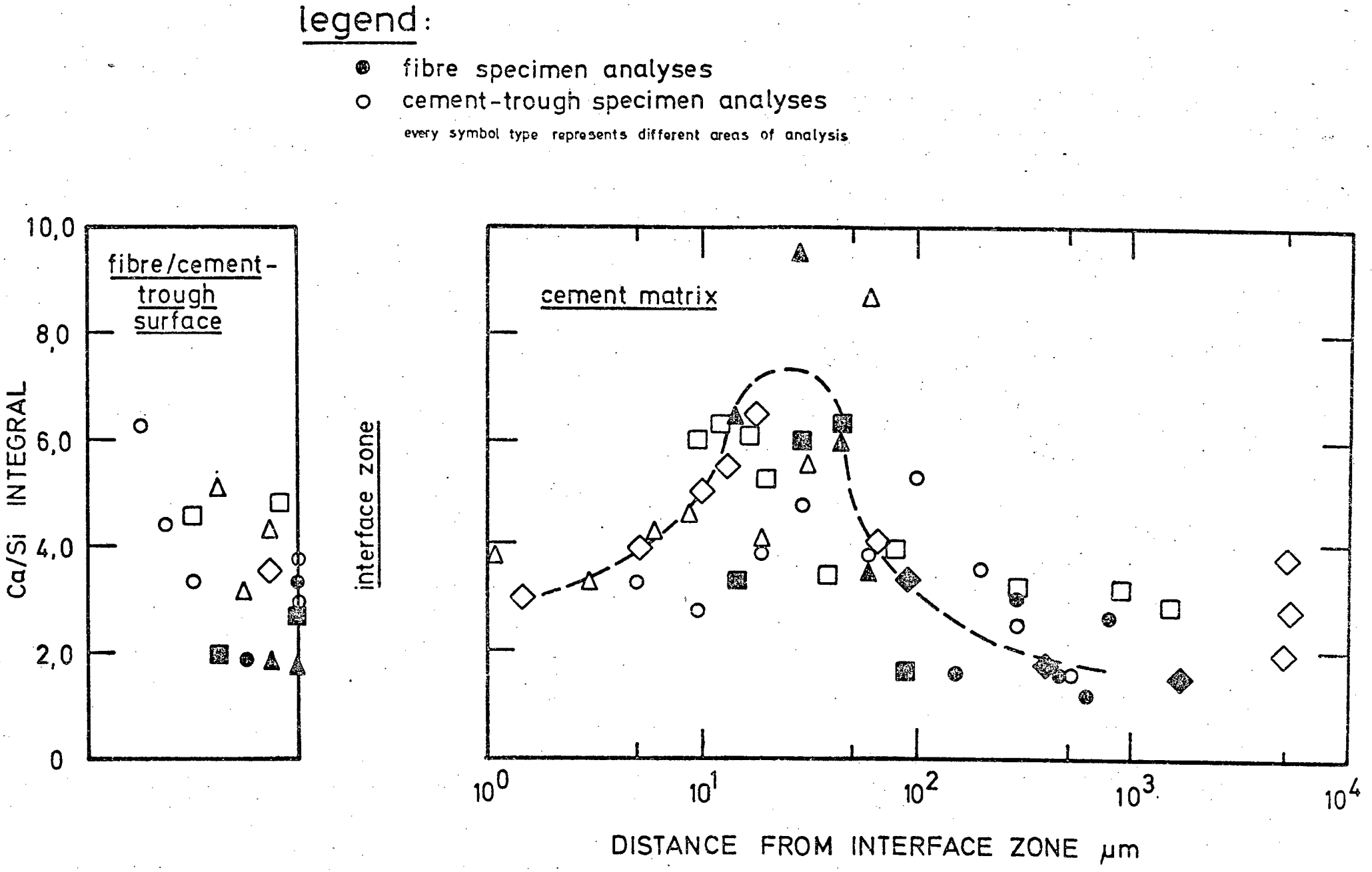

Fig. 6.17: Relationship between Ca/Si integral ratio with distance from fibre-matrix interface.

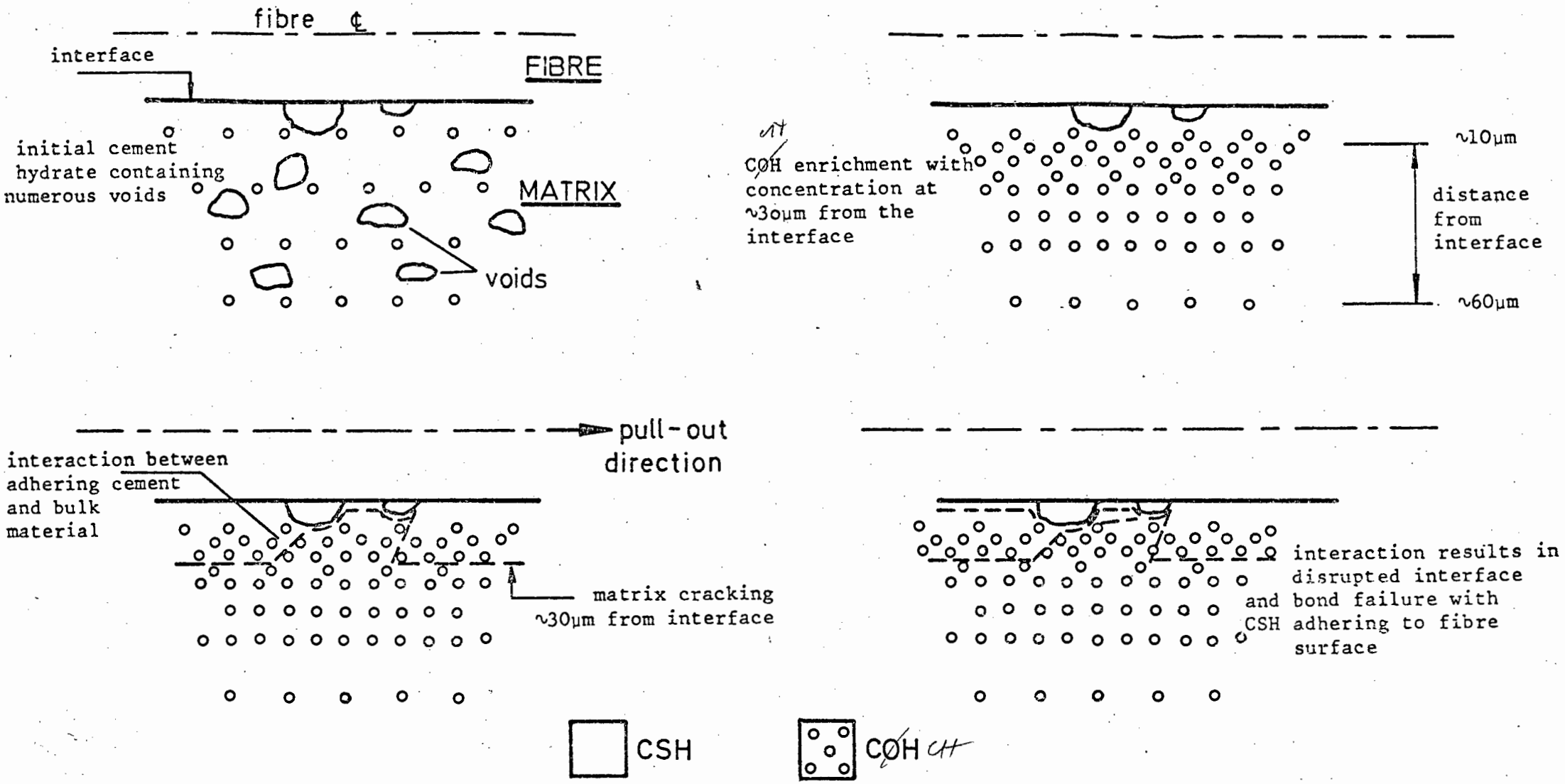

Fig. 6.18: Idealised representation of failure process at the fibre interface.

CHAPTER 7

7. SUMMARY AND CONCLUSIONS

It is well established that the relatively low tensile strength and ductility of cement-based materials is caused by the propagation of 'tensile' cracks which originate from inherent flaws within the cement matrix.

This thesis has been concerned with examining the effects of the addition of a uniform, but randomly-oriented distribution of short, discontinuous steel fibres to a plain mortar mix with the view to inhibiting, or at least retarding, the growth of such cracks thereby decreasing the unreinforced material's inherent deficiencies. This has involved an investigation of both the mechanical and microstructural effects of such additions.

Most previous experimental studies of plain cement-based materials have generally been concerned with investigating the compressive or flexural properties (for which concrete structural members are designed) rather than the tensile behaviour (tensile properties not being generally taken into account in design calculations). However, it is generally acknowledged that the failure of concretes (in compression or flexure) arises primarily from the propagation of 'tensile' cracks. Thus, the study of mechanical behaviour in this thesis has been concerned with comparative properties between fibrous and plain mortar in both compression (where it is logical to extend existing data analysis of plain cement-based materials to that of the fibrous composite) and tension (where the direct consequences of fibre reinforcement may be examined).

The addition of steel fibres was found to have no significant effect upon either the static or fatigue properties of plain mortar in compression, other than to substantially increase the load-bearing capacity after maximum load (i.e. toughness, measured as the area under the stress-strain curve). However, the dominating failure mechanisms of the mix are altered, and the fibres are shown to act in

a role both as crack-initiators (indicated by the earlier stress/strain at which microcracking initiates, measured by changes in ultrasonic pulse transit time (UPTT)) and crack-arrestors (the amount of damage sustained by the fibrous composite being substantially greater than that of plain mortar - also measured by UPTT). Fatigue loading resulted in an overall reduction of 30% in the elastic modulus at failure for both plain and fibrous mortar. Also, the accumulation of damage, measured by changes in UPTT and residual strain, was found to increase in a characteristic manner with up to three distinct regimes being obtained, depending on the maximum applied cyclic stress. Furthermore, several empirical relationships were obtained for compressive fatigue failure prediction for the mixes used in this thesis.

By contrast, when loaded statically in tension, fibre addition was observed to significantly increase the stress at the initiation of microcracking, ultimate failure stress (an increase of 60%), ultimate failure strain and toughness. The stress at the limit of proportionality of the fibrous mortar stress-strain curve was found to correspond precisely with the static failure stress of plain mortar, further stress/strain increases in fibrous mortar being a direct result of the fibres' ability to bridge cracks and support load.

The study of the corresponding fatigue properties in direct tension necessitated the development of a reliable and accurate testing method. The direct tensile fatigue properties of the plain mortar were found to be substantially improved by steel fibre additions as illustrated by marked increases in fatigue life. In addition, the fibres allow very extensive micro-cracking to occur during fatigue, which is not the case in the plain material. Results obtained also indicate that in direct tension the fibres behave solely as crack-arrestors and not also as crack-initiators as in compression.

The extensive cracking network shown to take place within the fibrous mortar, as measured by relatively large increases in ultrasonic pulse transit times during mechanical testing, was also observed to occur at initial debonding of

steel-fibres from the matrix by Scanning Electron Fractography studies. In conjunction with Energy Dispersion X-ray Analysis (EDXA) failure (or pull-out) in the reinforced composite has been found to initiate within an enriched calcium hydroxide region of the matrix adjacent to the fibre-matrix interface. This region is considered to arise from the calcium hydroxide filling up the concentration of voids initially present adjacent to the interface, the finer calcium silicate hydrates preventing the calcium hydroxides being deposited at the interface itself. These latter observations contradict previous reports made in the literature which suggest general fracture in the composite arises specifically due to bond failure between fibre and matrix. It is suggested, therefore, that before steel fibre reinforcement can be used more effectively, specific attention must be given to both the processing operations leading to regions of weakness adjacent to the interface, and indeed to the strength properties of the cement matrix itself.

why should the filling of voids weaken the structure if the voids are already there to weaken the structure. Although $Ca(OH)_2$ in itself is weak, it filling the voids should strengthen the structure.

REFERENCES

1. Kelly, A., 'Saving Energy with Inorganic Solids', Physics Bulletin, June 1977.

2. Van Ornum, J.L., 'Fatigue of Concrete' Transaction of American Soc. of Civil Engineers, Vol. 58, 1903.

3. Romualdi, J.P., Batson, G.B., 'The mechanics of crack arrest in concrete', Jour. of Mech. Div., Proc. A.S.C.E., Vol. 89, EM3, pp. 147-168, June 1963.

4. Porter, H.F., 'The preparation of Concrete from Selection of Materials to final disposition', Proc., National Association of Cement Users, A.C.I., Vol. 6, 1910.

5. Kelly, A., 'Strong Solids', 2nd ed., Clarendon Press, Oxford, 1973.

6. Aveston, J., Cooper, G.A., Kelly, A., 'The Properties of fibre composites', National Physics Lab., Nov. 1971, published by IPC Science and Technology Press, pp. 15-26.

7. Laws, V., 'The efficiency of Fibrous reinforcement of brittle matrices', Jour. Phys. D : Appl. Phys., Vol. 4, 1971, pp. 1737-1746.

8. Romualdi, J.P., Batson, G.B., 'Behaviour of Reinforced Concrete Beams with closely spaced reinforcement', Jour. A.C.I., Vol. 60, No. 6, pp. 775-789, June 1963.

9. Griffiths, A.A., 'The phenomena of rupture and flow in solids', Phil. Trans. Roy. Soc., A221, pp. 163-198, 1920.

10. Romualdi, J.P., Mandel, J.A., 'Tensile strength of concrete affected by uniformly distributed and closely spaced short lengths of wire reinforcement', Jour. A.C.I., Vol. 61, No. 6, June 1964.

11. Kaplan, M.F., 'Crack propagation and the fracture of concrete', Jour. A.C.I., Vol. 58, Nov. 1961, pp. 591-611.

12. Glucklich, J., 'The flexural static and fatigue failure of Portland Cement Mortar', T.A.M. report 622, Univ. of Illinois, 1962.

13. Glucklich, J., 'Fracture of Plain Concrete', Jour. of Eng. Mech. Div., A.S.C.E., EM6, Dec. 1963, pp. 127-137.

14. Moavenzadeh, F., Kuguel, R., 'Fracture of Concrete', Jour. of Materials, J.M.S.L.A., Vol. 4, No. 3, Sept. 1969, pp. 497-519.

15. Naus, J.D., Lott, J.L., 'Fracture Toughness of Portland Cement Concretes', Jour. A.C.I., June 1969.

16. Shah, S.P., McGarry, F.J., 'Griffith Fracture Criterion of Concrete', Jour. of Eng. Mech. Div., EM6, A.S.C.E., Dec. 1971, pp. 1663-1676.

17. Higgins, D.D., Bailey, J.E., 'Fracture measurements on Cement Paste', Jour. of Mat. Sci., Vol. 11, 1976, pp. 1995-2003.

18. Kesler, C.E., Naus, D.J., Lott, J.L., 'Fracture mechanisms - its applicability to concrete', Int. Conf. on Mech. Behaviour of Materials, Japanese Soc. of Mat. Sci., 1971.

19. Gjorv, O.Z., Sorensen, S.I., Arnesen, A., 'Notch Sensitivity and Fracture Toughness of Concrete', Cement and Concrete Res., Vol. 7, pp. 333-344, 1977.

20. Kanninnen, M.F., Rybicki, E.F., Brinson, H.F., 'A critical look at current Applications of fracture mechanics to the failure of fibre reinforcement composites', Composites, pp. 17-22, Jan. 1977.

21. Shah, S.P., Rangan, B.V., 'Fibre reinforced concrete properties', Jour. of A.C.I., Vol. 68, No. 2, pp. 126-135, Feb. 1971.

22. Johnston, C.D., Coleman, R.A., 'Steel fibre Reinforced mortar in uniaxial tension', Proc. of Int. Symp. of FRC, A.C.I., SP-44, Oct. 1973.

23. Edgington, J., 'Steel fibre reinforced concrete', Ph.D. thesis, Univ. of Surrey, Oct. 1973.

24. Swamy, R.M., 'Progress in fibre reinforced concrete', Civ. Eng. and Public Works review, Sept. 1973, pp. 745-754.

25. Aveston, J., Kelly, A., 'Theory of Multiple fracture of fibrous composites', Jour. of Mat. Sci., Vol. 8, 1973, pp. 352-362.

26. Majumdar, A.J., 'Properties of fibre cement composites', RILEM symp., 1975.

27. Kar, J.N., Pal, A.K., 'Strength of fibre reinforced concrete', Jour. Struct. Div., A.S.C.E., Vol. 98, May 1972.

28. Swamy, R.N., Mangat, P.S., Rao, C.V., 'The mechanics of fibre reinforcement of Cement Matrices', Int. Symp. on F.R.C., A.C.I., SP44-11, 1973.

29. Swamy, R.N., Fattuhi, N.I., Mangat, P.S., 'Mechanics of fibre reinforced concrete', Proc. of Int. Conf. on Mech. Behaviour of Materials, Vol. V, Composites, Testing and Evaluation, 1972, pp. 168-175.

30. Mangat, P.S., 'Tensile Strength of Fibre Reinforced Concrete', Cement and Concr. Res., Vol. 6, No. 2, pp. 245-252, March 1976.

31. Swamy, R.N., Mangat, P.S., 'A Theory for the flexural strength of steel-fibre reinforced concrete', Cem. and Concr. Res., Vol. 4, 1974, pp. 317-325.

32. Swamy, R.N., Mangat, P.S., 'The onset of Ductility and cracking of steel fibre concrete', Cem. and Concr. Res., Vol. 5, 1975, pp. 37-53.

33. Swamy, R.N., Mangat, P.S., 'The interfacial bond stress in steel fibre cement composites', Cement and Concr. Res., Vol. 6, pp. 641-650, 1976.

34. Batson, G.B., 'The state-of-the-art Report of fibre reinforced concrete', A.C.I. Jour., Nov. 1973.

35. Rajagopalan, K., Parameswaran, V.S., Discussion of ref. (32), Cem. and Concr. Res., Vol. 5, 1975, pp. 179-182.

36. Mayfield, B., Zelly, B., 'Steel fibre treatment to improve bonds', Concrete, pp. 35-37, March 1973.

37. Tattersall, G.H., Urbanowicz, C.R., 'Bond Strength in steel fibre reinforced concrete', Mag. of Conc. Res., Vol. 26, No. 87, June 1974.

38. Hughes, B.P., Fattuhi, N.I., 'Fibre bond strength in cement and concrete', Mag. of Conc. Res. Vol. 27, No. 92, Sept. 1975.

39. Neville, A.M., 'The failure of concrete compression test specimens', Civil Engineering, Vol. 52, No. 613, pp. 773-774, July 1957.

40. Gonnerman, H.F., 'Effect of size and shape of test specimen on compressive strength of concrete', Proc. A.S.T.M., Vol. 25, Part II, p. 237-250, 1925.

41. Murdock, J.W., Kesler, C.E., 'Effect of length to diameter ratio of specimens on the apparent compressive strength of concrete', A.S.T.M. Bulletin, p. 68-73, April 1957.

42. Swamy, R.N., Stravides, H., 'Some properties of high workability of steel fibre concrete', RILEM, 1975, p. 197.

43. Edgington, J., Hannant, D.J., and Williams, R.I.J., 'Steel fibre reinforced concrete', Building Research Establishment Current Paper, CP 69/74, July 1974.

44. Neville, A.M., 'Properties of Concrete', Pitman Int., 1975.

45. Walker, S., Bloem, D.L., 'Effects of curing and moisture distribution on measured strength of concrete', Proc. Highway Res. Bulletin, Vol. 36, pp. 334-346, 1957.

46. B.S. 1881: 1970, 'Methods of Testing Concrete', B.I.S., London.

47. Gonnerman, H.F., 'Effect of end conditions of cylinders on compressive strength of concrete', Proc. A.S.T.M., Vol. 58, pp. 1166-81, 1958.

48. Hannant, D.J., 'The tensile strength of concrete - a review paper', The Structural Engineer, Vol. 50, No. 7, July 1972, pp. 253-258.

49. Raithby, K.D., Galloway, J.W., 'Effects of moisture condition, age, and rate of loading on fatigue of plain concrete', SP 41-2, A.C.I., Abeles Symposium.

50. Antrim, J.D., 'The mechanism of fatigue in cement paste and plain concrete', Highway Res. Record, 210. 1968, pp. 95-107.

51. Antrim, J.D., 'A study of the mechanism of fatigue in cement paste and plain concrete', Ph.D. thesis, University of Purdue, Jan. 1964.

52. RILEM, 'Direct tensile test of concrete', RILEM Bulletin, No. 20, Sept. 1963, pp. 84-89.

53. Johnston, C.D., Sidwell, E.H., 'Testing concrete in tension and in compression', Mag. Conc. Res., Vol. 20, No. 65, Dec. 1968, pp. 221-228.

54. Raju, N.K., 'Small concrete specimens under repeated compressive loads by pulse velocity techniques', Jour. of Materials, J.M.L.S.A., Vol. 5, No. 2, pp. 262-272, June 1970.

55. Nwokoye, D.N., 'Predictions and Assessment of Concrete properties from pulse velocity tests', Mag. of Conc. Res., Vol. 25, No. 82, March 1973.

56. Kaplan, M.F., 'Ultrasonic pulse velocity, dynamic modulus of elasticity, Poisson's ratio and the strength of concrete made with 13 different aggregates', RILEM Bull., March 1959.

57. Jones, R., 'A method of studying the formation of cracks in a material subjected to stress', British Jour. of App. Physics, Vol. 3, No. 7, July 1952.

58. Spooner, D.C., 'Stress-Strain relationship for hardened cement pastes, 'Mag. of Conc. Res., Vol. 24, No. 79, June 1972.

59. Spooner, D.C., 'Stress-strain-time relationship for concrete', Mag. of Conc. Res., Vol. 23, No. 75-76, June-Sept., 1971.

60. Murdock, J.W., Kesler, C.E., 'Effect of Range of Stress on Fatigue strength of plain concrete beams', Proc. A.C.I., Vol. 35, 1959, pp. 221-231.

61. Neal, J.A., Kesler, C.E., 'The Fatigue of plain Concrete', Proc. of the Int. conf. on the structure of concrete and its behaviour under load, London 1968, pp. 226-237.

62. Hilsdorf, H.K., Kesler, C.E., 'Fatigue strength of concrete under varying flexural stresses', Proc. A.C.I., Vol. 63, pp. 1039-1076, 1966.

63. Kesler, C.E., 'Effect of speed of testing on Flexural Strength of Plain Concrete', Proc. Highway Res. Board, Vol. 32, 1953, pp. 251-258.

64. Sparks, P.R., Menzies, J.B., 'The effect of rate of loading upon the static and fatigue strengths of plain concrete in compression', Mag. of Concr. Res., Vol. 25, No. 83, June 1973.

65. Neville, A.M., Kennedy, J.B., 'Basic Statistical Methods for Engineers and Scientists', Int. Textbook Company, 1964.

66. Williamson, G.R., 'The effect of steel fibres on the compressive strength of concrete', Int. Symp. on F.R.C., A.C.I., SP-44-11, pp. 195-207, 1973.

67. Chen, Wai-Fah, Carson, J.L., 'Stress strain properties of Random Wire reinforced concrete', A.C.I. Jour., Dec. 1971.

68. Hughes, B.P., Fattuhi, N.I., 'Stress strain curves for fibre reinforced concrete in compression', Cem. and Conc. Res., Vol. 7, pp. 173-184, 1977.

69. Swamy, R.N., Al-Noori, K., 'Flexural properties of steel fibre reinforced concrete', Concrete, Vol. 9, No. 6, June 1975.

70. Snyder, M.J., Lankard, D.R., 'Factors affecting the flexural strength of steel fibrous concrete', A.C.I. Jour., Feb. 1972.

71. Hughes, B.P., Fattuhi, N.I., 'Improving the toughness of high strength cement paste with fibre reinforcement', Composites, July 1976, pp. 185-188.

72. Kaplan, M.F., 'Flexural and compressive strength of concrete as affected by the properties of coarse aggregates', Jour. A.C.I., Vol. 55, pp. 1193-1208, May 1959.

73. Bennett, E.W., Raju, N.K., 'Cumulative fatigue damage of Plain Concrete in compression', Struct., Solid Mech. and Eng. Design Proc., Southampton, 1969.

74. Shah, S.P., Chandra, S., 'Fracture of concrete subjected to cyclic and sustained loading', Jour. A.C.I., Oct. 1970, pp. 816-824.

75. Romualdi, J.P., 'The static cracking stress and fatigue strength of concrete reinforced with pieces of thin steel wire', Int. conf. on struct. of concrete and its behaviour under load, London, Sept. 1965, Cem. and Concr. Ass. 1968, pp. 190-201.

76. Batson, G., Ball, C., Bailey, L., Landers, E., Hooks, J., 'Flexural fatigue strength of steel fibre reinforced concrete beams', Jour. A.C.I., Nov. 1972.

77. Bennett, E.W., Muir, S.E., 'Some fatigue tests of high strength concrete in axial compression', Mag. of Conc. Res., Vol. 19, No. 59, June 1967.

78. Raju, N.K., 'Comparative study of Fatigue behaviour of concrete, mortar and paste in uniaxial compression', Jour. A.C.I., June 1970, pp. 461-463.

79. Lloyd, J.P., Lott, J.L., Kesler, C.E., 'Fatigue of concrete', T.A.M. report, No. 675, Univ. of Illinois, Sept. 1967.

80. Bennett, E.W., 'Fatigue in concrete', Concrete, Vol. 8, No. 5, May 1974, pp. 43-45.

81. Kesler, C.E., 'Fatigue and Fracture of Concrete', Stanton Walker lecture, Univ. of Maryland, Nov. 1970.

82. Neal, J.A., Kesler, C.E., 'Some Aspects of Fatigue of Concrete', T.A.M. report 657, Univ. of Illinois, July 1965.

83. Spooner, D.C., Doughill, R.A., 'A quantitative assessment of damage sustained in concrete during compressive loading', Mag. of Conc. Res., Vol. 27, No. 92, Sept. 1975.

84. Whaley, C.P., Neville, A.M., 'Non-elastic deformation of Concrete under cyclic compression', Mag. of Conc. Res., Vol. 25, No. 84, Sept. 1973.

85. Hilsdorf, H.K., Kesler, C.E., 'The behaviour of Concrete in flexure under varying repeated load', T.A.M. report No. 172, Univ. of Illinois, Aug. 1960.

86. Award, M.E., Hilsdorf, H.K., 'Strength and deformation characteristics of plain concrete subjected to high repeated and sustained loads', SP41-1, A.C.I., pp. 1-14.

87. Control of Cracking in Concrete Structures, Report by A.C.I. Committee 224, A.C.I. Jour., Dec. 1972, pp. 717-753.

88. Mindness, S., Nadeau, J.S., Hay, J.M., 'Effects of Different Curing Conditions on slow crack growth in cement paste', Cem. and Concr. Res., Vol. 4, pp. 953-965, 1974.

89. Clemmer, H.F., 'Fatigue of Concrete', Proc. of Amer. Soc. for Testing and Materials, Vol. 22, Part II, 1922, pp. 408-419.

90. Welsh, G.B., 'Tensile strains in unreinforced concrete beams', Mag. of Concr. Res., Vol. 18, No. 54, March 1966, p. 9-18.

91. Grant, J., 'Experiments on the Strength of Cement', Proc. of Inst. of Civil Engineers, Vol. XXV, No. 12, p. 66, Dec. 1865.

92. Todd, J.D., 'The Determination of tensile stress-strain curves for concrete', Proc. Inst. of Civil Engineers, Part I, Vol. 4, March 1955, pp. 201-211.

93. Humphreys, R., 'Direct tensile strength of concrete', Civil Eng. and Public Works Review, Vol. 52, No. 614, Aug. 1957, pp. 882-883.

94. Hughes, B.P., Chapman, B.P., 'Direct tensile test for concrete using modern adhesives', RILEM Bull., No. 26, March 1965, pp. 77-80.

95. Elvery, R.H., Haroun, W.A., 'Direct tensile test for concrete under long or short term loading', Mag. of Conc. Res., Vol. 20, No. 63, June 1968.

96. Samarai, M.A., Elvery, R.H., 'The influence of fibres upon crack development in reinforced concrete subject to uniaxial tension', Mag. of Conc. Res., Vol. 26, No. 89, Dec. 1974, pp. 203-211.

97. Elvery, R.H., Samarai, M.A., 'An Examination of the behaviour of fibres in reinforced concrete', Composites, July 1976, pp. 180-184.

98. Majumdar, A.J., 'The role of the interface in Glass Fibre Reinforced Cement', Cem. and Concr. Res., Vol. 4, pp. 247-266, 1974.

99. Stucke, M.S., Majumdar, A.J., 'Microstructure of glass fibre-reinforced cement composites', Jour. of Mat. Sci., Vol. II, 1976, pp. 1019-1030.

100. Diamond, S., Young, J.F., Lawrence, F.V., 'Scanning Electron microscopy-energy dispersive X-ray analysis of cement constituents - some cautions', Cem. and Concr. Res., Vol. 4, 1974.

101. Williamson, R.B., 'Solidification of Portland Cement', Progress in Materials, Vol. 15, 1973.

102. Berger, R.L., Cahn, D.S., McGregor, J.D., 'Calcium Hydroxide as a Binder in Portland Cement Paste', Jour. of Amer. Ceramic Society, Vol. 53, No. 1, Jan. 1970, pp. 57-58.

103. Jaras, A.C., Litherland, K.L., 'Microstructural features in glass fibre reinforced cement composites', RILEM Sym., 1975, pp. 327-334.

104. De Vekey, R.C., Majumdar, A.J., 'Determining Bond Strength in fibre-reinforced composites', Mag. of Concr. Res., Vol. 20, No. 65, Dec. 1968, pp. 229-234.

105. Pinchin, D.J., Tabor, D., 'Inelastic Behaviour in Steel wire pull-out from Portland cement mortar', submitted to Jour. of Mat. Sci., Private Comm.

106. Pinchin, D.J., Tabor, D., 'Mechanical properties of the steel/cement interface: some experimental results', RILEM Sym., pp. 521-526, 1975.

107. Argon, A.S., Shack, W.J., 'Theories of fibre cement and fibre concrete', Discussion, RILEM Sym., pp. 509-510, 1975.

108. Naaman, A.E., Shah, S.P., 'Bond studies on oriented and aligned steel fibres', RILEM Sym., pp. 171-178, 1975.

109. Pinchin, D.J., Tabor, D., 'Interfacial Phenomena in steel fibre reinforced cement. I: Structure and strength of Interfacial Region', Cem. and Concr. Res., Vol. 8, No. 1, January, 1978.

110. Pinchin, D.J., Tabor, D., 'Interfacial Phenomena in steel fibre reinforced cement. II: Pull-out behaviour of steel wires', Cem. and Concr. Res., Vol. 8, No. 2, March 1978.

111. Stucke, M.S., Majumdar, A.J., 'The composition of the gel phase in Portland Cement Paste', Proc. of Conf.: Hydraulic cement pastes - their structure and properties', Sheffield, 1976.

112. Diamond, S., 'Identification of hydrated cement constituents using a scanning electron microscope - energy dispersive X-ray spectrometer combination', Cem. and Concr. Res. Vol. 2, No. 5, Sept. 1972, pp. 617-632.

113. 'Discussion' Conf. on 'Polymers in Concrete', London, 1975, p. 107.

114. Walsh, D., Otooni, M.A., Taylor, M., Marcinkowski, 'Study of Portland Cement fracture surfaces by scanning electron microscopy techniques', Jour. of Mat. Sci., Vol. 9, 1974, pp. 423-429.

115. Diamond, S., 'Cement paste microstructure - An overview at several levels', Proc. of Conf., Hydraulic cement pastes, their structure and properties, Sheffield, 1976.

116. Shah, S.P., Naaman, A.E., 'Mechanical Properties of Glass and Steel - fibre reinforced mortar', Jour. A.C.I., Jan. 1976, pp. 30-53.

117. Shah, S.P., Rangan, B.V., 'Effects of Reinforcement on Ductility of Concrete', Jour. of Struct. Div., A.S.C.E., pp. 1167-1184, June 1970.

118. Majumdar, A.J., 'Fibre cement and concrete - a review', Composites, Jan. 1975, pp. 7-16.

119. Iyengar, K.T.S., Viswanatha, C.S., Discussion of ref. (67), Jour. A.C.I., June 1972, pp. 346-349.

120. Dixon, J., Mayfield, B., 'Concrete reinforced with Fibrous wire', Concrete, March 1971, pp. 73-76.

121. Nauda, V.K., 'A Laboratory Investigation of Fibre Reinforced Concretes', M.Sc. thesis, Univ. of Surrey, Oct. 1968.

122. Swamy, R.N., Mangat, P.S., 'Influence of Fibre-aggregate interaction on some properties of steel-fibre reinforced concrete', Matériaux et Constructions, Vol. 7, No. 41, Oct. 1973, pp. 301-313.

123. Pakotiprapha, B., Pama, R.P., 'Mechanical Properties of Cement Mortar with Randomly Oriented Short Steel Wires', Mag. of Concr. Res., Vol. 26, No. 86, March 1974.

ACKNOWLEDGEMENTS

I would like to express my appreciation to Dr. G.G. Garrett for the sustained and constructive guidance and encouragement he has given throughout this project.

Thanks also to my friends and colleagues in the Department for much useful discussion and assistance.

The assistance of the technical staff of the University, in particular Messrs. P. Duxbury and N. Dreze, is acknowledged.

I would like to express my gratitude to John Williams for assistance in mixing and casting of the test specimens, to Bernard Greeves for developing and printing the photographs, and to Lesley Hope-Sutterton for her assistance with draughting.

Financial support from the following is gratefully acknowledged:

Council for Scientific and Industrial Research,
University Research Administration,
Atomic Energy Board,
Portland Cement Institute.

Finally, I would like to thank Caroline Kingdon for her efficiency in typing the manuscript.